University of Technology, Sydney
Faculty of Engineering and IT
Centre of Real-Time Information Networks

Packet Scheduling for LTE-Advanced

Author: Nguyen, Sinh Chuong (John)
Student Number: 10928517
Supervisor: A/Prof Kumbesan Sandrasegaran

In accordance with the requirement for the Degree of
Master of Engineering by Research

2011

Certificate of Originality

I certify that the work in this thesis has not previously been submitted for a degree nor has it been submitted as part of requirements for a degree except as fully acknowledged within the text.

I also certify that the thesis has been written by me. Any help that I have received in my research work and the preparation of the thesis itself has been acknowledged. In addition, I certify that all information sources and literature used are indicated in the thesis.

Signature of Student

Abstract

LTE-Advanced has been approved by the International Telecommunication Union (ITU) as a 4G mobile communication system. It is also called IMT-Advanced or true 4G technology. LTE-Advanced is an evolution of LTE (Release-8) and backward compatible with LTE because they both use the same air-interface technologies such as OFDMA, MIMO, and the same core network.

Since radio spectrum is the most valuable resource in mobile technology, radio resource management (RRM) mechanisms are critical for the operation of a cellular network. One of the key RRM mechanisms is packet scheduling and it allocates suitable radio resources to each user for transmission of the downlink from the base station through the air interface to each mobile station.

The overall objectives of this project are to study packet scheduling mechanism for LTE-Advanced and find an optimized packet scheduling algorithm(s) to fully utilize new features and challenges of LTE-Advanced. This project is an extension of previous work done in packet scheduling in LTE at Centre for Real-time Information Networks (CRIN), UTS.

This thesis begins by explaining the design considerations used to create a computer simulation tool to model packet scheduling as well as other RRM mechanisms for LTE-Advanced. Thereafter, it will model, simulate, validate, and evaluate the performance of current well-known and new packet scheduling algorithms for LTE-Advanced. In this thesis, two new algorithms called optimized cross-CC proportional fair (OCPF) and optimized cross-CC M-LWDF (OCM) are proposed. (CC: component carrier)

The OCPF algorithm can overcome the weaknesses of current algorithms and improve system throughput. The OCM can provide a more effective solution for realistic traffic with strict requirement on the quality of services (QoS).

Acknowledgement

Firstly, I would like to express my deep gratitude to my supervisor Dr. Kumbesan Sandrasegaran for his guidance and support throughout this project.

Secondly, I would like to thank all the team members in CRIN center, Riyaj Basukala, Huda Adibah Mohd Ramli and others, for their contributions to help me gaining fundamental knowledge about this topic, their advice to make the simulation tool, as well as their valuable comments on my papers.

Finally, I would like to give grateful thank to my dear wife and my lovely parents. They have given me the excellent support and great encouragement to achieve the best education that I will never forget.

Table of Contents

List of Figures

List of Table

List of Acronyms

3G	3rd Generation Wireless Network
3GPP	3rd Generation Partnership Project
3GPP2	3rd Generation Partnership Project 2
4G	4th Generation Wireless Network
ACK	Acknowledgement
BLER	Block Error Rate
BS	Base Station
BSC	Base Stations Controller
CA	Carriers Aggregation
CC	Component Carrier
CDMA	Code Division Multiple Access
CoMP	Coordinated MultiPoint transmission and reception
CP	Cyclic Prefix
CQI	Channel Quality Indicator
CRIN	Centre of Real-Time Information Networks
Cross-CC	Cross-Component Carriers
CS/CB	Coordinated Scheduling/Beam-forming.
CSI	Channel State Information
EDGE	Enhanced Data rates for GSM Evolution
eNodeB	evolved NodeB
EPC	Evolved Packet Core
E-UTRAN	Evolved UTRAN
EXP/PF	Exponential/Proportional Fair
EVRC	Enhanced Variable Rate Coder
FDD	Frequency Division Duplex
FDMA	Frequency Division Multiple Access
FIFO	First-in-First-out
GSM	Global System for Mobile communications
HARQ	Hybrid-Automatic Repeat Request
HOL	Head of Line
HOM	Higher Order Modulations
HSDPA	High-Speed Downlink Packet Access
IEEE	Institute of Electrical and Electronics Engineers
IMT-2000	International Mobile Telecommunications-2000
In-CC	Independent-Component Carriers
IP	Internet Protocol
ITU	International Telecommunication Union
JP	Joint Processing
LTE	Long Term Evolution

LTE-A	Long Term Evolution Advanced
Max-Rate	Maximum-Rate
MCS	Modulation and Coding Scheme
MIMO	Multiple Input Multiple Output
M-LWDF	Modified-Largest Weighted Delay First
MME	Mobile Management Entity
NACK	Negative Acknowledgement
NRT	Non-Real Time
OCM	Optimized Cross-Component Carrier M-LWDF
OCPF	Optimized Cross-Component Carrier Proportional Fair
OFDM	Orthogonal Frequency Division Multiplex
OFDMA	Orthogonal Frequency Division Multiple Access
PCU	Packet Control Unit
PDF	Probability Density Function
PDN	Packet Data Network
PF	Proportional Fair
P-GW	PDN Gateway
PLR	Packet Loss Ratio
PS	Packet Scheduling
QAM	Quadrature Amplitude Modulation
QoS	Quality of Service
QPSK	Quadrature Phase Shift Keying
QSI	Queue State Information
RAN	Radio Access Network
RB	Resource Block
RMS	Root Mean Square
RN	Relay Node
RNC	Radio Network Controller
RNP	Radio Network Planning
RR	Round Robin
RRM	Radio Resource Management
RT	Real Time
RTT	Round-Trip Time
SA	Spectrum Aggregation
SC-FDMA	Single Carrier Frequency Division Multiple Access
SDF	Sub-band Discrimination Factor
S-GW	Serving Gateway
SINR	Signal to Interference-plus-Noise Ratio
SISO	Single-Input-Single-Output
SNR	Signal-to-Noise-Ratio
TB	Transport Block
TDD	Time Division Duplex
TDMA	Time Division Multiple Access

TFT	Time For Transmission
TTI	Transmit Time Interval
UDF	User Discrimination Factor
UE	User Equipment
UMB	Ultra Mobile Broadband
UMTS	Universal Mobile Telecommunications System
UTRAN	UMTS Terrestrial Radio Access Network
VoIP	Voice over IP
WCDMA	Wideband Code Division Multiple Access
WiMAX	Worldwide Interoperability for Microwave Access

CHAPTER 1: INTRODUCTION

1.1. Evolution of mobile technologies to 4^{th} Generation (4G)

Today, mobile phone is the most widely used electronic equipment over the world. In terms of daily usage, it surpasses any gadget that the human invented. According to the ITU (International Telecommunication Union) [1], there are more than 5.28 billion mobile subscribers in 2011 out of 6.8 billion or 77% of the world's population. In comparison to other widely used technologies, the number of users of Internet and television is around 2 billion [2] and fixed telephony users has dropped slightly below 1.2 billion, and the number of personal computers is nearly 1.2 billion. These facts have demonstrated the important contribution of mobile device usage in our day to day life.

An important change that is taking place is the shift from basic service of voice communication to data-based services such as web-surfing, video call, data transfer, and so on. Broadband wireless data usage is increasing faster than ever before with the appearance of new portable computers with wireless connection like iPad, laptop with 3G modem; and smartphones such as the iPhone and Android-OS phones. This is, consequently, driving the need to continue the innovation in wireless transmission technologies to provide more capacity and higher service quality.

Due to the efforts of the engineers & scientists, more technologies have been created to address the demand for broadband wireless data services. Researchers from vendors, operators, institutions and regulators around the world are gathering under three bodies that focus on the three main mobile technology families: **3GPP** (3^{rd} Generation Partnership Project) for GSM/UMTS [3], **3GPP2** for CDMA [4], and **IEEE** for WiMAX [5] (Figure 1-1).

After successfully deploying 3G technologies like WCDMA/HSDPA, 1xEVDO or WiMAX, these organizations have been researching on **4G** (or **IMT-Advanced**) technologies following the open call by the ITU-R (International Telecommunication Union- Radiocommunication Sector) for the "first invitation" of 4G candidates in 2008.

After around one year, there were six proposals submitted to ITU. All of them were aligned around two main technologies, the ***3GPP LTE Rel-10 and beyond (LTE-Advanced)*** technology and the ***IEEE 802.16m*** technology.

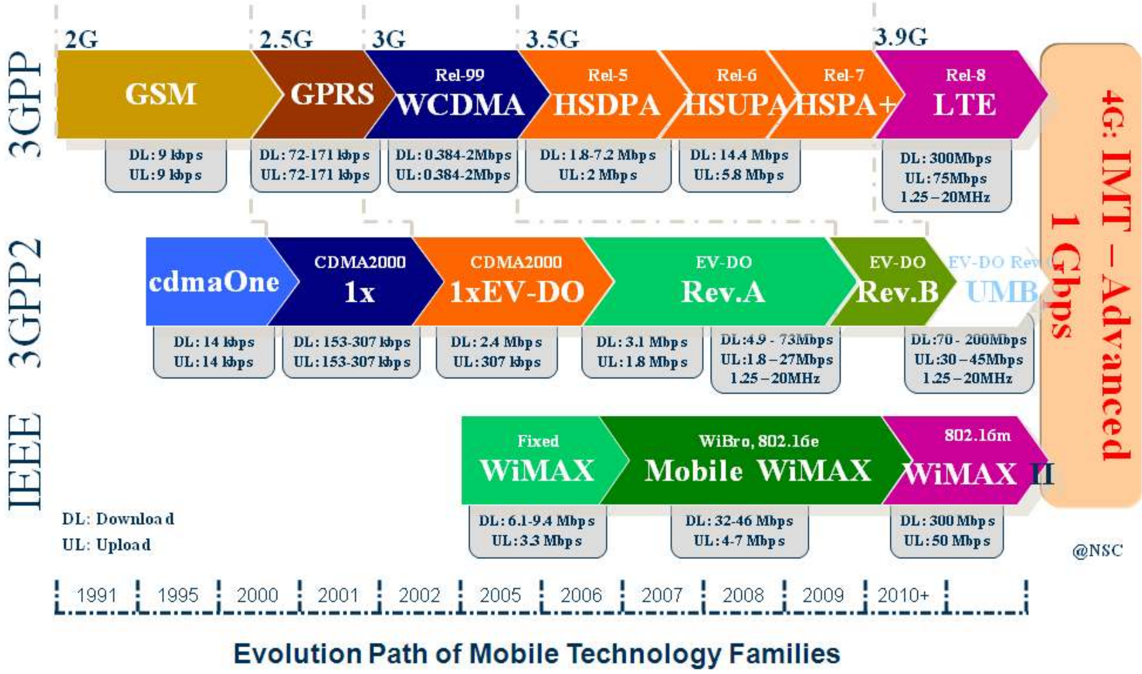

Figure 1-1: The evolution paths to 4G

The ITU-R officially announced the technologies that satisfied the IMT-Advanced requirement in a press release dated October 21st, 2010 [6]:

> *"ITU's Radiocommunication Sector (ITU-R) has completed the assessment of six candidate submissions for the global 4G mobile wireless broadband technology, otherwise known as IMT-Advanced. Harmonization among these proposals has resulted in two technologies,* ***LTE-Advanced*** *and* ***WirelessMAN-Advanced*** *being accorded the official designation of IMT-Advanced, qualifying them* ***as true 4G technologies****, … ITU-R Working Party 5D, which is charged with defining the IMT-Advanced global 4G technologies, reached a milestone in its work by deciding on these technologies for the first release of IMT-Advanced. In the ITU-R Report, which will be published shortly, the LTE-Advanced and WirelessMAN-Advanced technologies were each determined to have successfully met all of the criteria established by ITU-R for the first release of IMT-Advanced."*

Between these two 4G technologies, the 3GPP LTE-Advanced is more likely to be adopted by the most operators as the 3GPP market share account for 90% of total mobile subscriptions in the world. It is backward compatible and a natural evolution of 3GPP related technologies such as WCDMA, HSPA+ and LTE. Furthermore, recent publications [7] have shown that LTE-Advanced's performance far exceeds all the targets specified by requirements of IMT-Advanced.

1.2. 4G Technology and its technical requirements

As defined in the Report ITU-R M.2134 Requirements Related to Technical Performance for IMT-Advanced Radio Interface(s) [8], IMT-Advanced is defined by the following statement:

> *"International Mobile Telecommunications-Advanced (IMT-Advanced) systems are mobile systems that include the new capabilities of IMT that go beyond those of IMT-2000. Such systems provide access to a wide range of telecommunication services including advanced mobile services, supported by mobile and fixed networks, which are increasingly packet-based."*

One of the key features of 4G is that: "*Enhanced peak data rates to support advanced services and applications (**100 Mbit/s for high and 1 Gbit/s for low mobility** were established as targets for research)*".

A summary of the detailed requirements from the M.2134 report are enumerated below.

1. Minimum requirements of "Cell spectral efficiency" are listed in the table below:

Test environment	Downlink (bit/s/Hz/cell)	Uplink (bit/s/Hz/cell)
Indoor	3	2.25
Microcellular	2.6	1.80
Base coverage urban	2.2	1.4
High speed	1.1	0.7

Table 1-1: Cell spectral efficiency

2. The minimum requirements for peak spectral efficiencies are as follows:

- Downlink peak spectral efficiency is 15 bit/s/Hz
- Uplink peak spectral efficiency is 6.75 bit/s/Hz.

For example in a 100 MHz bandwidth, the downlink peak data rate is 1500 Mbit/s, uplink is 675 Mbit/s.

3. The bandwidth must be scalable, up to and including 40 MHz.

4. Cell edge user spectral efficiency: The cell edge user spectral efficiency is defined as the 5% point of the cumulative distribution function (CDF) of the normalized user throughput

Test environment	Downlink (bit/s/Hz)	Uplink (bit/s/Hz)
Indoor	0.1	0.07
Microcellular	0.075	0.05
Base coverage urban	0.06	0.03
High speed	0.04	0.015

Table 1-2: Cell edge user spectral efficiency

5. Mobility: the classes of mobility are defined in the following categories:

– Stationary: 0 km/h

– Pedestrian: > 0 km/h to 10 km/h

– Vehicular: 10 to 120 km/h

– High speed vehicular: 120 to 350 km/h

	Test environments			
	Indoor	**Microcellular**	**Base coverage urban**	**High speed**
Mobility classes supported	Stationary, pedestrian	Stationary, pedestrian, Vehicular (up to 30 km/h)	Stationary, pedestrian, vehicular	High speed vehicular, vehicular

Table 1-3: Mobility classes

6. Handover interrupt time has been specified in the table below. It is defined as the time duration during which a user terminal cannot exchange user plane packets with any base station

Handover type	Interruption time (ms)
Intra-frequency	27.5
Inter-frequency – **within a spectrum band** – **between spectrum bands**	 40 60

Table 1-4: Handover interrupt time

7. The VoIP capacity, which is the number of VoIP (Voice over IP) calls in one sector per MHz bandwidth, is specified in the table below:

Test environment	Min VoIP capacity (Active users/sector/MHz)
Indoor	50
Microcellular	40
Base coverage urban	40
High speed	30

Table 1-5: Voice capacity

1.3. Development in 3GPP from 2G to 4G

To understand the advanced 4G mobile technology, it is necessary to review the development history of mobile technologies, specifically in the 3GPP evolution path.

The first generation (1G) of the mobile telephony was commercialized around 1980 in various countries with different kinds of technologies. These technologies were not internationally standardized and as a result, could not work together. All 1G networks used analog technology with poor call quality, low traffic capacity and bulky terminal. The number of subscribers in 1G networks therefore was small, and its services were limited to voice only.

Ten years later, the second generation (2G) was introduced firstly with **GSM** technology standardized by ETSI (European Telecommunications Standards Institute) in 1991 [9]. It was a significant evolution as it employed digital technology which could provide better voice call quality, efficient usage of radio frequencies, and smaller user terminal. GSM is the most successful digital technologies to be deployed ever in human history since it is being used by billions of people around the world.

From a technology developed for voice services, **GSM** had been upgraded to a **GPRS/EDGE** (2.5G) network with a number of new network elements like PCU, SGSN and GGSN to support data services with slow data rate (around 14 – 171 kbps). Those technologies (GSM, GPRS and EDGE) are based on TDMA/FDMA radio access method with the basic idea that mobile users are allocated radio resources separated by time slot and frequency.

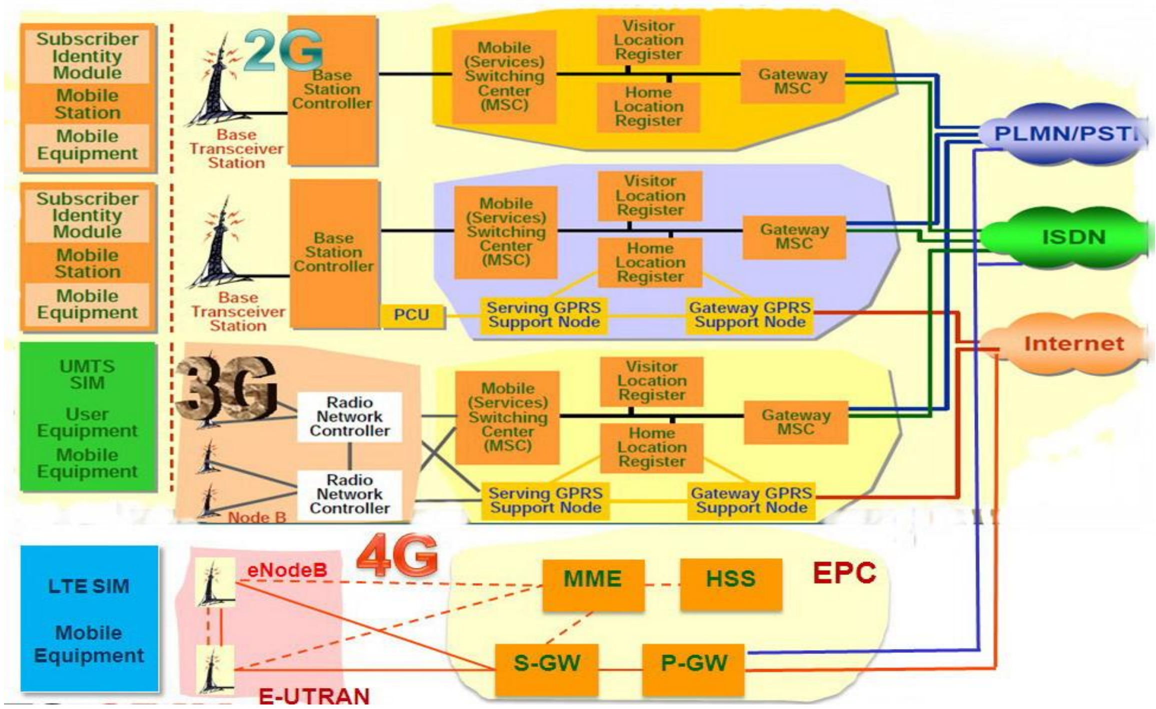

Figure 1-2: The transition from 2G to 4G in 3GPP family, adapted from [10]

The third generation (or 3G), also developed by ETSI, has further improved the mobile network performance in terms of the packet data rate as well as the system capacity. 3G employs new radio access method of CDMA where each user is distinguished by a unique code. This new radio interface operates concurrently with existing GSM in other frequency bands. It is supported by the new network elements called RNC and NodeB (Figure 1-2), which make the UTRAN network different from the RAN network in GSM that combines BSCs and BTSs although their main functions are similar. Technology in earliest stage of 3G is UMTS or **W-CDMA**, filed as Release (Rel)-99, launched in January 1998.

On December 1998, the 3GPP (3rd Generation Partnership Project) was formed by many partner organizations all over the world (no more limited within Europe researchers) to coordinate the research and development of GSM system. The task of developing GSM/UMTS was transferred from ETSI to 3GPP.

After minor changes in Release-4, Release-5 specification, frozen on June 2002 with the name **HSDPA** (High Speed Downlink Packet Access), has significantly increased the system throughput to 7.2 – 14.4 Mbps, thanks to the application of 16QAM modulation scheme, which means that one symbol contains 4 bits of information, or 2 to 4 times the data rate. This release also introduces the "IP everywhere" vision and IMS (IP Multimedia Subsystem) in the core network to control every multimedia service on the IP platform.

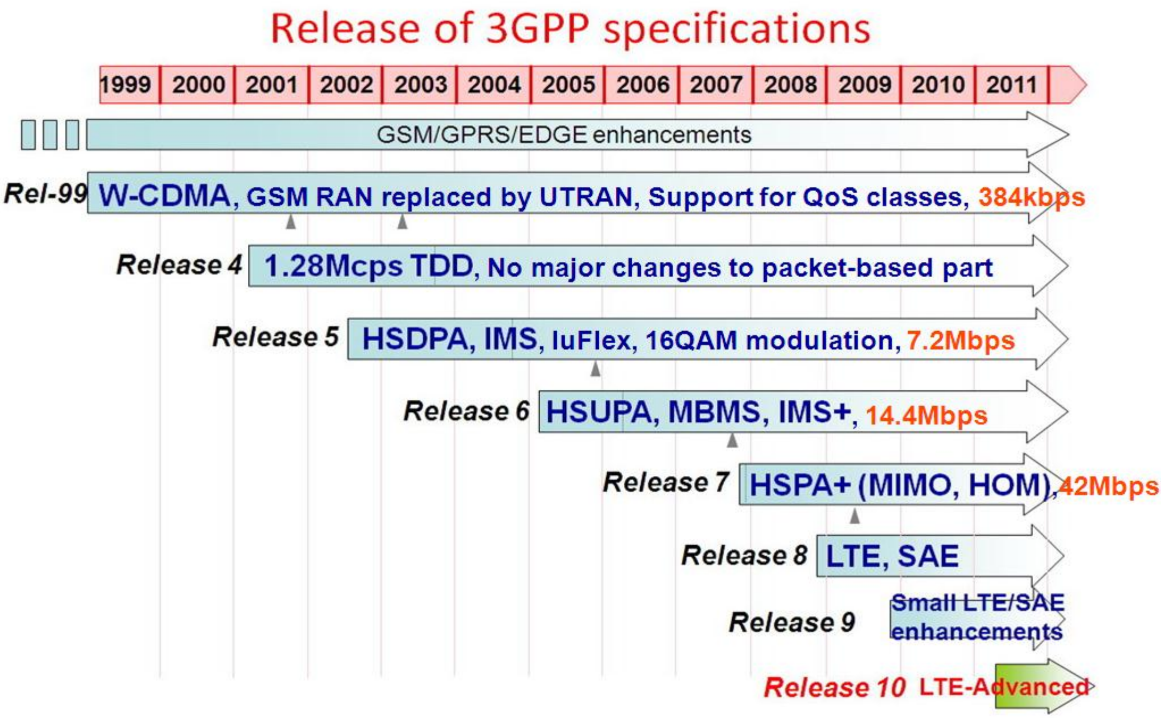

Figure 1-3: 3PPP standardization & its key evolutionary features, adapted from [11]

Release-6, also named **HSUPA** (High Speed Uplink Packet Access), was released on March 2005 and was designed to speed up the uplink data rate to 5.8 Mbps from 2 Mbps in Release-5. The main features in this release are MBMS (Multimedia Broadcast/Multicast Services) and HARQ (Hybrid Automatic Retransmission Request).

The next release Rel-7, was named Evolved HSPA or **HSPA+,** was completed on December 2007. It supports data rates up to 42 Mbps in the downlink, thanks to the implementation of MIMO (Multiple Input Multiple Output) and HOMs (Higher Order Modulations) up to 64QAM (6 bits/symbol).

The radio access technologies from Rel-99 to Rel-7 are all based on variants of CDMA and operate on the same frequency band, similar to previous technologies GSM, GPRS and EDGE working on the same frequency band with the same access method of TDMA/FDMA. At Rel-7, CDMA seemingly reached its maximum capacity and the mobile technology evolution path needed a new technology to support higher data rate and better performance. This is expected to be provided by OFDMA (Orthogonal Frequency Division Multiple Access), a new radio access method with many advantages over CDMA and TDMA/FDMA.

3GPP had completed the Rel-8 specifications in March of 2009, which defines a new OFDMA-based radio access technology known as **LTE** (Long Term Evolution) work item. This new OFDMA-based air interface, is also often referred to as the Evolved UMTS Terrestrial Radio Access (E-UTRA), again operates on new frequency band. E-UTRA does not have Base Station Controller (BSC or RNC), and instead of NodeB the base-station in LTE is known as eNodeB. Core network also is migrated to total new structure which is flat IP-based all-packet network (SAE/EPC). One again, a totally new radio interface has been added to 3GPP family to support the new evolution in wireless network, apart from TDMA/FDMA in 2G, CDMA in 3G. The 3GPP devices, up to this stage, will run on three modes with three frequency spectrum and three radio interfaces (TDMA/FDMA, CDMA and OFDMA).

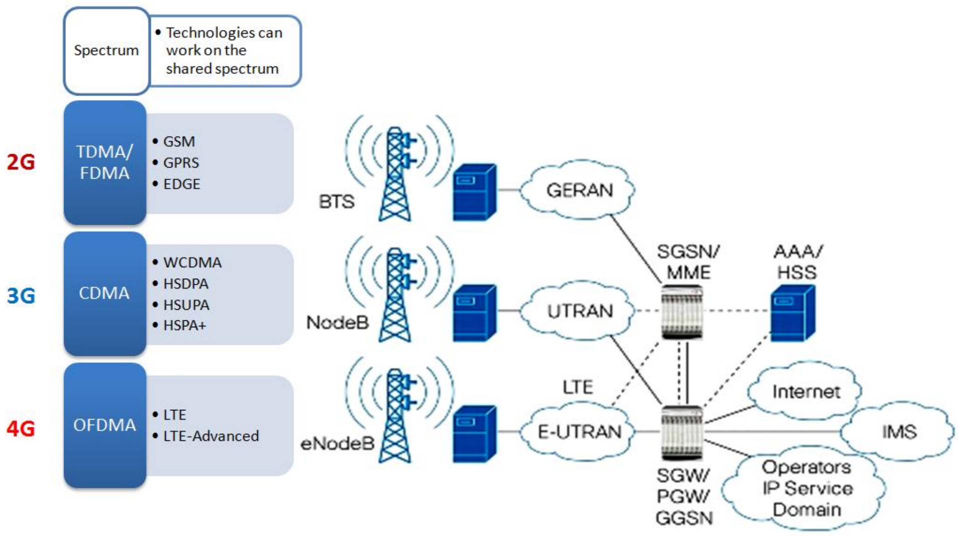

Figure 1-4: The spectrum of three radio interfaces with its technologies, adapted from [12]

Rel-9 was completed in March 2010 and it has added new features and functionalities for performance enhancements to both HSPA+ and LTE. For HSPA, additional multicarrier and MIMO options are introduced. For LTE, additional features and enhancements to support emergency services, location services and broadcast services are the focus.

While work for Rel-9 was being completed, significant progress has already been made by 3GPP in regards to Rel-10. In fact, 3GPP has already submitted proposals for the IMT-Advanced evaluation and certification process led by the ITU. A study item in 3GPP, called **LTE-Advanced**, evaluated and selected technology enhancements to LTE that meet the requirements of IMT-Advanced (4G) and was submitted to the ITU for consideration and approval in October 2009 [13]. Later on, as mentioned in previous section, LTE-Advanced was approved by ITU as true 4G on October 2010.

The evolution of 3GPP will continue in the coming years with further enhancements to LTE-Advanced, SAE in Rel-11 (planned to be frozen in 9/2012) and so forth.

1.4. LTE-Advanced

LTE-Advanced is an upgraded version of LTE Rel-8 and backward compatible with LTE Rel-8 in the sense that a LTE terminal can work in a LTE-Advanced network and LTE-Advanced terminal can work in a LTE network [11].

According to recent reports [7] from 3GPP, LTE-Advanced has been evaluated and compared with LTE Rel-8 and IMT-Advanced requirements. The results in the table below have confirmed that LTE-Advanced meet and exceed all requirements of IMT-Advanced.

		LTE Rel-8	LTE-Advanced	IMT-Advanced Requirement
Peak data rate	DL	300 Mbps	1 Gbps	1 Gbps
	UL	75 Mbps	500 Mbps	
Peak spectrum efficiency [bps/Hz]	DL	15	30	15
	UL	3.75	15	6.75
Capacity [bps/Hz/cell]	DL (4x2)	1.87	2.6	2.2
	UL (2x4)	-	2.0	1.4
Cell-edge user spectrum efficiency [bps/Hz/cell/user]	DL (4x2)	0.06	0.09	0.06
	UL (2x4)	-	0.07	0.03

Table 1-6: LTE-Advanced performance

For example, with the peak spectrum efficiency of 30 bps/Hz, the LTE-Advance peak data rate in a 100 MHz bandwidth can reach as high as 3 Gbps. This far exceeds the requirement of IMT-Advanced. To get this achievement, LTE-Advanced has applied a number of new features such as support for wider bandwidth, advanced MIMO techniques, coordinated multipoint transmission and reception (CoMP) and relaying. All these features will be discussed in detail in the next chapter.

1.5. Radio Resource Management

For every telecommunication operator, the company who run the mobile network, resources to invest and expand its radio network are always finite, such as frequency bandwidth and capital. But the demand to provide the best service for customers with broad coverage, good quality, no black holes, variety of services, etc. is always pushing the telecom engineers to find better solutions with limited resources. There are four objectives that the network designers and RF (Radio Frequency) engineers are focusing:

- Capacity: how to support highest capacity such as number of subscribers, number of calls in busy hour, data throughput, etc.
- Coverage: provide the widest coverage area with the limited number of base stations.
- Efficiency: maximize the system efficiency with the limited resources such as radio frequency and equipment infrastructure.
- Quality: guarantee the best quality of services such as: least number of black holes, call drop rate, or the best call success rate.

These objectives are quite contradictory and compete with each other and it needs a considerable effort to design, plan, control and optimize a mobile network.

In beginning stage, it is the Radio Network Planning (RNP) task, which includes design, dimensioning, planning, etc. Later stage is Radio Resource Management (RRM). While radio network planning makes the network setup and run, RRM makes it optimize, as illustrated in the below figure.

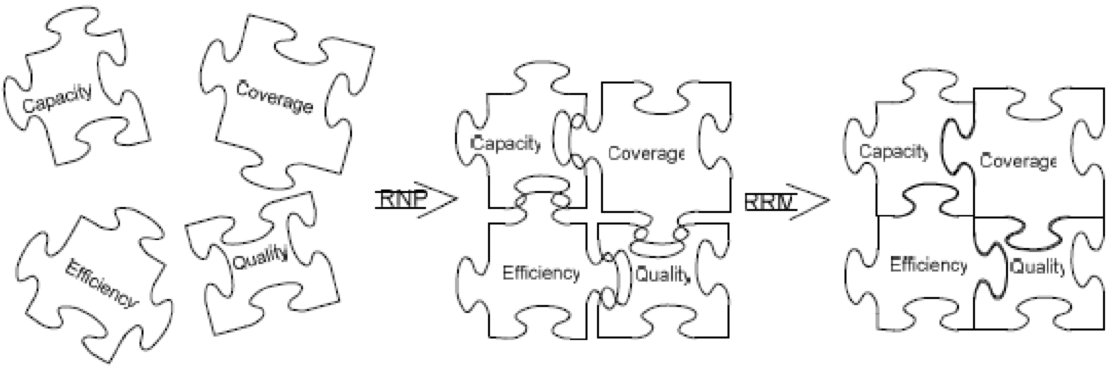

Figure 1-5: Radio Network Planing & Radio Resources Management [14]

Radio Resource Management refers to a group of mechanisms:

- Radio Admission Control – Guarantee QoS and maximize system's throughput by controlling an admission of a new call.
- Power Control – Minimize the power levels and provide adequate quality of signals.
- Handover Control – Handle the mobility of UEs across cell boundaries.
- Congestion Control & Load Balancing – Ensure that system is not overloaded, especially when RRM mechanisms are not working properly.
- Packet Scheduling – Control the traffic size of each user and allocate suitable radio resources to a user based on its radio condition & other's in the same cell.

The job of optimization engineers as well as telecom researchers is to find the best method/algorithm and optimized parameters for these mechanisms. Within this project, we focus on the packet scheduling mechanism.

1.6. Research question and objectives

Among the RRM mechanisms, packet scheduling is the most interesting subject to analyze since there are many papers about it. From cdma2000, W-CDMA, HSDPA, to LTE, each technology has received a large number of algorithm proposals. It is because this mechanism is not specified by 3GPP/3GPP2 specification and is open for the infrastructure vendors to develop a suitable algorithm. It is also because each proposed algorithm has its own pros and cons, in other words, the improvement of some performance criteria degrades others. Depending on the technology, network status or traffic patterns, each network should apply a suitable packet scheduling algorithm. In addition to the fact that LTE-Advanced technology is new and the standards development was frozen recently, the work of finding the best algorithm for LTE-A is quite challenging and interesting.

Correspondingly, the research questions that this project is trying to answer are:

- How to create a new computer simulation tool to model and simulate the LTE-Advanced system?

- How to design a new packet scheduling algorithm that can efficiently utilize all radio resources while guaranteeing fairness and QoS requirements of every user, both LTE and LTE-Advanced, in the downlink LTE-Advanced system?

The overall goal of the research is to develop and evaluate a set of advanced packet scheduling algorithms for LTE-Advanced.

The objectives of this project are as follows:

- To develop a modulation tool to model the LTE-Advanced technology
- To model, simulate, validate, and evaluate current well known and the new packet scheduling techniques for LTE-Advanced.
- To identify the suitability of various packet scheduling algorithms.
- To develop new packet scheduling algorithms and compare it with the simulated results.

1.7. Research signification

Demand for radio spectrum in future wireless network will be very expensive and competitive. The future mobile technologies like LTE-Advanced will also play an essential role in every aspect of our life, in government, business, entertainment, and personal communication. Advanced techniques that can improve the usage of these precious radio resources are significant. The models, tools, algorithms, protocols and framework which were developed in this research project will lead to efficient management of the LTE-Advanced networks. The applications of the outcomes of this project will optimize the usage of limited radio spectrum in the mobile networks and also considerably influence the investment required for radio spectrum. The better quality of service will be delivered using less radio resources and consequently at a lower price to the customer.

Moreover, Australian government has deployed the biggest ever telecommunication project. It's National Broadband Network – NBN, with $43 billion investments on a nationwide high-speed broadband network throughout Australia [15]. For the remote area or 7% of this network, LTE has been considered as an alternative solution [16] for FTTN (Fiber to the Node) technology which runs on the fiber optic. When LTE-Advanced is commercially available, the percentage of wireless LTE users using NBN services may increase since it reduces the deployment cost considerably while still maintaining the high data rate for the end-customers. Therefore, any research on LTE and LTE-Advanced to enhance its capacity and efficiency is important for the development of Australian telecom industry as well as the global industry.

1.8. Research Methodology and Plan

This research adopts a research methodology that combines hypothesis-based theory building in combination with empirical evaluation and refinement of the candidate models and algorithms on a LTE-Advanced packet scheduling simulator. The project builds on the know-how and experience gained from Dr. Sandrasegaran's current research team working in the areas of packet scheduling, link adaptation and handovers in LTE and LTE-Advanced as well as knowledge from a number of related engineering subjects and disciplines undertaken by the candidate.

The steps taken for the completion of this research work are:

1. Develop a comprehensive understanding of the LTE-Advanced network and to undertake a comprehensive survey of packet scheduling algorithms in LTE-A.

2. Analyse the current LTE simulation code, modify and develop the code to model the LTE-Advanced technology.

3. Model, simulate, and validate the performance of well known packet scheduling algorithms in LTE-Advanced.

3. Compare and contrast the performance of various PS algorithms under various radio propagation, user mobility, and user traffic conditions.

4. Develop new PS algorithms and obtain theoretical performance of these algorithms.

5. Document the project and the results of the project and present the results in a professional manner.

1.9. Publications

For this research degree, I have three papers published in conferences, one journal paper and one article in telecom magazine about LTE-Advanced, 4G and packet scheduling. Title and abstract of these papers are:

1. Nguyen, S.C., Sandrasegaran, K., and Madani, F.M.J, "***Modeling and Simulation of Packet Scheduling in the Downlink LTE-Advanced***", The 17th Asia-Pacific Conference on Communications (APCC 2011), 2-5 October, 2011, Kota Kinabalu, Malaysia.

Abstract - LTE-Advanced, the true 4G technology of the 3GPP family, is a complex radio access technology with co-existence of many types of user equipments. As it is a new technology, there are few published research focusing on modeling and simulation of the LTE-Advanced system. A simulation tool is indispensable for the research relating to the Radio Resource Management mechanisms such as packet scheduling. This paper presents detailed descriptions of a computer simulation tool that can effectively model packet scheduling, as well as the simulation results.

2. Nguyen, S.C., and Sandrasegaran, K., "***Design Considerations for Packet Scheduling Simulation from LTE to LTE-Advanced***", The 2010 International Conference on Communication and Vehicular Technology (ICCVT 2010), 30-31 December, 2010, Hanoi, Vietnam.

Abstract – LTE-Advanced, 3GPP's proposal for IMT-Advanced or 4G, is quite complex network with co-existence of many types of user equipments in terms of radio access technology. Our current research projects have focused on LTE and we are in the process of upgrading simulation tools from LTE to LTE-Advanced. This paper discusses the design considerations to extend an existing LTE-based Packet Scheduling simulation tool to LTE-Advanced. The modifications are presented in detail to develop a new LTE-Advanced Packet Scheduling Simulator.

3. Nguyen, S.C., and Sandrasegaran, K., "***Adaptations of Proportional Fair Algorithm for Packet Scheduling in LTE-Advanced***", The 2010 International Conference on Communication and Vehicular Technology (ICCVT 2010), 30-31 December, 2010, Hanoi, Vietnam.

Abstract – 3GPP has proposed LTE-Advanced as its 4G technology with many new features supplementing the current LTE technology. These new techniques lead to the demand of new Packet Scheduling Algorithms to distribute packets optimally from eNodeB to mobile stations in LTE-Advanced network. This paper presents the survey of these new algorithms that have been proposed, studies how the most well-known algorithm–proportional fair– has been propositionally modified, and discusses the new challenges for scheduling task in the downlink of LTE-Advanced system.

4. Nguyen, S.C., and Sandrasegaran, K., "***Optimized Proportional Fair Algorithm for LTE-Advanced System with Multiple Component Carriers***", IET Communications, Waiting for approval.

Abstract – LTE-Advanced, the true 4G technology of the 3GPP family, has a new feature that aggregates multiple LTE carriers so that users can be served on multiple component carriers. This characteristic plays an important role to increase the data rate multiple times for LTE-Advanced users with its corresponding multiple component carriers. However, the current proposed packet scheduling algorithms ignore this effect in the effort of providing new solution that increases system performance. The modified proportional fair algorithm proposed by this paper can provide optimized algorithm for packet scheduling mechanism in LTE-Advanced system as well as other technologies that use multiple carriers.

One feature in Vietnamese magazine:

5. "***What is 4G***?" for eChip Mobile magazine, published in 8 September, 2010

CHAPTER 2: LITERATURE REVIEW

2.1. LTE Technology Review

LTE-Advanced is an enhanced version of LTE in the sense that it uses the network architecture and radio interfaces of LTE as the foundation, and adds more features to boost the system performance. Therefore, it is necessary to understand the LTE technology before discussing about LTE-Advanced.

From an architecture point of view, LTE Rel-8 is a major development in radio access network (RAN) of 3GPP families to date. In previous technologies, the RNC controls the base stations and plays an intermediate role in connecting base stations (NodeB) to the core network. But in LTE Rel-8, this network element does not exist; instead the evolved NodeB (eNodeB) is connected directly to the core network (MME/UPE), as shown in Figure 2-1. The functions of the removed RNC are split between the remaining parts, the eNodeB and the core network. Most of these functionalities were inherited by eNodeB, such as radio resource management mechanisms. The eNodeB will have more tasks to do but the architecture of LTE is neater, as the number of nodes is minimized. [17]

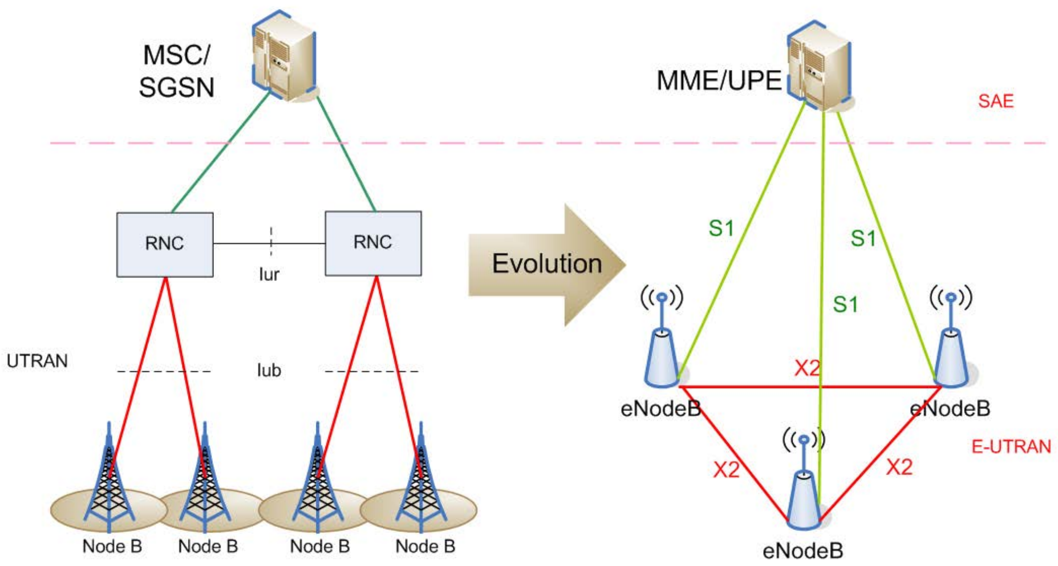

Figure 2-1: The evolution in the Radio Access Network from 3G to LTE

In the radio interface, LTE employs Orthogonal Frequency Division Multiple Access (OFDMA) in the downlink and Single Carrier Frequency Division Multiple Access (SC-FDMA, or DFTS-OFDM) in the uplink (Figure 2-2). The basic concept of OFDMA is that the system bandwidth is divided into multiple narrowband orthogonal sub-carriers with equal frequency spacing, so that at a sampling point of a single sub-carrier, all the other sub-carriers have zero crossing. In other words, the signal in each sub-carrier doesn't affect the others; as illustrated in Figure 2-3 all signals in all colors (red, green, yellow, etc) can be transmitted independently although their spectra are close together.

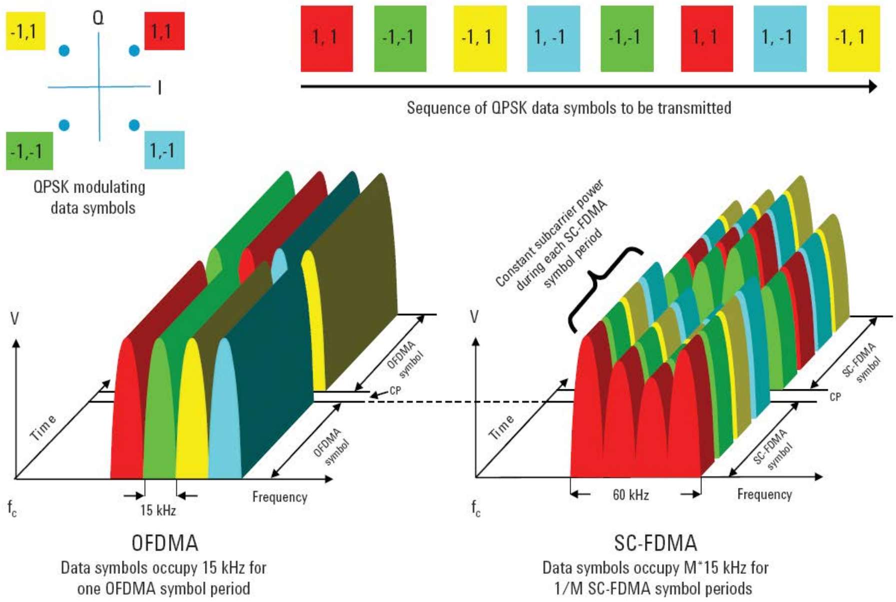

Figure 2-2: Radio interfaces in the downlink and uplink of LTE [18]

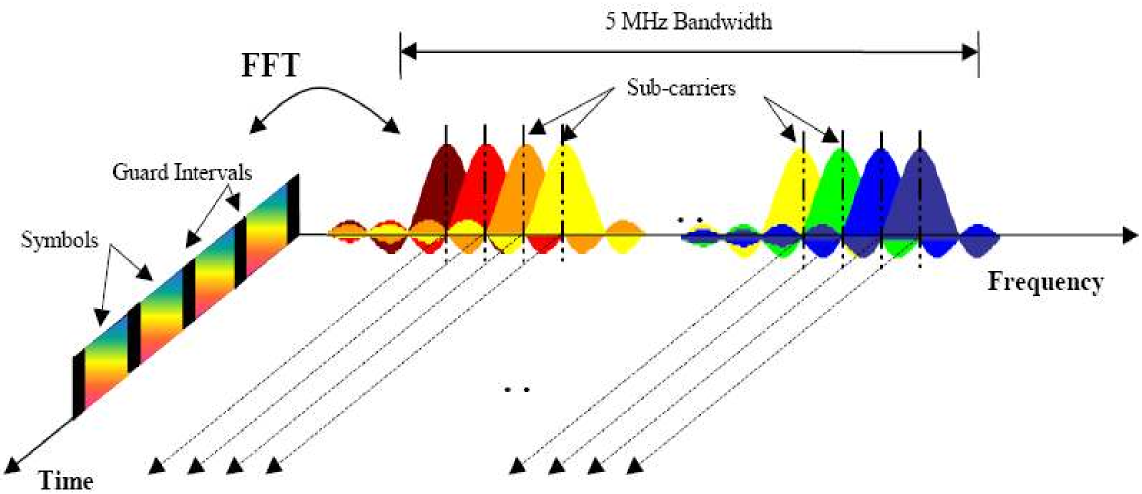

Figure 2-3: Maintaining the Subcarriers' Orthogonality [18]

Each OFDM symbol is transmitted on a particular radio resource element, whose bandwidth is 15 KHz and lasts for 0.07 (0.5/7) ms. The combination of 84 adjacent resource elements, which is composed of 12 sub-carriers and 7 time-slots or 180 KHz x 0.5 ms (Figure 2-4), forms a radio **resource block** (RB), which is the basic unit for all LTE radio resource activities and functionalities.

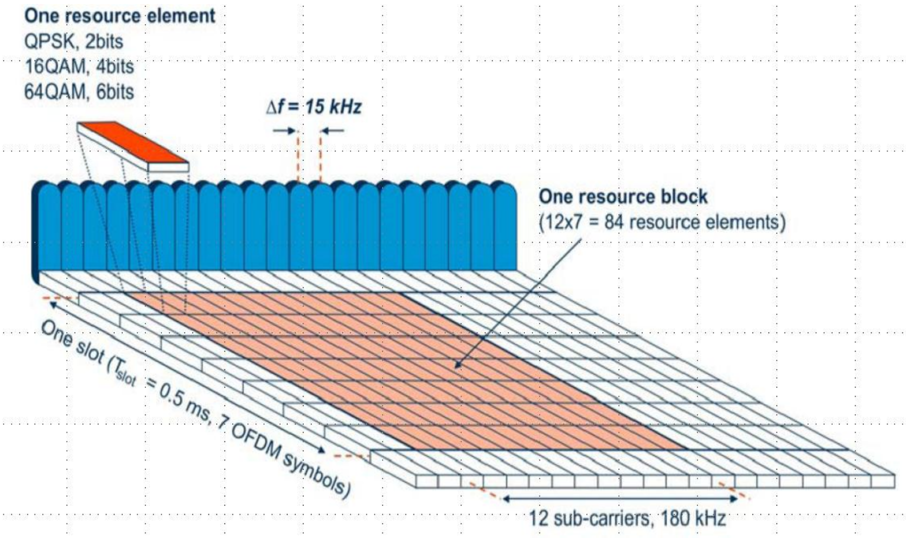

Figure 2-4: Radio Resource Block (RB) component [19]

From this basic radio resource unit, LTE can form a system bandwidth of variable size, from 1.4 MHz with 6 RBs to 20 MHz with 100 RBs as shown in the Figure 2-5. This feature is called scalable bandwidth (unlike UMTS/HSPA, which has a fixed 5 MHz bandwidth).

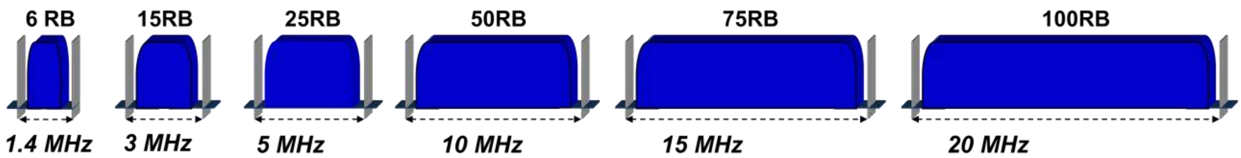

Figure 2-5: The LTE scalable bandwidths

LTE applies three modulation schemes: QPSK (4QAM), 16QAM, and 64QAM, corresponding to 2 bits, 4 bits and 6 bits per symbol. Depending on the channel conditions, a mobile station or eNodeB will adjust the selection of modulation and channel coding schemes (MCS). If the channel quality is good, it will use the best MCS to transmit at the highest data rate. This feature is called as link adaptation.

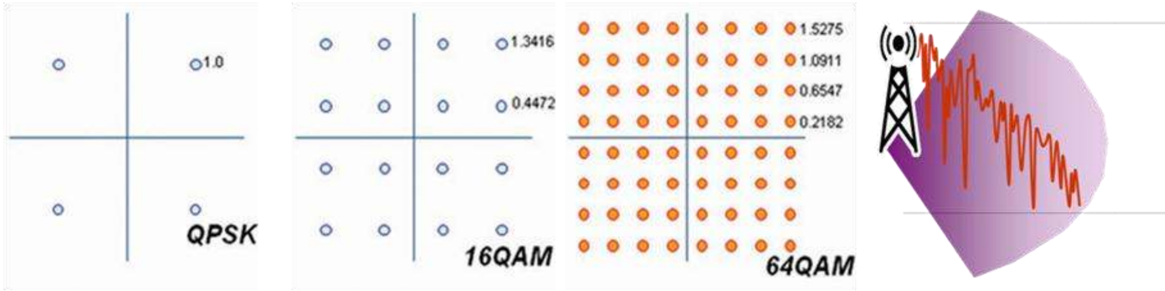

Figure 2-6: Modulation scheme & Link adaptation

A number of reference signals are inserted into the OFDM frequency-time domain signal to aid in the downlink channel estimation. There are four reference signals (R) within an RB (using the normal cycling prefix) available to be used in the downlink channel estimation as shown in the Figure 2-7.

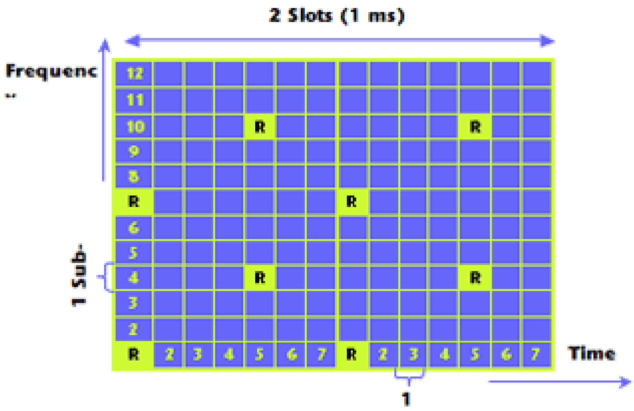

Figure 2-7: Reference signals mapping [20]

LTE can operate in a different spectrum using technology that supports FDD and TDD, which means uplink and downlink can be separated by frequency or by time domain.

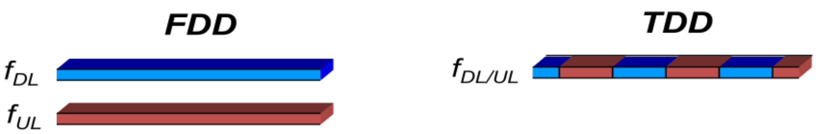

Figure 2-8: FDD & TDD in LTE

As introduced in Rel-7, 3GPP also adopts MIMO (Multi-Input Multi-Output) in LTE. This is a new advanced technique that employs multiple antennas at transmitter (network) and receiver (terminal) side to transmit simultaneously multiple data streams over a single radio link. For instance, a 2x2 MIMO configuration means 2 transmit antennas at the base station and 2 receive antennas at the mobile station. Depending on the channel condition, one of two MIMO schemes is chosen: spatial multiplexing or transmit diversity.

Spatial multiplexing refers to the transmission of different streams (or layers) of data simultaneously on a resource block. These data streams can belong to one single user (single user MIMO/SU-MIMO) or to different users (multi user MIMO/MU-MIMO), as illustrated in Figure 2-9. While SU-MIMO significantly increases the peak data rates of one user over the same radio link, MU-MIMO helps to increase the system capacity.

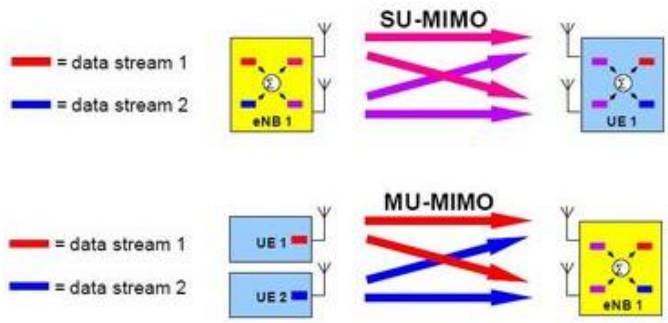

Figure 2-9: MIMO technology [21]

If the mobile radio channel is not allowed, MIMO can be switched to transmit diversity scheme. This mode is used to exploit diversity, which is already applied in WCDMA.
The basic characteristic of LTE can be summarized in Table 2-1, in comparison to other competitive technologies, 3GPP2 UMB and Mobile WiMAX.

	3GPP LTE	3GPP2 UMB	Mobile WiMAX
Channel bandwidth	1.4, 3, 5, 10, 15, and 20 MHz	1.25, 2.5, 5, 10, and 20 MHz	5, 7, 8.75, and 10 MHz
DL multiple access	OFDMA	OFDMA	OFDMA
UL multiple access	SC-FDMA	OFDMA and CDMA	OFDMA
Duplexing	FDD and TDD	FDD and TDD	TDD
Subcarrier mapping	Localized	Localized and distributed	Localized and distributed
Subcarrier hopping	Yes	Yes	Yes
Data modulation	QPSK, 16QAM, and 64QAM	QPSK, 8PSK, 16QAM, and 64QAM	QPSK, 16QAM, and 64QAM
Subcarrier spacing	15 kHz	9.6 kHz	10.94 kHz
FFT size (5 MHz)	512	512	512
Channel coding	Convolutional coding and turbo coding.	Convolutional coding, turbo coding, and LDPC coding	Convolutional coding and convolutional turbo coding. Block turbo coding and LDPC coding optional.
MIMO	Multi-layer precoded spatial multiplexing space-time/frequency block coding, switched transmit diversity, and cyclic delay diversity	Multi-layer precoded spatial multiplexing, space-time transmit diversity, spatial division multiple access, and beamforming.	Beamforming, Space-time coding, and spatial multiplexing

Table 2-1: LTE Characteristics [22]

2.2. Major characteristics of LTE-Advanced

LTE-Advanced (LTE-A) inherits all the features of LTE. It is also backward compatible with LTE. There are several key technical improvements of LTE-A as compared to LTE.

- **Support of wider bandwidth:** LTE-A aggregates multiple LTE carrier bandwidths (maximum 20 MHz each carrier) to form up to 100 MHz operating bandwidth. It is easy to observe that carrier aggregation is the most straightforward approach to accelerate the peak data rate to meet the requirements of IMT-Advanced.[23]

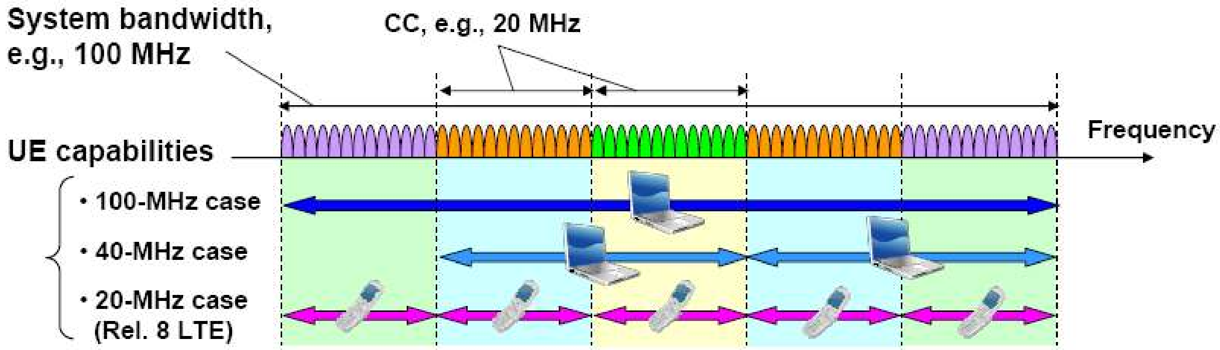

Figure 2-10: Wider bandwidth [11]

Each carrier is called component carrier (CC). In the case where these CCs are adjacent and symmetric to each other, this model is named as Carrier Aggregation (Figure 2-11). If these CCs are non-continuous and asymmetric, it is called Spectrum Aggregation [24]. The maximum number of CC is 5 [23]. This spectrum flexibility is very beneficial for a network provider as they can use all available spectrum they were assigned from government regulator for LTE-A.

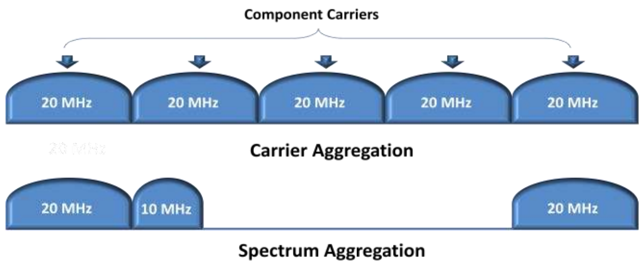

Figure 2-11: Supporting wider bandwidth with multiple component carriers feature

- **Asymmetric transmission bandwidth:** In the 3GPP family, up to LTE, equal bandwidths are specified for uplink and downlink for the FDD (Frequency Division Duplex) mode. But in LTE-Advanced, the bandwidth for the downlink can be different from the uplink due to the imbalance between download and upload traffic [25], as shown in Figure 2-12.

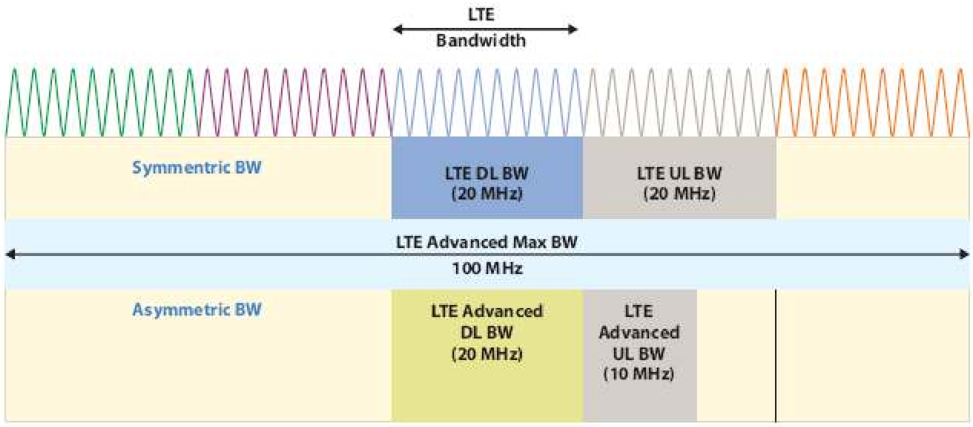

Figure 2-12: Asymmetric bandwidth of uplink and downlink [25]

- **Advanced MIMO technique:** From 4 layers (streams) in LTE spatial multiplexing, LTE-A extends to up to 8-layer transmission in downlink. Single-user MIMO up to 4 layers was also introduced in the uplink. In other words, it increases the spatial channels (streams) so that more data can be transmitted on a physical channel defined by time and frequency. Moreover, LTE-A will apply Multi-User (MU) MIMO techniques, upgrading from current Single-User (SU) MIMO. These mechanisms greatly improve the peak spectrum efficiency, system data rate, capacity, and cell-edge user throughput.[23]

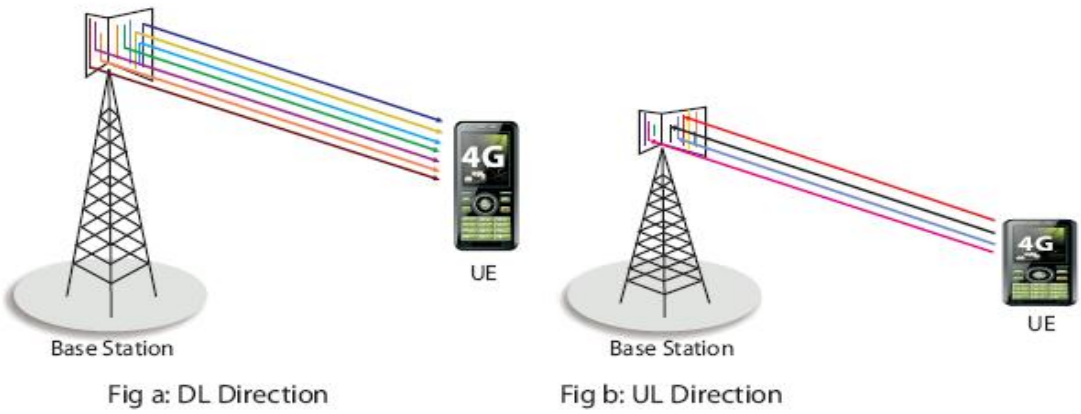

Figure 2-13: Advanced MIMO techniques [25]

- **Coordinated multipoint transmission and reception (CoMP)**: This mechanism refers to data that can be transmitted and received from multiple coordinated cells to and from UEs to help increase user throughput and extend the cell coverage. It is divided by two types, Coordinated Scheduling/Beamforming (CS/CB) and Joint Processing (JP) [11].
  For CS/CB, the transmission to a single UE is transmitted from the serving cell, exactly as in the case of non-CoMP transmission. However, the scheduling, including any

beamforming functionality, is dynamically coordinated between the cells in order to control and/or reduce the interference between different transmissions. In principle, the best serving set of users will be selected so that the transmitter beams are constructed to reduce the interference to other neighbouring users, while increasing the served user's signal strength.

With joint processing, the transmission to a single UE is simultaneously transmitted from multiple transmission points, across cell sites. The multi-point transmissions will be coordinated as a single transmitter with antennas that are geographically separated. This function helps LTE-A increase cell-edge user throughput, expand the coverage, and accelerate the deployment flexibility.

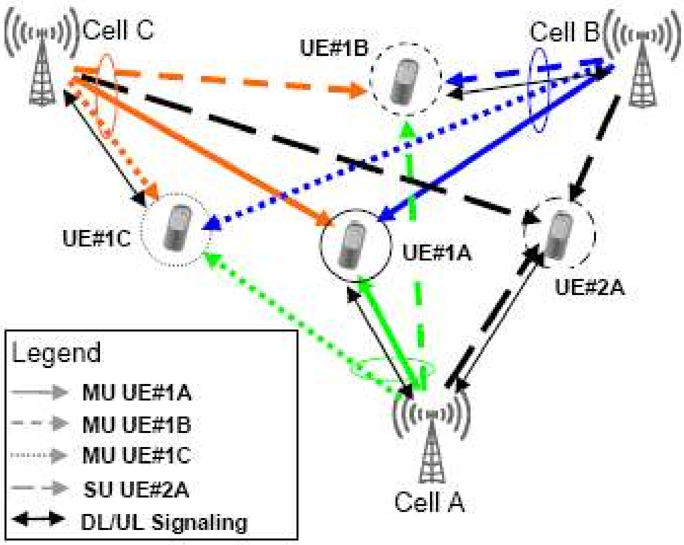

Figure 2-14: Cooperative MultiPoint techniques [26]

- **Relaying**: In LTE-A architecture, there is one new network element called Relay Node (RN) which receives signal from eNodeB and re-transmits it to create a new coverage area. The link from eNodeB to RN is named backhaul link and from RN to UE is named access link. The backhaul link could be in-band or out-band with the operating frequency band or access link. Basically, there are two types of RN, Type 1 operates as a separate cell while Type 2 is transparent to UEs [27]. Users under RN will have more processing delay to eNodeB.

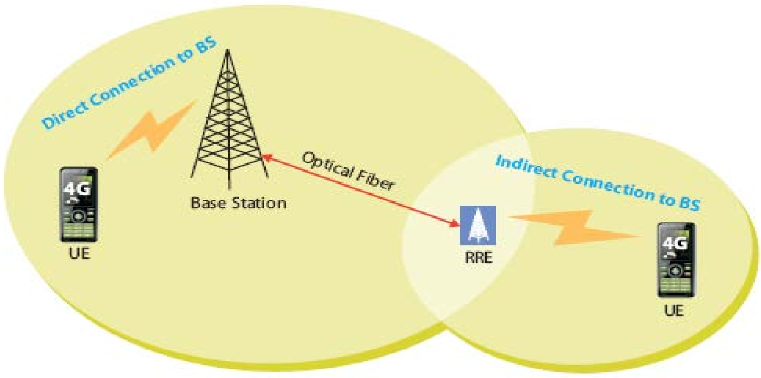

Figure 2-15: Relaying function [25]

Table 2-2 summarizes all new characteristics of LTE-A and compares it to LTE:

Technology	LTE	LTE--A
Peak data rate Down Link (DL)	150 Mbps	1 Gbps
Peak data rate Up Link (UL)	75 Mbps	500 Mbps
Transmission bandwidth DL	20MHz	100 MHz
Transmission bandwidth UL	20MHz	40 MHz (requirements as defined by ITU)
Mobility	Optimized for low speeds(<15 km/hr) High Performance At speeds up to 120 km/hr Maintain Links at speeds up to 350 km/hr	Same as that in LTE
Coverage	Full performance up to 5 km	a) Same as LTE requirement b) Should be optimized or deployment in local areas/micro cell environments.
Scalable Band Widths	1.3,3, 5, 10, and 20 MHz	Up to 20–100 MHz
Capacity	200 active users per cell in 5 MHz.	3 times higher than that in LTE
Bandwidth	Symmetric	Asymmetric
MIMO	Downlink: 2x2, 4x2, 4x4 Uplink: 1x2, 1x4	DL: Up to 8x8 UL: Up to 4x4
Coordinate MultiPoint	No	Yes
Relaying	No	Yes

Table 2-2: LTE vs. LTE-Advanced [25]

2.3. Packet Scheduling

In LTE and LTE-Advanced, with the removal of Radio Network Controller (RNC), all RRM functions including Packet Scheduling are conducted by eNodeB. Scheduling in the downlink LTE system is performed at 1 ms interval (as known as Transmit Time Interval, TTI) which consists of 2 time slots, or resource-block-pair basis (RB, one subframe of 0.5ms over 180 kHz). Within this TTI, two consecutive RBs are assigned to a user. [28]

In each TTI, each user computes its received signal strength or signal to interference plus noise ratio (SINR) on the reference signals received from the serving eNodeB. The computed SINR values of each user vary on each sub-carrier and at each TTI due to the frequency-selective fading nature of multi-path propagation and the time-selective fading nature due to the user movement. Once the effective SINR values in each RB are determined, each user reports these values to the serving eNodeB in each TTI.

The received effective SINR values of each user in each RB are used by the serving eNodeB to determine the modulation and coding scheme (MCS) to be used for downlink packet transmission. Thereafter, the data rate (which is the number of bits that a user can support in two consecutive RBs in a TTI) is computed based on the determined modulation and coding scheme. The downlink LTE system uses QPSK, 16QAM and 64QAM together with channel coding to provide support for high data rates. Besides being used to determine the number of bits that a user can support in two consecutive RBs in each TTI, the effective SINR value is used to determine a user's priority in channel-dependent scheduling, as discussed later.

At eNodeB, the packet scheduler assigns a buffer for each user. Packets that arrive into the buffer are time stamped and queued for transmission on a First-in-First-out (FIFO) basis. For each packet in the queue at the eNodeB buffer, the Head of Line (HOL) packet delay which is the time difference between the current time and the arrival time of a packet is computed. Different delay deadlines are assigned to packets of different services and a user is usually assumed to be either real-time (RT) or non real-time (NRT) services. If the HOL packet delay exceeds the delay deadline, the packet is discarded.

The packet scheduler determines a user's priority based on a packet scheduling algorithm. These algorithms use scheduling criteria when making scheduling decisions. Once a user has been selected for transmission, the number of bits (packet sizes) to be transmitted is based on the user's reported SINR value.

Figure 2-16 shows a generalized model of packet scheduling in the downlink LTE system that consists of N RBs and K users.

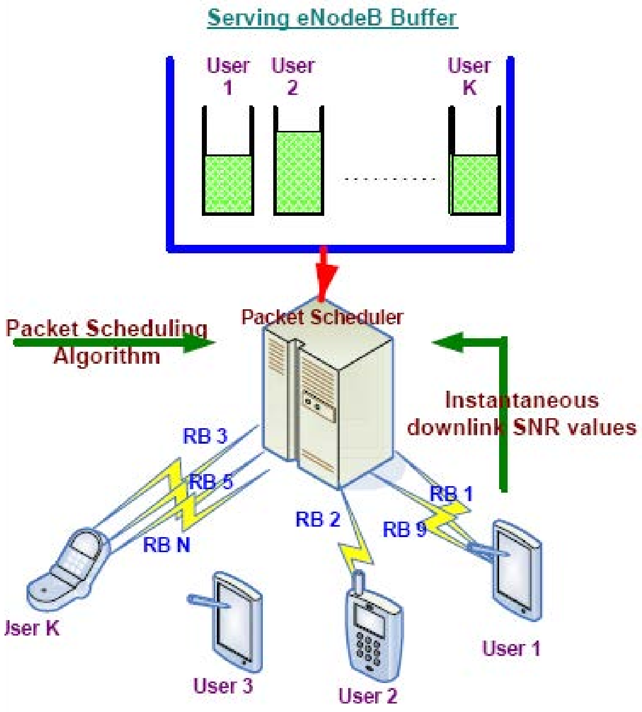

Figure 2-16: Packet scheduling operation [29]

2.3.1. Packet Scheduling Algorithms

There are many packet scheduling algorithms for real-time services (conversational, streaming) and non-real time services (interactive, background) in wireless systems. The table below shows some of the widely accepted packet scheduling algorithms in wireless systems.

Aspects	WCDMA	HSDPA	LTE
Function allocation	RNC	Node B	eNode B
Scheduling speed	TTI=10ms; High RRT and channel setup time consumption	TTI=2ms; Fast scheduling	TTI=1ms; Dynamic scheduling
Scheduling controller	MAC-c in RNC	MAC-hs in Node B	MAC of Control-plane in eNode B

Scheduling mechanism	User-Specific PS; Cell-specific PS;	Based on favourable channel condition of user	Frequency-Time based; OFDMA based;
Scheduling algorithms	Maintaining capacity for existing user while dividing remaining capacity into new arrivals	-Round Robin (*RR*) scheduler; -*Maximum C/I* scheduler; -Proportional Fair (*PF*) algorithm;	-Request Activity Detection (*RAD*) scheduler and PF scheduler; -OFDMA scheduling; -*Max-Max* with *OFDM PF*

Table 2-3: Packet scheduling in wireless technologies [14]

Several well known and recently proposed PS algorithms will be described in the following paragraphs.

A. Round Robin (RR)

The Round Robin (RR) algorithm [30] assigns equal portions of packet transmission time to each user in a circular order.

RR algorithm achieves the best fairness performance if the users have similar channel conditions and similar sized packet arriving at their buffers. Since RR algorithm does not take the channel conditions for each user into consideration, it may have a comparatively worst throughput performance comparing to other algorithms.

B. First-in-First-out (FIFO)

The First-In-First-Out (FIFO) algorithm [31] gives transmission priority to the user with the highest HOL packet delay at each time slot.

Similar to RR algorithm, FIFO algorithm has a good fairness performance but a low throughput performance.

C. Maximum Rate (Max Rate)

The Maximum Rate (Max Rate) algorithm [30] transmit the packets of the user with highest achievable data rate, as given in (2-1).

$$M = \arg\max r_i(t) \tag{2-1}$$

where $r_i(t)$ is the instantaneous achievable data rate of user i at time t which depends on the reported SINR value. The higher the SINR, the higher the $r_i(t)$.

Max Rate algorithm maximizes the system throughput since it always select(s) user(s) with the best channel condition(s). On the contrary, users with low SINR values might never be selected for transmission, which leads to the poor fairness performance of Max Rate algorithm.

D. Proportional Fair (PF)

Proportional Fair (PF) algorithm [32] was proposed to provide a balanced performance between the fairness and system throughput. The scheduling metric *M* is defined as

$$M = \arg\max \frac{r_i(t)}{R_i(t)} \tag{2-2}$$

and

$$R_i(t) = (1 - \frac{1}{t_c}) * R_i(t-1) + \frac{1}{t_c} * r_i(t-1) \tag{2-3}$$

where $r_i(t)$ is the instantaneous achievable data rate and $R_i(t)$ is the average data rate of user *i* at time *t*. Parameter t_c is the update window size (the number of previous slots that its correspondent data rate were calculated for average value) and controls the latency of the system.

As the PF algorithm incorporates the feasible data rate with the average throughput, it achieves a good throughput and fairness performance.

E. Modified-Largest Weighted Delay First (M-LWDF)

The Modified-Largest Weighted Delay First (M-LWDF) algorithm [33] is proposed to support RT services. The scheduling criteria metric *M* is defined as follows:

$$M = \arg\max a_i W_i(t) \frac{r_i(t)}{R_i(t)} \tag{2-4}$$

with

$$a_i = -\frac{(\log \delta_i)}{\tau_i} \tag{2-5}$$

where $W_i(t)$ is the HOL packet delay of user *i* at time *t*, τ_i is the delay threshold of user *i* and δ_i denotes the maximum probability for HOL packet delay of user *i* to exceed the delay threshold of user *i*.

Since M-LWDF jointly considers HOL packet delay along with PF properties, it obtains a good throughput and fairness performance along with a relatively low PLR.

F. Exponential/Proportional Fair (EXP/PF)

The Exponential/Proportional Fair (EXP/PF) [34, 35] is designed to support multi-media applications with RT and NRT services concurrently. The scheduling criterion metric, *M*, for NRT and RT services of each user is defined as

$$M = \arg\max \begin{cases} \exp \dfrac{a_i W_i(t) - \overline{aW(t)}}{1 + \sqrt{\overline{aW(t)}}} \dfrac{r_i(t)}{R_i(t)} & i \in RT \\ \dfrac{w(t)}{P(t)} \dfrac{r_i(t)}{R_i(t)} & i \in NRT \end{cases} \tag{2-6}$$

and

$$\overline{aW(t)} = \frac{1}{N_{RT}} \sum_{i \in RT} a_i W_i(t) \tag{2-7}$$

$$w(t) = \begin{cases} w(t-1) - \varepsilon & W_{\max} > \tau_{\max} \\ w(t-1) + \dfrac{\varepsilon}{k} & W_{\max} < \tau_{\max} \end{cases} \tag{2-8}$$

where *P(t)* is the average number of waiting packets for all RT services at time t, ε and k are constant, and W_{max} and τ_{max} are the maximum HOL packet delay out of RT service users and maximum delay constraint of all RT service users, respectively.

The EXP/PF algorithm gives a higher priority to the RT service users whose packets are approaching the transmission deadline than NRT service users.

2.4. Theoretical Throughput Analysis of Packet Scheduling Algorithms

In [36], the thesis presented a mathematical analysis for throughput of two PS algorithms, PF and M-LWDF in the downlink of LTE system. Based on the step-by-step derivations, it explained how to obtain the mathematical expressions of the expected throughput for PF algorithm and M-LWDF algorithm. This section has been added to this thesis to demonstrate the complexity and the assumptions needed to derive a mathematical result for performance analysis of LTE. It also justify simulation as the best method of performance analysis for LTE-A. It is important to note that this section is not claimed as a thesis contribution.

2.4.1. Theoretical Throughput Analysis of PF Algorithm

Consider a scenario in which *K* users are competing for the data transmission from one base station over Rayleigh fading channel. The proportional fair (PF) algorithm, as described in Section 2.3.1, is adopted by the base station. The theoretical throughput analysis of this system has been discussed in [37-40].

The instantaneous achievable data rate of user *i* at time *t+1* is denoted by $r_i(t+1)$. The *k*-point moving average throughput of user *i* up to time *t* is given by $R_i(t)$, which is defined as the average throughput of user *i* in the last *k* time slots. The moving average throughput of user *i* up to time *t+1* can be updated by

$$R_i(t+1) = (1-\frac{1}{k}) * R_i(t) + \frac{r_i(t+1)}{k} * I_i(t+1) \tag{2-9}$$

in which $I_i(t+1)$ is defined as the indicator function specifying whether user *i* is scheduled for transmission at time slot *t+1*.

$$I_i(t+1) = \begin{cases} 1, & user\ i\ scheduled\ in\ slot\ t+1 \\ 0, & else \end{cases} \tag{2-10}$$

There is a relationship between the SINR and the instantaneous achievable data rate *r(t)*. [41] states that in a Rayleigh fading environment, the achievable data rate could be approximated by a Gaussian distribution. For Single-Input-Single-Output (SISO) case, it reduces to

$$E[r] = \int_0^\infty \log(1+SINR\times\lambda)\times e^{-\lambda}d\lambda \tag{2-11}$$

and

$$\begin{aligned}\sigma_r^2 &= \int_0^\infty \log(1+SINR\times\lambda)^2\times e^{-\lambda}d\lambda \\ &-\left(\int_0^\infty \log(1+SINR\times\lambda)\times e^{-\lambda}d\lambda\right)^2\end{aligned} \tag{2-12}$$

where *E[r]* and σ_r are the mean value and the standard deviation of *r(t)*.

From (2-9), assuming wide-sense stationary $R_i(t)$, the expected value of the average throughput of user *i* up to time *t+1* is given as

$$
\begin{aligned}
&E[R_i(t+1)] = E[R_i(t)] \\
&= E[(1-\frac{1}{k})R_i(t) + I_i(t+1) \times \frac{r_i(t)}{k}] \\
&= (1-\frac{1}{k})E[R_i(t)] + \frac{1}{k}E[I_i(t+1) \times r_i(t)]
\end{aligned} \quad (2\text{-}13)
$$

Hence,

$$
E[R_i(t)] = E[I_i(t+1) \times r_i(t)] \quad (2\text{-}14)
$$

On substitution (2-10) to (2-14), we can obtain

$$
\begin{aligned}
&E[R_i(t)] = E[I_i(t+1) \times r_i(t)] \\
&= E\left[1 \times r_i(t+1) \middle| I_i(t+1) = 1\right] \times \Pr(I_i(t+1) = 1) \\
&+ E\left[0 \times r_i(t+1) \middle| I_i(t+1) = 0\right] \times \Pr(I_i(t+1) = 0) \\
&= E\left[1 \times r_i(t+1) \middle| I_i(t+1) = 1\right] \times \Pr(I_i(t+1) = 1)
\end{aligned} \quad (2\text{-}15)
$$

where $Pr(I_i(t+1)=1)$ is the probability that user i will be chosen for transmission at time $t+1$.

Applying Bayes's theorem, which is $P(a|b) \times P(b) = P(b|a) \times P(a)$, (2-15) can be written as

$$
\begin{aligned}
&E[R_i(t)] = \Pr(I_i(t+1) = 1) \times \int_0^\infty x f_{r_i}(x | I_i(t+1) = 1) dx \\
&= \int_0^\infty x f_{r_i}(x) \Pr(I_i(t+1) = 1 | r_i(t+1) = x) dx
\end{aligned} \quad (2\text{-}16)
$$

where $Pr(I_i(t+1)=1 | r_i(t+1)=x)$ is the conditional probability that user i will be scheduled to transmit at time $t+1$, if the instantaneous achievable date rate of user i at time $t+1$ is assigned with the value x and $f_{r_i}(\cdot)$ denotes the probability density function of r_i.

According to the scheduling criterion of PF algorithm given in (2-2), user i will be selected for transmission only if any other user j, $j \neq i$, has smaller value of the scheduling criterion than user i, which is $\frac{r_j(t+1)}{R_j(t+1)} < \frac{r_i(t+1)}{R_i(t+1)}$. It holds for large t, k that

$$\Pr(I_i(t+1)=1|r_i(t+1)=x)=\Pr(\forall j\neq i,\frac{r_j(t+1)}{R_j(t+1)}<\frac{r_i(t+1)}{R_i(t+1)}|r_i(t+1)=x)$$
$$=\prod_{j=1,j\neq i}^{K}F_{r_j}(R_j(t+1)\frac{x}{R_i(t+1)})\approx\prod_{j=1,j\neq i}^{K}F_{r_j}(\frac{E[R_j]}{E[R_i]}x) \tag{2-17}$$

in which $F_{r_i}(\cdot)$ is the accumulated distribution function of r_i.

For Gaussian distribution r_i as given in (2-11) and (2-12), applying (2-17) to (2-16) yields

$$E[R_i(t)]\approx\int_0^{\infty}xf_{r_i}(x)\prod_{j=1,j\neq i}^{K}F_{r_j}(\frac{E[R_j]}{E[R_i]}x)dx$$
$$=\int_{-\frac{E[r_i]}{\sigma_{r_i}}}^{\infty}(y\sigma_{r_i}+E[r_i])\frac{1}{\sqrt{2\pi}}e^{-\frac{y^2}{2}} \tag{2-18}$$
$$\times\prod_{j=1,j\neq i}^{K}F_{r_j}(\frac{E[R_j]}{E[R_i]}(y\sigma_{r_i}+E[r_i]))dy$$

For the instantaneous achievable data rate as described in (2-11) and (2-12), one can verify that

$$\begin{cases}E[r_i]>E[r_j]\ \ and\ \ \frac{E[r_i]}{\sigma_{r_i}}>\frac{E[r_j]}{\sigma_{r_j}}, & if\ \ \sigma_{r_i}>\sigma_{r_j}\\ E[r_i]>E[r_j], & if\ \ \sigma_{r_i}=\sigma_{r_j}\end{cases} \tag{2-19}$$

Using (2-19), we can prove [38]

$$\frac{E[R_i]E[r_j]-E[R_j]E[r_i]}{E[R_j]\sigma_{r_i}-E[R_i]\sigma_{r_j}}<0,\quad for\quad \sigma_{r_i}\neq\sigma_{r_j} \tag{2-20}$$

When all σ_{ri} *(i=1,2,…,K)* are equal, according to (2-19) all users have the same expected value of instantaneous data rate $E[r_i]$ *(i=1,2,…,K)*.

Since $F_{r_i}(x)=F_{(0,1)}((x-E[r_i])/\sigma_{r_i})$ for Gaussian r_i, where $F_{(0,1)}(.)$ denotes the standard normal distribution function with zero mean and unit variance, we have

$$E[R_i(t)] = \int_{-\frac{E[r_i]}{\sigma_{r_i}}}^{\infty} (y\sigma_{r_i} + E[r_i]) \frac{1}{\sqrt{2\pi}} e^{-\frac{y^2}{2}}$$
$$\times \prod_{j=1, j\neq i}^{K} F_{r_j}\left(\frac{E[R_j]}{E[R_i]}(y\sigma_{r_i} + E[r_i])\right)dy \qquad (Guess \frac{E[R_j]}{E[R_i]} = \frac{E[r_j]}{E[r_i]} = 1)$$
$$= \int_{-\frac{E[r_i]}{\sigma_{r_i}}}^{\infty} (y\sigma_{r_i} + E[r_i]) \frac{1}{\sqrt{2\pi}} e^{-\frac{y^2}{2}} \times (F_{r_j}(y\sigma_{r_i} + E[r_i]))^{K-1} dy$$
$$= \int_{-\frac{E[r_i]}{\sigma_{r_i}}}^{\infty} (y\sigma_{r_i} + E[r_i]) f_{(0,1)}(y) \times (F_{(0,1)}(y))^{K-1} dy \tag{2-21}$$

When not all σ_{ri} *(i=1,2,…,K)* are equal, denote $Z = \arg\max_j \frac{E[R_i]E[r_j] - E[R_j]E[r_i]}{E[R_j]\sigma_{r_i} - E[R_i]\sigma_{r_j}}$. Then it is can be proved that $Z \geq \arg\max_j \frac{E[R_i]E[r_j] - E[R_j]E[r_i]}{E[R_j]\sigma_{r_i} - E[R_i]\sigma_{r_j}} \geq -\frac{E[r_i]}{\sigma_{r_i}}$ and $Z \leq -\max_j[-\frac{E[r_j]}{\sigma_{r_j}}]$. So (2-18) can be written as

$$E[R_i(t)] = \int_{-\frac{E[r_i]}{\sigma_{r_i}}}^{z} (y\sigma_{r_i} + E[r_i]) \frac{1}{\sqrt{2\pi}} e^{-\frac{y^2}{2}}$$
$$\times \prod_{j=1, j\neq i}^{K} F_{r_j}\left(\frac{E[R_j]}{E[R_i]}(y\sigma_{r_i} + E[r_i])\right)dy$$
$$+ \int_{Z}^{\infty} (y\sigma_{r_i} + E[r_i]) \frac{1}{\sqrt{2\pi}} e^{-\frac{y^2}{2}}$$
$$\times \prod_{j=1, j\neq i}^{K} F_{r_j}\left(\frac{E[R_j]}{E[R_i]}(y\sigma_{r_i} + E[r_i])\right)dy \tag{2-22}$$

Since the first integral in the right hand side of (2-22) is not less than 0, we obtain

$$E[R_i(t)] \geq \int_{Z}^{\infty} (y\sigma_{r_i} + E[r_i]) \frac{1}{\sqrt{2\pi}} e^{-\frac{y^2}{2}}$$
$$\times \prod_{j=1, j\neq i}^{K} F_{r_j}\left(\frac{E[R_j]}{E[R_i]}(y\sigma_{r_i} + E[r_i])\right)dy \tag{2-23}$$

Using (2-20), we can obtain the following equation:

$$\frac{E[R_j]}{E[R_i]}(y\sigma_{r_i} + E[r_i]) > y\sigma_{r_j} + E[r_j]. \tag{2-24}$$

Applying (2-23) to (2-24), we then have

$$E[R_i(t)] \geq \int_Z^{\infty}(y\sigma_{r_i} + E[r_i])\frac{1}{\sqrt{2\pi}}e^{-\frac{y^2}{2}}$$
$$\times\prod_{j=1,j\neq i}^{K} F_{r_j}(\frac{E[R_j]}{E[R_i]}(y\sigma_{r_i} + E[r_i]))dy \tag{2-25}$$
$$= \int_Z^{\infty}(y\sigma_{r_i} + E[r_i])f_{(0,1)}(y)\times(F_{(0,1)}(y))^{K-1}dy$$
$$\geq \int_M^{\infty}(y\sigma_{r_i} + E[r_i])f_{(0,1)}(y)\times(F_{(0,1)}(y))^{K-1}dy$$

where M=-$argmax_j[E[r_j]/\sigma_{rj}]$ (j=1,2,…,K).

We express (2-21) and (2-25) by the same equation,

$$E[R_i(t)] \geq \int_M^{\infty}(y\sigma_{r_i} + E[r_i])f_{(0,1)}(y)\times(F_{(0,1)}(y))^{K-1}dy$$
$$= \frac{E[r_i]}{K} + \int_M^{\infty} y\sigma_{r_i}f_{(0,1)}(y)\times(F_{(0,1)}(y))^{K-1}dy$$
$$= \frac{E[r_i]}{K} + \int_M^{\infty} y\sigma_{r_i}\times\frac{1}{\sqrt{2\pi}}e^{-\frac{y^2}{2}}\times\left(\frac{1}{2}\times\left(1+erf(\frac{y}{\sqrt{2}})\right)\right)^{K-1}dy \tag{2-26}$$
$$= \frac{E[r_i]}{K} + \int_M^{\infty} y\sigma_{r_i}\times\frac{1}{\sqrt{2\pi}}e^{-\frac{y^2}{2}}\times\left(\frac{1}{2}\times\left(1+\frac{2}{\sqrt{\pi}}\int_0^{\frac{y}{\sqrt{2}}}e^{-t^2}dt)\right)\right)^{K-1}dy$$

This is the mathematical expression for the users' mean throughput when the PF scheduling algorithm is used.

2.4.2. Theoretical Throughput Analysis of M-LWDF Algorithm

The theoretical throughput analysis of M-LWDF algorithm in the downlink LTE system will be presented in this section.

The Rayleigh fading system with K users and N RBs is modeled. Assume that all sub-bands in OFDMA system have independent identical fading characteristic for all users. Thus instantaneous capacities of different users on the same RBs are independent. Then, the average network throughput can be calculated by:

$$Average\ \ Network\ \ Throughput = K\times N\times E[R_{ij}(t)] \tag{2-27}$$

where $R_{ij}(t)$ denotes the average throughput of user i on RB j at time slot n and $E[R_{ij}(t)]$ is the expectation value of $R_{ij}(t)$.

As discussed in Section 2.4.1, the instantaneous achievable data rate $r(t)$ is approximated by the Gaussian distribution and follows (2-11) and (2-12) for the single user case.

If we assume $R_{ij}(t)$ to be wide-sense stationary, then (2-16) can be modified as

$$E\left[R_{ij}(t)\right] = \int_0^{\infty} x f_{r_{ij}}(x) \Pr(I_{ij}(t+1) = 1 | r_{ij}(t+1) = x) dx \tag{2-28}$$

where $f_{r_{ij}}(x)$ is the probability density function of r_{ij} and $\Pr(I_{ij}(t+1) = 1 | r_{ij}(t+1) = x)$ is the conditional probability that user i will be scheduled on RB j at time $t+1$, given that the instantaneous achievable rate of RB j at time $t+1$ is x.

Based on the scheduling criterion of M-LWDF algorithm which has been discussed in Section 2.3.1, for statistically independent r_{ij}, the probability of user i being selected for transmission on each RB at each TTI can be computed by

$$\begin{aligned}
&\Pr(I_{ij}(t+1) = 1 | r_{ij}(t+1) = x) \\
&= \Pr(\forall m \neq i, \mathrm{a_m} W_m(t+1) \frac{r_{mj}(t+1)}{R_{mj}(t+1)} < \mathrm{a_i} W_i(t+1) \frac{r_{ij}(t+1)}{R_{ij}(t+1)}) \\
&= \Pr(\forall m \neq i, r_{mj}(t+1) W_m(t+1) < \frac{\mathrm{a_i}}{\mathrm{a_m}} \frac{R_{mj}(t+1)}{R_{ij}(t+1)} x W_i(t+1))
\end{aligned} \tag{2-29}$$

in which $W_i(t)$ represents the HOL waiting time of user i at time t.

Further assuming that all users have the same delay requirements (e.g. $a_i = a_m, \forall m \neq i$), it holds for the large values of t and k that

$$\begin{aligned}
&\Pr(I_{ij}(t+1) = 1 | r_{ij}(t+1) = x) \\
&= \Pr(\forall m \neq i, r_{mj}(t+1) W_m(t+1) < \frac{\mathrm{a_i}}{\mathrm{a_m}} \frac{R_{mj}(t+1)}{R_{ij}(t+1)} x W_i(t+1)) \\
&\approx \Pr(\forall m \neq i, r_{mj}(t+1) W_m(t+1) < x W_i(t+1)) \\
&= \int_{w=0}^{\infty} f_{W_i}(w) \times \prod_{m=1, m \neq i}^{K} F_{r_{mj} W_m}(xw) dw
\end{aligned} \tag{2-30}$$

in which f_{Wi} is the probability density function of W_i and $F_{r_{mj}W_m}$ is the product cumulative distribution function of $r_{mj} * W_m$.

On substitution of (2-30) to (2-28), we obtain

$$
\begin{aligned}
E[R_{ij}(t)] &= \int_0^{\infty} x f_{r_{ij}}(x) \int_{\tau=0}^{\infty} f_{W_i}(\tau) \times \prod_{m=1,m\neq i}^{K} F_{r_{mj}W_m}(x\tau) d\tau dx \\
&= \int_0^{\infty} x f_{r_{ij}}(x) \int_{\tau=0}^{\infty} f_{W_i}(\tau) \times \left[\prod_{m=1,m\neq i}^{K} \int_0^{x\tau} f_{r_{mj}W_m}(m) dm \right] d\tau dx
\end{aligned} \tag{2-31}
$$

where $f_{r_{mj}W_m}$ is the probability density function of $r_{mj}*W_m$.

According to [42], we can get

$$
f_{r_{mj}W_{mi}}(m) = \int_{-\infty}^{\infty} \left| \frac{1}{w} \right| f_{r_{mj},W_m}\left(w, \frac{m}{w} \right) dw \tag{2-32}
$$

Since r_{mj} and W_m are independent and the waiting time is no less than zero, we can rewrite (2-32) as

$$
\begin{aligned}
f_{r_{mj}W_{mi}}(m) &= \int_{-\infty}^{\infty} \left| \frac{1}{w} \right| f_{r_{mj}}(w) f_{W_m}\left(\frac{m}{w} \right) dw \\
&= \int_0^{\infty} \frac{1}{w} f_{r_{mj}}(w) f_{W_m}\left(\frac{m}{w} \right) dw
\end{aligned} \tag{2-33}
$$

On substitution of (2-33) to (2-31), we obtain

$$
\begin{aligned}
E[R_{ij}(t)] &= \int_0^{\infty} x f_{r_{ij}}(x) \int_{\tau=0}^{\infty} f_{W_i}(\tau) \times \left[\prod_{m=1,m\neq i}^{K} \int_0^{x\tau} f_{r_{mj}W_m}(m) dm \right] d\tau dx \\
&= \int_0^{\infty} x f_{r_{ij}}(x) \int_{\tau=0}^{\infty} f_{W_i}(\tau) \times \left[\prod_{m=1,m\neq i}^{K} \int_0^{\infty} f_{r_{mj}}(w) F_{W_m}\left(\frac{x\tau}{w} \right) dw \right] d\tau dx
\end{aligned} \tag{2-34}
$$

where F_{Wm} is the cumulative distribution function of W_m.

According to [43], we assume that the HOL waiting time of user i follows an exponential distribution as

$$
f_{W_i}(t) = E[r_i] e^{-E[r_i]t} \tag{2-35}
$$

and

$$
F_{W_i}(t) = 1 - e^{-E[r_i]t} \tag{2-36}
$$

Then, (2-34) can be rewritten as

$$E[R_{ij}(t)] = \int_0^\infty x f_{r_{ij}}(x) \int_{\tau=0}^\infty f_{W_i}(\tau) \times \left[\prod_{m=1, m\neq i}^{K} \int_0^\infty f_{r_{mj}}(w) F_{W_m}\left(\frac{x\tau}{w}\right) dw \right] d\tau dx$$

$$= \int_{-\frac{E[r_i]}{\sigma_{r_i}}}^\infty (y\sigma_{r_i} + E[r_i]) \frac{1}{\sqrt{2\pi}} e^{-\frac{y^2}{2}} \int_{\tau=0}^\infty E[r_i] e^{-E[r_i]\tau} \tag{2-37}$$

$$\times \left[1 - \frac{\sigma_{r_m}}{\sqrt{2\pi}} \int_0^\infty e^{-\frac{m^2}{2}} e^{-E[r_m]\frac{(y\sigma_{r_i} + E[r_i])\tau}{m\sigma_{r_m}}} dm \right]^{K-1} d\tau dy$$

It can be proven that

$$\int_0^\infty e^{-\frac{m^2}{a}} e^{-\frac{b}{m}} dm = \frac{b G_{0,3}^{3,0}(\frac{ab^2}{4} \left| -\frac{1}{2}, 0, 0 \right.)}{4\sqrt{\pi}}, \; if \; a > 0 \; and \; b > 0 \tag{2-38}$$

where the G-function is the Meijer G-function which is defined as

$$G_{p,q}^{m,n}(z \left| \begin{matrix} a_1, \ldots, a_p \\ b_1, \ldots, b_q \end{matrix} \right.) = \frac{1}{2\pi i} \int_L \frac{\prod_{j=1}^m \Gamma(b_j - s) \prod_{j=1}^n \Gamma(1 - a_j + s)}{\prod_{j=m+1}^q \Gamma(1 - b_j + s) \prod_{j=n+1}^p \Gamma(a_j - s)} z^s ds \tag{2-39}$$

On substitution of (2-38) to (2-37), we can have

$$E[R_{ij}(t)] \le \int_{-\frac{E[r_i]}{\sigma_{r_i}}}^\infty (y\sigma_{r_i} + E[r_i]) \frac{1}{\sqrt{2\pi}} e^{-\frac{y^2}{2}} \int_{\tau=0}^\infty E[r_i] e^{-E[r_i]\tau}$$

$$\times \left[1 - \frac{\sigma_{r_m}}{\sqrt{2\pi}} \int_0^\infty e^{-\frac{m^2}{2}} e^{-E[r_m]\frac{(y\sigma_{r_i} + E[r_i])\tau}{m\sigma_{r_m}}} dm \right]^{K-1} d\tau dy \tag{2-40}$$

$$= \int_{-\frac{E[r_i]}{\sigma_{r_i}}}^\infty (y\sigma_{r_i} + E[r_i]) \frac{1}{\sqrt{2\pi}} e^{-\frac{y^2}{2}} \int_{\tau=0}^\infty E[r_i] e^{-E[r_i]\tau} \times [1 - \frac{E[r_m]}{4\sqrt{2\pi}} (y\sigma_{r_i} + E[r_i])\tau$$

$$\times G_{0,3}^{3,0}(\frac{1}{2} \times \left(\frac{E[r_m]}{\sigma_{r_m}} (y\sigma_{r_i} + E[r_i])\tau \right)^2 \left| -\frac{1}{2}, 0, 0) \right. \Bigg]^{K-1} d\tau dy$$

Finally, the theoretical average network throughput for M-LWDF algorithm can be expressed as:

$$Average\ \ Network\ \ Throughput$$

$$\leq K\times N\times\int_{-\frac{E[r_i]}{\sigma_{r_i}}}^{\infty}(y\sigma_{r_i}+E[r_i])\frac{1}{\sqrt{2\pi}}e^{-\frac{y^2}{2}}\int_{\tau=0}^{\infty}E[r_i]e^{-E[r_i]\tau}\times\Bigg[1-\frac{E[r_m]}{4\sqrt{2\pi}}\times \tag{2-41}$$

$$(y\sigma_{r_i}+E[r_i])\tau\times G_{0,3}^{3,0}\left(\frac{1}{2}\times\left(\frac{E[r_m]}{\sigma_{r_m}}(y\sigma_{r_i}+E[r_i])\tau\right)^2\middle|-\frac{1}{2},0,0\right)\Bigg]^{K-1}d\tau dy$$

2.5. Packet Scheduling in LTE-Advanced

In LTE-Advanced, there are many new features/mechanisms being proposed to upgrade an LTE system so that it can meet the requirements of IMT-Advanced to become the true 4G system. In terms of packet scheduling, new algorithms are needed to support and make use of these new capacities.

2.5.1. New proposed Packet Scheduling Algorithms for LTE-Advanced

Since most of the new packet scheduling algorithms are proposed based on the new techniques of LTE-A, it is easier to review the literature by categorizing them with respect to the LTE-A features they incorporate.

A. Support wider bandwidth:

To the best of the author's knowledge, there are five papers related to this specific technique, four of them [24, 44-46] proposed the algorithm that performs scheduling over multiple CCs instead of scheduling independently on each CC and the other [47] proposed a PS algorithm that does scheduling based on grouping users with the same number of CCs.

The CC-independent scheduling is illustrated in Figure 2-17. Each CC has its own scheduler which does not consider the transmission characteristics on other CCs.

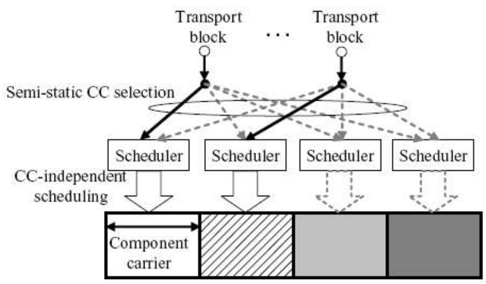

Figure 2-17: Independent-Component Carrier scheduling [45]

All three papers used Proportional Fair (PF) algorithm to demonstrate their proposal. The scheduling metric $M_{k,i,j}$ of user k, on the i^{th} CC at the j^{th} resource block (RB) is calculated by the equation:

$$M_{k,i,j} = \frac{r_{k,i,j}}{R_{k,i}} \quad (2\text{-}42)$$

$r_{k,i,j}$ is the achievable data rate of user i, on the k^{th} CC at the j^{th} RB, $R_{k,i}$ is the average data rate of that user in the k^{th} CC in the past as defined in the Equation (2-3) .The scheduler then compares all $M_{k,i,j}$ metric and assigns j^{th} RB to the user with the maximum value of $M_{k,i,j}$.

Developed from the traditional scheduler mentioned above, Figure 2-18 shows a new scheduler which controls over multiple CCs, or cross-CC scheduler. By taking the statistics from all CCs into consideration, the scheduler can achieve better decisions on resource allocation.

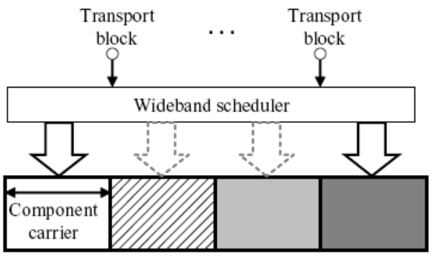

Figure 2-18: Cross-Component Carriers scheduling [45]

Follow this cross-CC scheduler concept, [44] proposed a scheduling framework that can manage cross-CC in Figure 2-19.

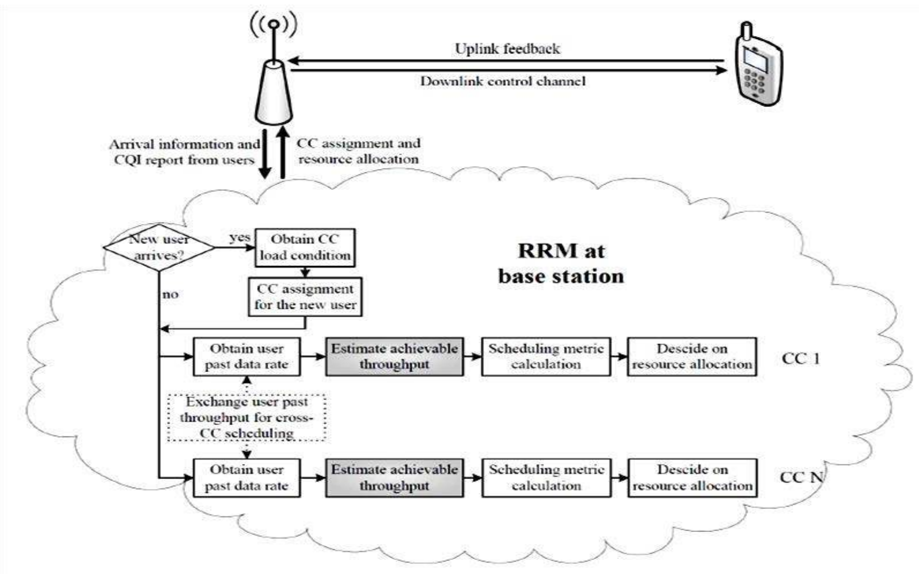

Figure 2-19: Simple cross-CC Scheduling framework [44]

The formula proposed for this algorithm is defined by the Equation (2-43). The PF metric was modified to take into account the average data rate of all aggregated CCs.

$$M_{k,i,j} = \frac{r_{k,i,j}(t)}{\sum_{k=1}^{N} R_{k,i}(t)} \tag{2-43}$$

N is the total number of CC.

Alternately, for real cross-CC scheduling with only one cross-CC scheduler for all CCs in Figure 2-18 (no scheduler for each CC as in Figure 2-17), it might not have separate calculator to calculate average data in each CC or $R_{k,i}$. Therefore, the cross-CC PF algorithm in cross-CC scheduler is expressed better in the equation below, as proposed by [24, 45, 46]:

$$M_{k,i,j} = \frac{r_{k,i,j}(t)}{R_i(t)} \tag{2-44}$$

with

$$R_i(t) = (1 - \frac{1}{t_c}) * R_i(t-1) + \frac{1}{t_c} * r_i(t-1) \tag{2-45}$$

R_i is total average data rate of user i in all CCs, r_i is total instantaneous data rate in all assigned RBs in all CCs of that user in previous time slot that had been transmitted.

With these formulas (2-43 and (2-44), the metric of LTE-A user will be reduced as its aggregated average data rate is higher than a LTE user, but the LTE user metric remains the same as Equation (2-42). It means that the priority of LTE users is higher which leads to better system fairness between LTE and LTE-A users.

Moreover, the simulation results in these papers have shown that the cell throughput increases by 18% as compared to the CC-independent scheduler [45] (Figure 2-20) while cell-edge user throughput increases up to 90% [44] (Figure 2-21). The latency in case of carrier aggregation scheduling also improves, the system can support a load factor of 0.8 in cross-CC whereas 0.4 in independent-CC scheduler (Figure 2-22) [24].

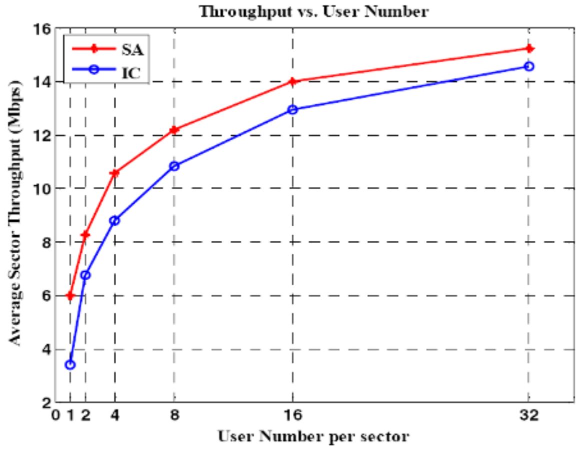

Figure 2-20: Throughput of cross-CC vs. In-CC [24]

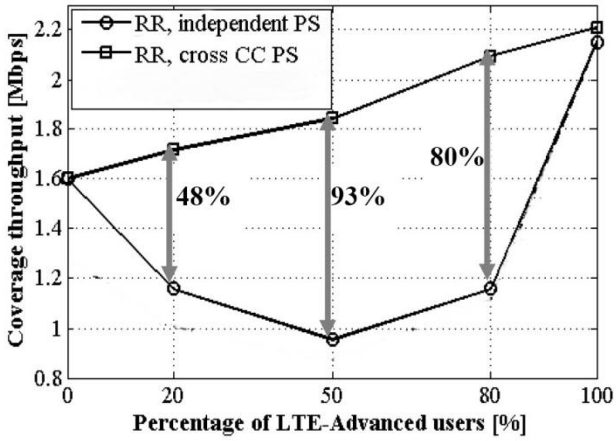

Figure 2-21: Cell-edge user throughput [48]

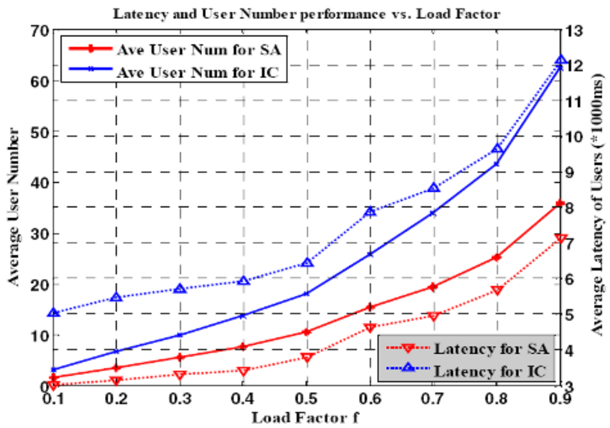

Figure 2-22: Latency of cross-CC vs. In-CC [24]

(Note: IC: In-CC scheduler, SA: Spectrum aggregation or cross-CC scheduler)

There are differences in the above mentioned papers. Paper [24] evaluates the proposed PS algorithm in TDD LTE-A while others in FDD LTE-A; paper [44] studies the CCs load balancing method, i.e. how to assign CCs to each user, with the result that round robin achieves better performance than the mobile hashing (or random assignment); and [45] proposes a new mechanism with Transport Block (TB) assignment over multiple CCs (together with scheduling over multiple CCs) which is still not considered by 3GPP RAN WG1 (Work Group 1) or current 3GPP specifications.

Another aspect of carrier aggregation in LTE-A relates to coverage area of a cell, [47] proposed a new PS algorithm based on the characteristic that the coverage of each CC is different as their frequency bands are not the same, especially in non-continuous case.

Figure 2-23 shows that the coverage area of lower frequency band f1 (e.g. 800 MHz) is bigger that of the frequency band f2 (e.g. 2000 MHz). Therefore, User 1 located further away from base station will operate on fewer CC than the User 2 who is closer to the base-station.

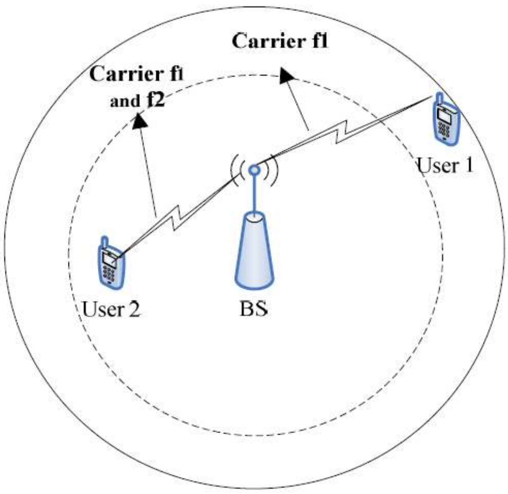

Figure 2-23: Coverage of difference frequency bands [47]

The number of CCs to be allocated to a LTE-A user is determined by the threshold pathloss and actual pathloss experienced by the user. Based on its location, user reports its SINR on each CC to the base station.

Using the PF algorithm, the simulation result shows that user group (UG) scheduling can accomplish better fairness among all users (Figure 2-24) while causing minor throughput degradation as compared with the original PF scheduling algorithm (Figure 2-25).

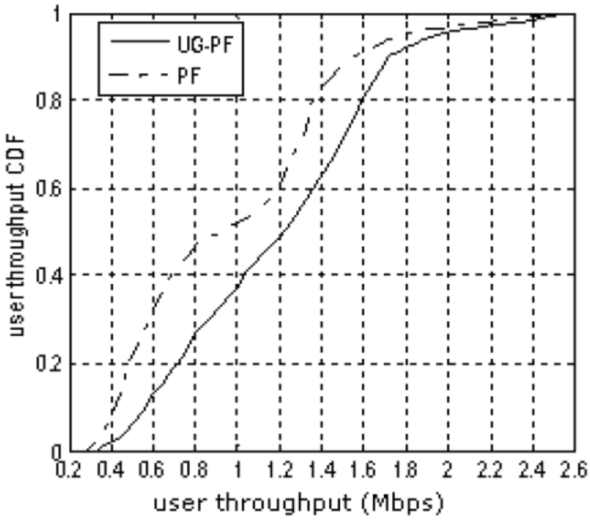

Figure 2-24: User throughput CDF

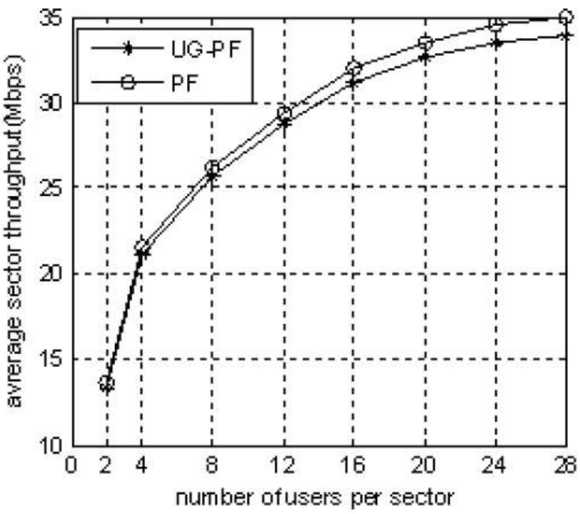

Figure 2-25: Average sector throughput

B. Advanced MIMO technique:

A new PS algorithm proposal related to this technique does not take into account the 8-layer upgraded feature since it does not affect packet scheduling, but does consider the Multi-User MIMO feature. [49] suggests a scheduling algorithm based on the PF in the context of MU MIMO for both Single-Cell (SC) and Multi-Cell (MC) scenario.

For SC-MU MIMO, this paper proposes modified formula of PF metric of *n* users' pairing:

$$\boldsymbol{M_n = \max_{S_n \in \Omega_n} \sum_{k \in S_n} \frac{r_k^n}{R_k}}, \tag{2-46}$$

n is the number of users in one simultaneous MIMO transmission among total N users in one base station, S_n is the set of one simultaneous MIMO users, r_k^n is the achievable rate of user k^{th} in these n users, R_k is the average data rate of that k^{th} user. This equation implies the scheduler find a subset of $S_n \in \Omega_n$ with the maximum value. Then, it selects the optimal value of M_n:

$$\boldsymbol{n_{opt} = arg\,max_{n=1,\dots,N}\, M_n,} \tag{2-47}$$

For MC-MU MIMO, the PS algorithm uses the formula used in the SC case to calculate the metric for SC $M^{SC}$and for MC M^{MC}, and simply compares the two optimal metric, and then determines which set of users have to be scheduled.

The simulation results in Figure 2-26 and table below show that this PS algorithm can tremendously improve the average cell throughput as well as cell-edge user throughput.

	ITU Targets	SC-SU-MIMO	SC-MU-MIMO	MC-MU-MIMO
Cell-average user throughput (bps/Hz)	2.2	1.5673	1.969	2.346
	Gains from SC-SU-MIMO	0%	25.63%	49.67%
Cell-edge user throughput (bps/Hz)	0.06	0.0452	0.0479	0.0667
	Gains from SC-SU-MIMO	0%	5.97%	47.57%

Table 2-4: Throughput of new algorithm

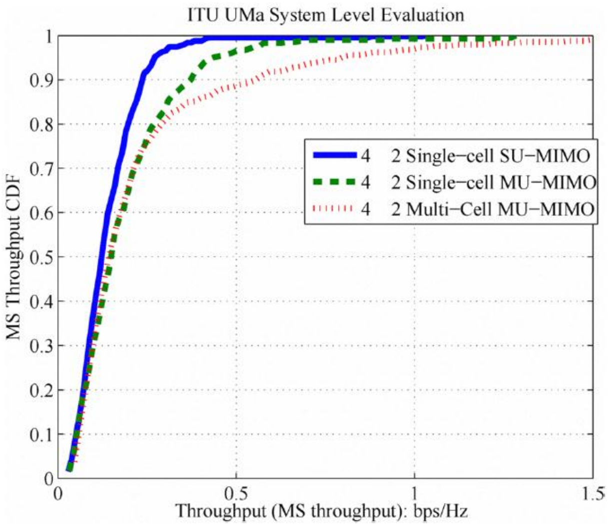

Figure 2-26: Throughput

This PS algorithm can be applied to any operation modes of complex network including single-cell SU-MIMO, single-cell MU-MIMO, multi-cell SU-MIMO and multi-cell MU-MIMO.

C. Coordinated multipoint transmission and reception (CoMP)

In [50], a simple PF scheduling mechanism for downlink cooperative transmission system is proposed that splits the users into two groups: CoMP users who receive data from multiple base stations, and single-cell users who receive from a single-cell transmission. It is assumed that OFDMA bandwidth consisting of RBs is divided into two groups, one group of RBs is exclusively reserved for CoMP and the other group for single-cell transmission.

The proposed User-Grouping (UG) method will find the optimal number of CoMP users and use the traditional PF metric to assign the best CoMP user for each CoMP RB. This is also the same method for single-cell user for single-cell RB. Comparing to this UG, it uses two reference methods: the No-UG method, in which users are not grouped and can be scheduled in any RBs, and no CoMP method, or all users use single-cell transmission.

The simulation results show that the easy-to-implement algorithm significantly enhances the average user throughputs over no CoMP method (Table 2-5) and also maintains the same user resource fairness (Table 2-6). The cell-edge performance of the proposed method is slightly worse than the No-UG method for smaller number of RBs reserved for CoMP (Table 2-7). But the proposed method would involve simpler scheduling and control complexity as a user can only undergo either single cell or CoMP transmissions.

Scheme	P = 2	P = 4	P = 6
UG	1.99	1.74	1.69
No-UG	1.67	1.71	1.70
SC	1.66		

Table 2-5: Average user throughput in Mbps, 30 Users/cell

Scheme	P = 2	P = 4	P = 6
UG	0.80	0.79	0.79
No-UG	0.84	0.83	0.82
SC	0.79		

Table 2-6: Fairness index

Scheme	P = 2	P = 4	P = 6
UG	0.70	0.53	0.45
No-UG	0.65	0.59	0.57
SC	0.36		

Table 2-7: Average cell-edge user throughput in Mbps

D. Relaying

Regarding Relay function in the LTE-A network, paper [51] proposes applying a semi-persistent scheduling algorithm for VoIP service. On the access link, the process is the same as the traditional network, persistent scheduling for initial transmissions and dynamic scheduling for retransmissions. On the backhaul link, the eNodeB schedules several users to one RN for each TTI, then the main process is defined as:

i. When relay users change to active, both eNodeB and RN persistently allocate the resource of backhaul link and access link to the users respectively based on the average quality of backhaul link and access link.
ii. When user needs retransmission in the backhaul or access link, eNodeB or RN schedules retransmission in the backhaul link and access link independently.

This algorithm was applied to evaluate the performance of the LTE-A network with and without Relay Node, and it is not compared with other PS algorithms. The simulation results show that the VoIP capacity is increased with the number of RN increases, while the packet delay of Relay users increases under the QoS requirements.

2.5.2. Challenges Faced to Implement Scheduling

These papers have shown the new challenges that the scheduling task and other RRM tasks must solve in the new LTE-A network. It includes:

- *Quicker computations*: Since LTE-A usually has more Resource Blocks (RB), Transport Block (TB), component carriers, etc. It requires quicker processing capacity for all network elements such as eNodeB and UEs, as well as for the simulation program to model the scheduling task, in order to maintain the processing time for smooth operation.

- *The transition of user mode*: With co-existence of new types of users and its modes, the scheduling task now deals with more input attributes of each user and must have better solutions to handle all of the users' change of modes. For example, one active user during its connection session may switch from normal mode to CoMP mode, and later to relaying mode. eNodeB should acknowledge all these transitions and provide different solutions to optimize the performance of this user, as well as the whole system for every instance.

- *More complexity*: New features like CoMP and MU-MIMO are complicated in terms of the co-ordination of many users and several eNodeBs. The serving cell must play the role of control unit (like BSC or RNC in previous technologies) to gather all related information from users directly and from neighbor eNodeBs, and deliver the specific task for each radio channel to serve its active users.

- *Brand new algorithms*: As most algorithms are the modified version of existing PF algorithm, the main challenge will be to develop a new algorithm optimized for LTE-A which incorporates all its new features and can address the user and system requirements.

On the other hands, the challenges above have shown some drawbacks of current works:

- *They focus on one feature of LTE-A*: Each new feature was considered separately in each paper. The scheduling algorithm proposals, therefore, only solve for one technique independently. For example, the user-grouping by number of CCs solution could not apply for CoMP or relay technique and vice versa.

- *The simplicity of proposed algorithms and modeling*: some papers have proposed the mathematical solutions in the simplest way, as well as the simulation model. In reality, with the presence of many users and eNodeB, it is not certain that the proposed formula is feasible or not. For example, in [49], only two eNodeB for MC-MU MIMO are studied but the mathematical solution is quite complicated with the combination of many possible subsets of MIMO types. It is a question of whether it can be applied in reality.

2.6. Summary

In this chapter, literature regarding LTE and LTE-A has been carefully discussed. All main features of LTE and LTE-A has been presented to provide the necessary knowledge to understand the project. Packet scheduling mechanisms as well as some well-known packet scheduling algorithms have been explained in detail. It also explained the mathematical analysis for throughput in the downlink of LTE system.

In addition, this chapter has presented a survey of proposed scheduling algorithms for LTE-A. Most of the algorithms were developed based on the new features of LTE-A and on the

Proportional Fair algorithm. Some challenges to implementing the scheduling task are presented, as well as the drawbacks of these papers. The work to be carried out after this chapter is to develop a new solution for packet scheduling in LTE-A. It includes implementing a PS simulation tool, evaluating the above algorithm proposals as well as the existing PS algorithms such as round-robin, max-rate, PF, etc., and ultimately creating an optimal scheduling algorithm for LTE-A.

CHAPTER 3: SYSTEM MODELLING & SIMULATION

In order to study packet scheduling in LTE-Advanced, it is necessary to build a simulation tool that can model and simulate the LTE-A system. This chapter presents descriptions on LTE-A system's model and operation which related to the RRM mechanisms. It also explains how the simulation tool model operations of LTE-A system in downlink using a C++ programming language.

3.1. New model in LTE-A network

As discussed in LTE-A review section, LTE-A adopts several new features which create many types of LTE-A users co-existing in the LTE-A network, apart from the LTE users:

1. **Single/multi CC users:** LTE-A UEs can operate on multiple carriers, but due to its on-demand services, or network balance control, an UE can be assigned some specific CCs only. For example, the cell-edge users can use the 800 MHz band if an eNodeB has three CCs operating at 800, 1900, 2100 MHz, as lower frequency band has bigger coverage [47].

2. **Relay users**: UEs which are under the coverage of Relay Node. These users have more delay than users with direct connection with eNodeB.

3. **CoMP users**: In LTE-A, UEs transmit and receive data from coordinated multiple cells [50]. A user can be determined to use CoMP function if the reference signal strengths at the user location from neighboring eNodeBs are nearly equal (lower than a pre-defined threshold value)

4. **MIMO users**: UEs that use MIMO, or spatial multiplexing [49]. MIMO users will use more Transport Blocks (TB), 2 TBs instead of 1 [17].

This complex network can be illustrated by the Figure 3-1.

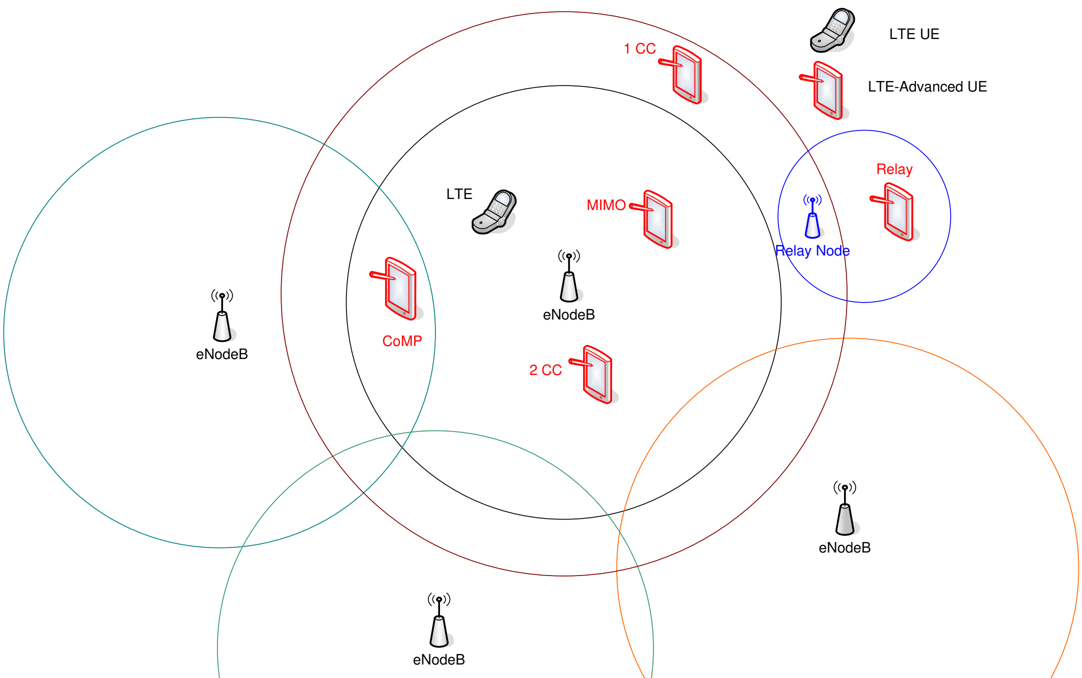

Figure 3-1: New model of LTE-Advanced with many kinds of user co-existence

3.2. Packet Scheduling Simulation Tool

Computer simulation is essential to evaluate the performance of current and proposed packet scheduling algorithms since the LTE-A network is not commercialized and realistic at the moment. Thanks to current works of Dr. Sandraseragan's research team, the computer simulation tool for LTE is available to be modified and upgraded to LTE-Advanced. This tool is written in C++ language and can be compiled in C++ platforms like Microsoft Visual C++ or Eclipse C/C++.

Most RRM mechanisms in the downlink LTE system, which operates on OFDMA technology, are performed at 1 ms interval (known as Transmit Time Interval, TTI). When a user is moving during a connection with the mobile network, in each TTI (or several TTIs, depending on network configuration setting), it measures the eNodeBs' signal strength and calculates the signal to noise and interference ratios (SINRs). UE uses the SINR to generate the CQI and then sends CQI to eNodeB. Based on the CQI, eNodeB communicates with UE to decide camping cells and handover process. eNodeB also collects hybrid automatic repeat request (HARQ) feedback and incoming traffic to control traffic buffer of each UE. By comparing CQI of all users on each RB, depending PS algorithm, eNodeB decides which user will be allocated on each RB with corresponding packets of that user. This traffic (user's packets) will be passed to the transmission modules, through the air interface to related UE.

All the above operations were modeled and simulated by our simulation tool. The tool can be described in the diagram below.

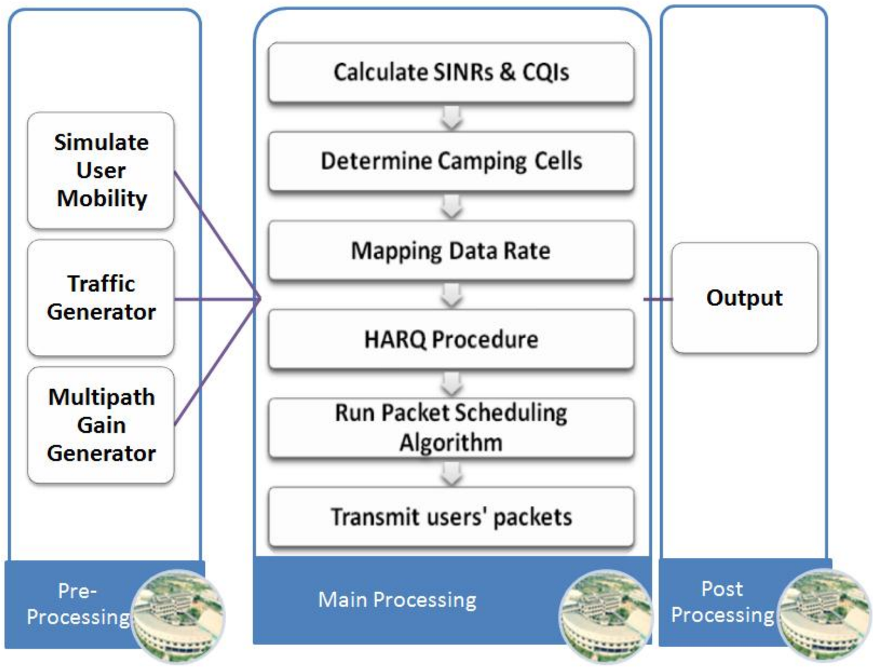

Figure 3-2: LTE-Advanced Simulation Tool Block Diagram

3.2.1. Pre-processing block

There are three pre-processing modules that are run independently before the main processing program. The reasons of this separation are to reduce the computation of the main program and to create the same conditions of incoming users' traffic, environment's multipath gain and users' movement so that the results of different simulation runs can be easily compared.

i. **User Mobility Module**: The location of users is randomly distributed in the simulation area. At each time interval, users move at a predefined speed in random directions [52]. The new location $loc_i(t+1)$ of user i is determined using the following equation:

$$loc_i(t+1) = loc_i(t) + v_i(t) * dir_i(t) \quad (3\text{-}1)$$

where $v_i(t)$, $dir_i(t)$ are the speed and direction of user *i* at time *t*.

This module generates a file which contains the locations of every user for the simulation time. As the main program reads it from the same file, the movements of all users are unchanged for different simulation runs; so that the simulation results can be easily compared.

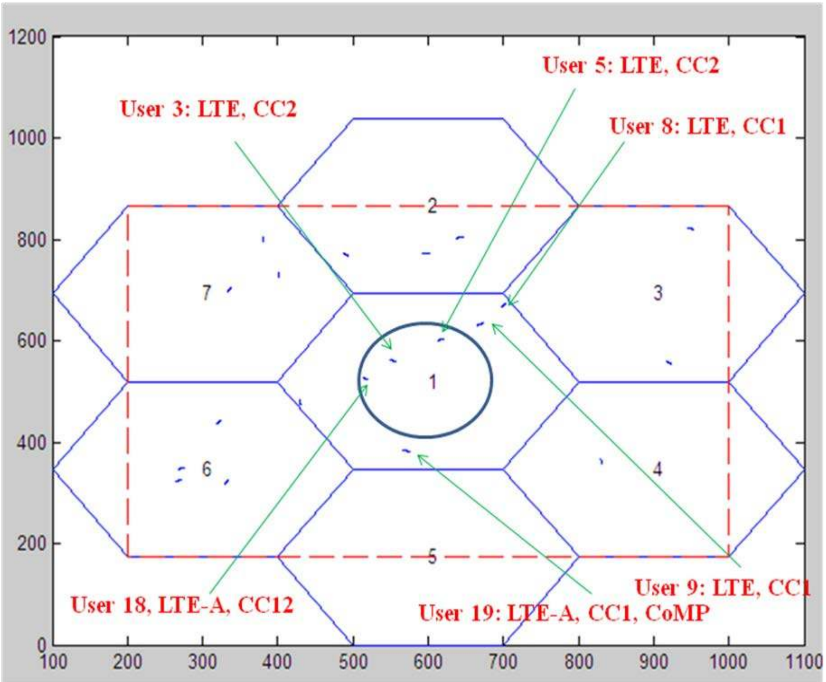

Figure 3-3: Sample picture of users' location and movement in new simulation

ii. **Multipath Gain Generator Module**: This module uses the speed and carrier frequency to generate the multipath gain for every TTI [53] and for each CC.

The multi-path fading refers to the addition of multi-path components caused by the reflection and scattering of the radio signal. The received signals from different path have different attenuations and delays, which result in fluctuations of the received signal.

In this thesis, the multi-path fading is approximated as a complex random Gaussian process $\mu(t)$, which is given as

$$\mu(t) = \sqrt{\mu_1^2(t) + \mu_2^2(t)} \tag{3-2}$$

where $\mu_1(t)$ and $\mu_2(t)$ are uncorrelated filtered white Gaussian noises with zero means $E[\mu_i(t)] = =0$ and identical variances $Var[\mu_i(t)]=\sigma_{\mu i}^2 = \sigma_{\mu 0}^2$, $i=1,2$.

As discussed in [54], the approximation of each Gaussian process $\mu_i(t)$ ($i=1,2$) can be expressed as a finite sum of weighted sinusoids with evenly distributed phases.

$$\tilde{\mu}_i(t) = \sum_{n=1}^{N_{s,i}} c_{i,n} \cos(2\pi f_{i,n} t + \theta_{i,n}), \qquad i = 1,2 \tag{3-3}$$

where $N_{s,i}$, $c_{i,n}$, $f_{i,n}$ and $\theta_{i,n}$ denote the number of sinusoids, Doppler coefficient, discrete Doppler frequency and Doppler phase of the i^{th} process, respectively.

The Monte Carlo Method (MCM) [55] is deployed to determine the value of parameters $c_{i,n}$, and $f_{i,n}$. The approximated Gaussian process can be modified as below:

$$\tilde{\mu}_i(t) = \sum_{n=1}^{N_i} \sigma_{\mu_0} \sqrt{\frac{2}{N_i}} \cos(2\pi f_{\max} \sin(\frac{\pi}{2}\mu_n)t + \theta_{i,n}), \qquad i = 1,2\,. \tag{3-4}$$

in which f_{max} is the maximum Doppler frequency.

The envelope of the Gaussian process $\mu(t)$ is a Rayleigh process $\xi(t)$ [56], which is expressed as

$$\xi(t) = |\mu(t)| \tag{3-5}$$

The model of multi-path fading is given in Figure 3-4.

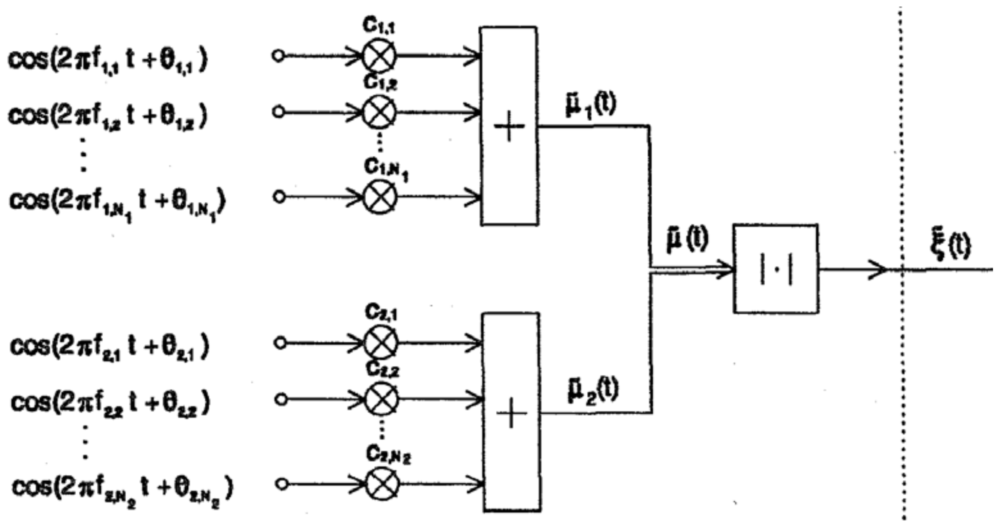

Figure 3-4: Model of Multi-path Fading [55]

iii. **Traffic Generator Module**: This module generates the packet arrivals for each user for the duration of the simulation and queues packets in the buffer. It basically models the traffic arrivals at eNodeB from the Core Network [57, 58].

The video streaming packets, arriving from the network, as seen by the serving eNodeB buffer are modeled using parameters given in Table 3-1. The video frames arrive at a regular interval and consists of fixed number of packets. The packet sizes are of variable in length and are based on a Truncated Pareto distribution (followed 3GPP recommendation). Similarly, the inter-arrival time of each packet in a frame follows the Truncated Pareto distribution.

Information types	Distribution	Distribution Parameters
Inter-arrival time between the beginning of successive frames	Deterministic (Based on 20fps)	50ms
Number of packets (slices) in a frame	Deterministic	8
Packet (slice) size	Truncated Pareto (Mean=100bytes, max=125bytes)	K=40bytes, α=1.2
Inter-arrival time between packets (slices) in a frame	Truncated Pareto (Mean=6ms, Max=12.5ms)	K=2.5ms, α=1.2

Table 3-1: Traffic pattern [59, 60]

The packets are streamed into users' buffers from variable bit rate (VBR) source encoders running at 50 Mbps in average. The video streaming applications are assumed to be "played" as the packets are being streamed through the air interface, instead of being downloaded first and then played. In this paper, the threshold for HOL packet delay of each user is set to 20 ms which is the maximum waiting time of a video streaming packet at the serving eNodeB buffer. The buffer of each user is assumed to be infinite and a packet is considered lost when it is discarded. [57]

3.2.2. Main processing block

In the main program, after reading the configuration input file (number of LTE users, LTE-A users, speed, etc.) and three files from above modules, the simulation will be performing the following steps for every TTI:

i. **Calculate SINRs, CQIs**: this step includes the following calculations:

- ***Compute pathloss***: Based on the UE locations from the previous step (User Mobility Module), Extended COST-231 Hata model for urban environment [61] is used to compute the pathloss of each user.

$$PL_i(t) = 46.3 + 33.9 * \log_{10}(f) - 13.82 * \log_{10}(h_b) - a(h_m) + (44.9 - 6.55 * \log_{10}(h_b)) * \log_{10}(d_i(t)) \quad (3\text{-}6)$$

with

$$a(h_m) = (1.1 * \log_{10}(f) - 0.7) * h_m - (1.56 * \log_{10}(f) - 0.8) \quad (3\text{-}7)$$

where $PL_i(t)$ is the path loss (in dB) and $d_i(t)$ is distance (in km) of user i at time t. f is the carrier frequency (in MHz), h_b and h_m are the heights of eNodeB and mobile phone (in meters), respectively and $a(h_m)$ is the mobile antenna correction factor.

- ***Generate shadowing gain***: Shadow fading refers to the signal attenuations caused by signal reflection, diffraction and shielding phenomenon from obstructions such as building, trees, and rocks. Following the approach proposed in [62, 63], it can be modeled by the equation below:

$$\xi_i(t+1) = \rho_i(t) * \xi_i(t) + \sigma * \left(\sqrt{1 - \rho_i(t)^2}\right) * W(t) \quad (3\text{-}8)$$

where $\xi_i(t+1)$ is shadow fading gain for user i at time $(t+1)$, σ is the shadow fading standard deviation, and $W(t)$ is a Gaussian random variable at time t. The shadow fading autocorrelation function $\rho_i(t)$ of user i at time t is computed using the equation below:

$$\rho_i(t) = \exp\left(\frac{-v_i(t)}{d_0}\right) \quad (3\text{-}9)$$

where $v_i(t)$ is the speed of user i at time t, and d_0 is the shadow fading correlation distance.

The channel gain $Gain_{i,j}(t)$ of user i on RB j at time t can be computed using the following equation:

$$Gain_{i,j}(t) = 10^{\left(\frac{PL_i(t)}{10}\right)} * 10^{\left(\frac{\xi_i(t)}{10}\right)} * 10^{\left(\frac{mpath_{i,j}(t)}{10}\right)} \quad (3\text{-}10)$$

where $mpath_{i,j}(t)$ is the multi-path fading gain of user i on a RB j at time t. From the computed channel gain, the SINR value ($SINR_{i,j}(t)$) of user i on RB j at time t is computed using the approach proposed in [64] and is given as below:

$$SINR_{i,j}(t) = \frac{P_{total} * Gain_{i,j}(t)}{N_{RB}\left(I + N_o\right)} \quad (3\text{-}11)$$

where P_{total} is the total eNodeB downlink power, N_{RB} is the number of RBs, N_o is the thermal noise and i is the inter-cell interference.

This module calculates SINR, and corresponding CQI (refer to Table 3-2) of every user in every frequency band.

ii. **Determine Camping Cell**: this step will assign the camping cell for all UEs according to the SINR calculated from Equation (3-11) and pre-defined handoff algorithms [65]. For LTE-A users, it also determines the following:

- ***The number of CCs per LTE-A users***: Based on the distance, cell edge users may not use high frequency band CC bands [47]. For coverage requirements, the maximum pathloss on a carrier cannot be higher than a threshold PL_{th}. This requirement is implemented as follows. For user i in carrier f_k at the distance d from a base station, user's pathloss can be calculated using Equation (3-6) and this is used to determine if user i can operate on carrier f_k.

- ***Number of CoMP users***: Based on the SINRs calculated from the above module, the CoMP users can be identified. UEs with comparable reference signal strengths from different eNodeBs (difference lower than a pre-defined threshold value) can be classified as CoMP users.

iii. **Mapping data rate**: data rate for each UE at each RB can be estimated by eNodeB from received CQI and target BLER.

The number of bits per symbol of user i on a subcarrier within RB j at time t ($nbits_{i,j}(t)/symbol$) can be computed according to the approach discussed in [60, 66, 67]. The achievable data rate $date\_rate_i(t)$ for user i at time t can be obtained by

$$data\_rate_i(t) = \frac{nbits_{i,j}(t)}{symbol} \times \frac{nsymbols}{slot} \times \frac{nslots}{TTI} \times \frac{nsc}{N} \quad (3\text{-}12)$$

where *nsymbols/slot* is the number of symbols per time slot, *nslot/TTI* is the number of time slots per TTI, *nsc/N* is the number of subcarriers per RB and *N* is the number of available RBs.

Therefore, based on the computed SINR value given in (3-11), the achievable data rate can be determined by (3-12), and an appropriate modulation and coding scheme (MCS) can be chosen according to Table 3-2.

BLER>0.1

Minimum SINR (dB)	CQI index	Modulation	Code rate x 1024	Data Rate/TTI
$-\infty$	0	Out of range		
-5.504	1	QPSK	78	22
-4.88	2	QPSK	120	34
-3.879	3	QPSK	193	55
-2.435	4	QPSK	308	89
-0.79	5	QPSK	449	129
0.835	6	QPSK	602	174
2.335	7	16QAM	378	218
4.305	8	16QAM	490	283
6.265	9	16QAM	616	356
7.435	10	64QAM	466	404
9.369	11	64QAM	567	491
11.086	12	64QAM	666	577
12.819	13	64QAM	772	669
14.456	14	64QAM	873	757
15.712	15	64QAM	948	822

Table 3-2. CQI Mapping table

iv. **HARQ procedure**: erroneous packet retransmission procedure.

v. **Run PS algorithms**: This is where PS algorithm is performed or edited. As specified by 3GPP [27], the packet scheduler can perform scheduling on each CC independently or all CCs together (cross-carrier). This simulation tool has two mechanisms, cross-CC and independent-CC (in-CC) scheduler.

vi. **Transmit users' packets**: Transmit user's traffic its allocated RB. Depending on user's CQI on that RB, this module will transmit number of packets corresponding to its data rate on this RB.

These steps above will run in a loop until the simulation time is completed. For each interval, the main process block generates output files with information of all packet attribute: the UE that packet belongs to, packet's arrival time, packet's depart time, packet's status (e.g. normal, discarded or rejected), etc.

3.2.3. Post processing block

The LTE system is designed as a packet-optimized network supporting both Real-Time (RT) and Non-Real-Time (NRT) traffic. Packet scheduling plays an important role in guaranteeing the system performance. The vital target of PS algorithms is to meet the QoS and fairness requirements of each user while ensuring the efficient usage of the available radio resources. In this simulation tool, the performance of various algorithms is evaluated in terms of system throughput, average packet delay, packet loss rate and fairness.

By using the outputs of the main process block, the post processing block calculates the following system performance metrics:

- Throughput for each UE and eNodeB, and system throughput.
- System (packet) delay.
- Packet loss ratio.
- Fairness.

i. System throughput:

The system throughput indicates the average transmission rate of the system. It is defined as the sum of transmitted packet size of all users per second, which is given by

$$system\ throughput = \frac{1}{T}\sum_{i=1}^{K}\sum_{t=1}^{T} ptransmit_i(t) \quad (3\text{-}13)$$

where K is the total number of users, T represents the total simulation time, and $ptransmit_i(t)$ denotes the number of transmitted bits of user i at time t.

ii. Packet delay:

Packet delay is one of the QoS requirements. The Head of Line (HOL) delay is defined as the time duration from the packet's arrival time in the buffer to the current time. Average packet delay describes the average HOL waiting time of all users' packets throughout the simulation time, which is given as follows:

$$packet\ delay = \frac{1}{K}\sum_{i=1}^{K}\frac{1}{T}\sum_{t=1}^{T}W_i(t) \tag{3-14}$$

where $W_i(t)$ denotes the HOL delay of user *i* at time *t*.

iii. Packet loss ratio

RT and NRT traffic require different delay deadlines for the packet transmission. A packet will be discarded when the HOL delay of the packet goes beyond the user traffic delay deadline. Packet Loss Rate (PLR) is defined as the proportion of total discarded packet size to total arrived packet size. PLR is mathematically expressed as:

$$PLR = \frac{\sum_{i=1}^{K}\sum_{t=1}^{T} pdiscard_i(t)}{\sum_{i=1}^{K}\sum_{t=1}^{T} psize_i(t)} \tag{3-15}$$

in which $psize_i(t)$ denotes the total size of all received packet and $pdiscard_i(t)$ is the total size of all discarded packet of user *i* at time *t*.

iv. Fairness

Fairness measures if users are receiving a fair resource block allocation. Fairness evaluates the difference between the users who have the most and least transmitted packet size. The maximum value of fairness is one and occurs when all users transmit an equal amount of packets. The mathematical expression of fairness is given as:

$$fairness = 1 - \frac{ptotaltransmit_{max} - ptotaltransmit_{min}}{\sum_{i=1}^{K}\sum_{t=1}^{T} psize_i(t)} \tag{3-16}$$

where $ptotaltransmit_{,max}$ and $ptotaltransmit_{min}$ are maximum and minimum values of all users' total transmitted packets size respectively.

To measure fairness, another approach [68] that also being used in this thesis is defined as:

$$fairness = \frac{1}{K}\sum_{i=1}^{K}\frac{|UT_i - UT_{aver}|}{UT_{aver}} \tag{3-17}$$

where UT_i is the throughput of user i, UT_{aver} is the average user throughput of all users.

The fairness metric of this algorithm can higher than one. With the Equation (3-16), the higher the metric is, the fairer the system performs. But with the second formula (Equation (3-17)), the system performs fairer when the metric is lower.

3.3. Summary

This chapter has described how a new simulation tool was developed to model LTE-Advanced technology. It was developed from an existing simulation tool for the LTE system. All of the tool modules were modified to adapt the LTE-Advanced system. Modules that are intensively modified during this project were: User Mobility, Traffic Generator, Multipath Gain Generator, Calculate SINR & CQIs, Determine Camping Cells, and Run PS Algorithms.

The final outcome of the simulation tool has two scheduler, in-CC and cross-CC scheduler. The results of this tool (which will be presented in next chapter), in comparison to other papers, prove that this simulation tool is working as anticipated. Although it does not support spatial multiplexing (MIMO) and relaying functions, this simulation is efficient for researchers in studying and evaluating the PS algorithms. Based on this tool, any concept for developing a new algorithm for LTE-Advanced can be applied and performed. Its performance can be evaluated and compared with the existing algorithms.

CHAPTER 4: PACKET SCHEDULING ALGORITHMS FOR LTE-ADVANCED

In this chapter, several well-known algorithms will be evaluated by the LTE-Advanced simulation tool with two schedulers, in-CC and cross-CC. These algorithms are: Round Robin, Max Rate, Proportional Fair and M-LWDF. The comparison between cross-CC and in-CC scheduler is also discussed. Most importantly, the objective of the project, which is the finding of optimized algorithms for packet scheduling in LTE-A, will be presented in this chapter.

4.1. Cross-CC vs. In-CC scheduler with PF algorithm

4.1.1. Theory discussion

A survey of all papers related to the packet scheduling mechanism in LTE-A revealed that the proportional fair (PF) algorithm [69] and its variants are the most popular solutions [70], as mentioned in Chapter 2. Therefore, the PF algorithm is the best to compare the in-CC and cross-CC scheduler.

For independent-CC (in-CC) scheduling, a scheduler calculates a metric $M_{k,i,j}$ for all users in all RBs of each CC in each time slot t. For each RB, the user with the highest metric will be allocated to the RB

$$M_{k,i,j} = \frac{r_{k,i,j}(t)}{R_{k,i}(t)} \tag{4-1}$$

$r_{k,i,j}$ is the instantaneous supportable data rate of user i, on the k^{th} CC at the j^{th} RB, $R_{k,i}$ is the average data rate of user i in the k^{th} CC (containing the RB) in the past t_c time slots as defined below:

$$R_{k,i}(t) = (1 - \frac{1}{t_c}) * R_{k,i}(t-1) + \frac{1}{t_c} * r_{k,i}(t-1) \quad (4\text{-}2)$$

For cross-CC scheduling, the PF metric was modified to take into account the total average data rate of all CCs in which the user can operate. The paper [44] proposed a Cross-CC PF metric defined by the equation below:

$$M_{k,i,j} = \frac{r_{k,i,j}(t)}{\sum_{k=1}^{N} R_{k,i}(t)} \quad (4\text{-}3)$$

N is the total number of CC.

While other papers [24, 45, 46] had proposed Cross-CC PF metric defined by:

$$M_{k,i,j} = \frac{r_{k,i,j}(t)}{R_i(t)} \quad (4\text{-}4)$$

with

$$R_i(t) = (1 - \frac{1}{t_c}) * R_i(t-1) + \frac{1}{t_c} * r_i(t-1) \quad (4\text{-}5)$$

R_i is total average data rate of user i in all CCs, r_i is total instantaneous data rate in all assigned RBs in all CCs of that user in previous time slot that had been transmitted.

The meaning of the two Equations, (4-3) and (4-4), is the same with the denominator of both metrics referring to the total average throughput of a user. But for cross-CC scheduling with only one cross-CC scheduler for all CCs (no separate calculator for each CC), it cannot calculate average data in each CC or $R_{k,i}$. Therefore, cross-CC PF algorithm in cross-CC scheduler is expressed better in the Equation (4-4).

With this algorithm, the value of the metric of LTE-A users operating on multiple CCs will be reduced as its denominator is higher than the in-CC equation ($R_i > R_{k,i}$, since total average data rate in all CC is always higher than average data rate in one CC), but the LTE users' metric remains the same. It means the priority of LTE-A users decrease, leading to the better system fairness between LTE and LTE-A users.

According to these papers, Cross-CC PF algorithm has advantages over in-CC PF. In terms of system throughput, it can increase from 12% [46] up to 18% [45] than the in-CC scheduler. For cell-edge users throughput, the improvement is as high as 90% [44]. The latency in case of carrier aggregation scheduling also improves [24]. The simulation conducted in [24] also concludes that the Cross-CC PF algorithm provides the best fairness even comparing to round robin algorithm [71] or Figure 4-15. So far, the Cross-CC PF is the most recommended algorithm for the LTE-A system.

4.1.2. Simulation results

The simulation parameters can be summarized in Table 4-1. This table does not include the input variables like number of users and PS algorithms as they will be set differently in each scenario.

Parameter	Value/description
Test scenario	7 hexagon cells with wrap-around function
Cell radius	200m
Mobile height	1.6m
Base station height	**18m**
Number of Component Carriers	2 CC of 5MHz (25RB each CC)
Component Carriers band	800MHz, 2GHz
User type	LTE & LTE-A users co-existence with different percentage
User location	Uniformly distributed in all cells
User speed	3kmph
Traffic pattern	Real-time traffic, full buffer and finite buffer (Poisson arrival with fixed buffer size of 1 Mbps)
Propagation model	Okumura-Hata
Operations involve	Handover, CoMP, Multiple Carrier Components.

Table 4-1: System simulation configuration

The simulation can model multiple CCs in different or same frequency. In case of the same frequency band, it is assumed that the coverage area of two bands of a base station are the same. The first result to be presented in the graph below is simulated in the setting of two CCs in the same band of 800 MHz. This simulation result recalls the paper [44], with its correspondent graph is nearly comparable with this.

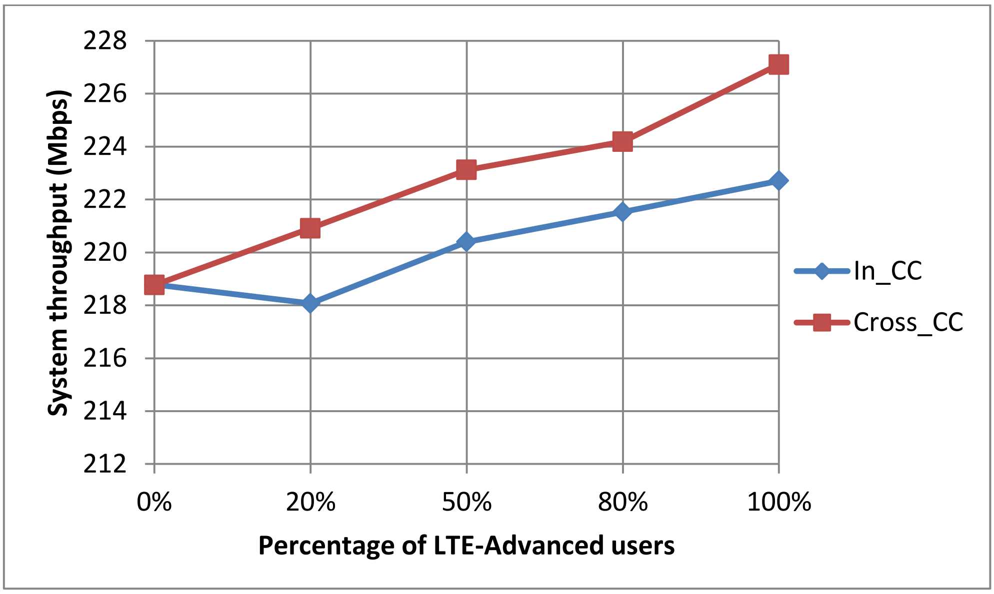

Figure 4-1: System throughput, in-CC vs. cross-CC

By using the Proportional Fair algorithm in cross-CC and independent-CC (in-CC) schedulers according to the Equations (4-1) and (4-3), the cross-CC is seen to have a better performance over in-CC scheduler. System throughputs of cross-CC in most cases are slightly higher than that of in-CC by around 1%.

Moreover, the cell edge users' throughputs in cross-CC are better than in-CC. The biggest improvement is seen in the 50-50 scenario with 69% improvement. This result correctly reflects the graph in Figure 2-21 of [44].

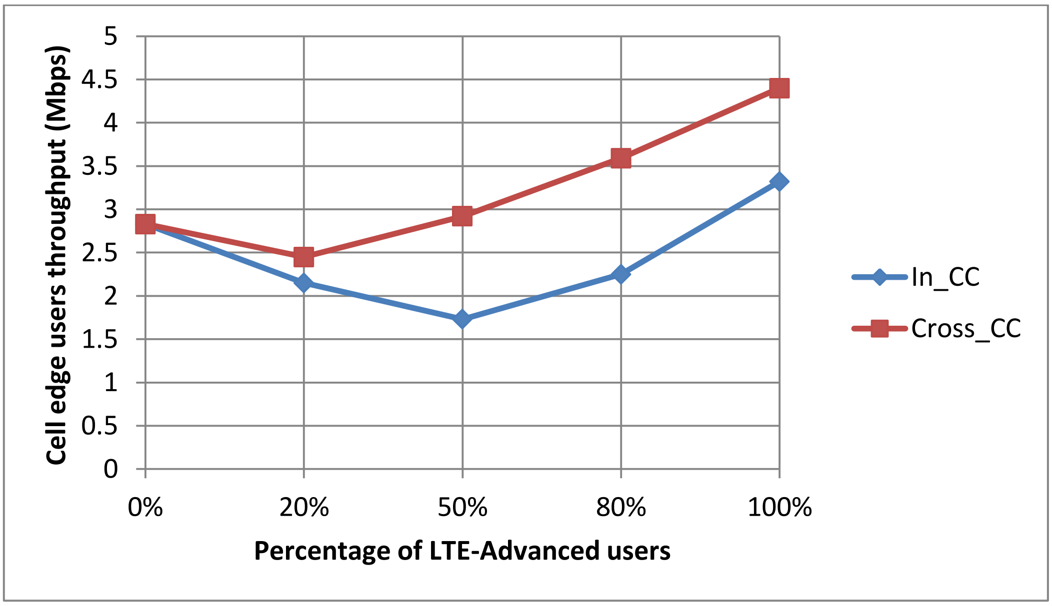

Figure 4-2: Cell edge users throughput, in-CC vs. cross-CC

The graph shown in the figure below displays the differences of the system throughputs in two cases (in-CC and cross-CC) as number of users increases. Cross-CC always has better performance over in-CC scheduler. This result consistently reflects result obtained in paper [24] with Figure 2-20 in the previous session, and in paper [45].

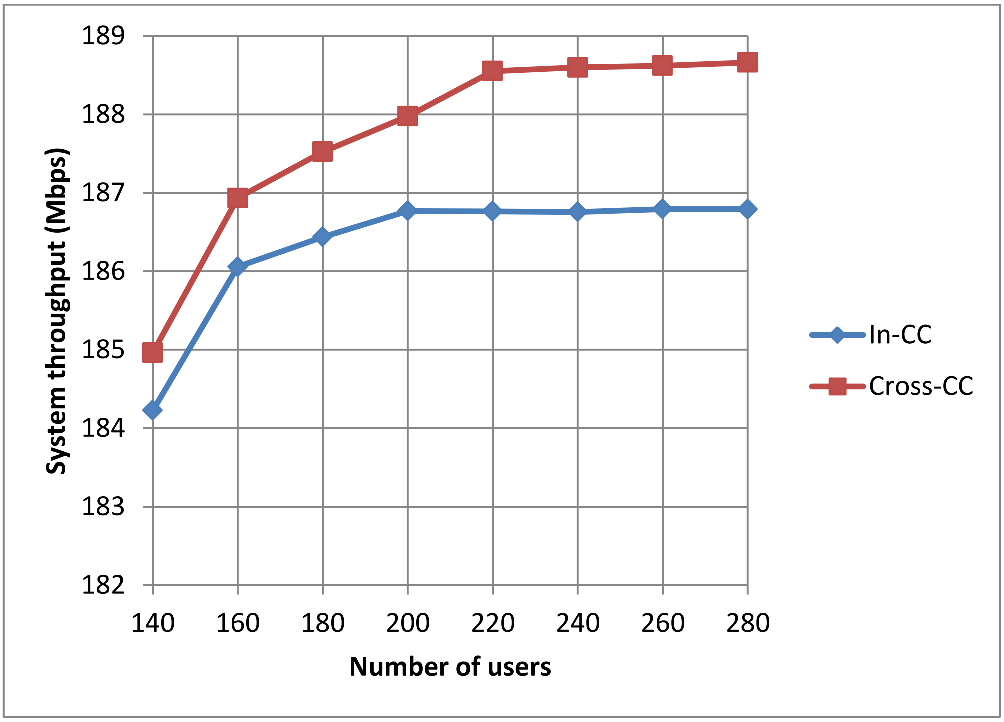

Figure 4-3: System throughput

4.2. Cross-CC vs. In-CC scheduler with other algorithms

4.2.1. Theory discussion

The advantage of this simulation tool is that it can simulate PS mechanism with 2 schedulers, in-CC and cross-CC. Therefore, each algorithm can be compared in two scenarios. The difference between two schedulers with PF algorithm has been presented in previous section. However, in algorithms (such as Round Robin and Max-Rate) whose concept does not involve with multiple CCs, there is no difference between in-CC and cross-CC.

For Round Robin algorithm (as discussed in the literature review section) allocates active users to each RB consecutively and equality in rotation within each CC. For example, in a particular CC, if there are three active users (User 2, 5 and 7), then the scheduler will allocate RB to the three users continuously (2, 5, 7, 2, 5, 7 …) in each TTI. The change from in-CC scheduler to cross-CC scheduler does not affect this logic. Therefore, the system performance is unchanged between the two schedulers using Round Robin algorithm.

Regarding Max Rate algorithm, its concept is to allocate user with the best CQI in a particular RB to this RB. The decision is made among the collection of active users operating within each CC. The cross-CC scheduler also must follow this concept, consequently, there is no difference between in-CC and cross-CC scheduler.

In terms of M-LWDF algorithm, the formula for in-CC scheduler is

$$M_{k,i,j} = a_i W_i \frac{r_{k,i,j}(t)}{R_{k,i}(t)} \tag{4-6}$$

with

$$a_i = -\frac{(\log \delta_i)}{\tau_i} \tag{4-7}$$

where W_i is the head-of-line (HOL) packet delay of user i at time t, τ_i is the delay threshold of user i and δ_i denotes the maximum probability for HOL packet delay of user i to exceed the delay threshold.

Following the same approach with PF, the formula for cross-CC scheduler is defined as:

$$M_{k,i,j} = a_i W_i \frac{r_{k,i,j}(t)}{R_i(t)} \tag{4-8}$$

Since the change of M-LWDF from in-CC to cross-CC formula is the same with PF (the same change of denominator in the metric formula), we can expect the same effect that cross-CC scheduler can make to the system performance with this M-LWDF algorithm.

4.2.2. Simulation results

In the setting of two CCs in different bands, one in 800 MHz and one in 2 GHz, the simulation can model more complex network. The current simulation code can perform four algorithms in two types of scheduler (in-CC and cross-CC). The implemented algorithms are Round Robin, Max Rate, Proportional Fair and M-LWDF. Totally, eight different scheduling scenario can be examined with this simulation tool.

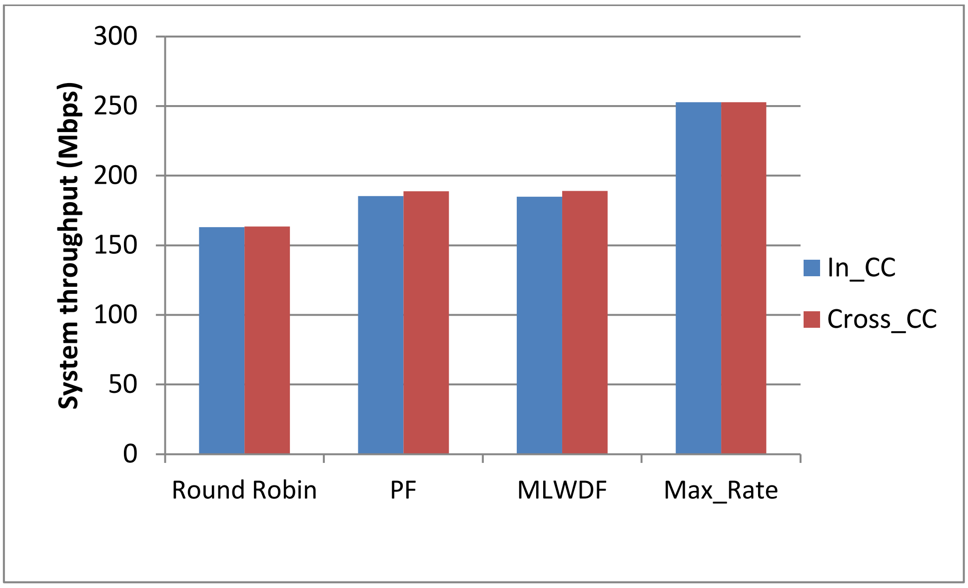

Figure 4-4: System throughput, algorithms comparison

The above graph reflects exactly the performance of eight algorithms. Max Rate always have the highest throughput, Round Robin is the worst while PF and M-LWDF are in the middle.

In terms of comparison of cross-CC and in-CC, with Round Robin and Max Rate, the system throughputs are similar for cross-CC and in-CC. This is logical since there are no difference factor in the two types of scheduler when applying these algorithms. But for PF as well as M-LWDF, the cross-CC scheduler takes into account the average user data rate over multiple CCs while the in-CC does not. Then it creates the difference that the cross-CC scheduler provides better system throughput than in-CC.

In terms of fairness, the simulation shows that Max Rate is worst in all cases. It is obvious because this algorithm allocates RBs for the best users which usually locate near the eNodeB. Many cell-edge users might never be scheduled. It causes unfairness, or low fairness performance of this algorithm. For in-CC, Round Robin is fairest, while PF and M-LWDF have moderate fairness. However, for cross-CC, **PF and M-LWDF are the best algorithm in terms of fairness**. This interesting result proves the advantage of cross-CC over in-CC scheduler.

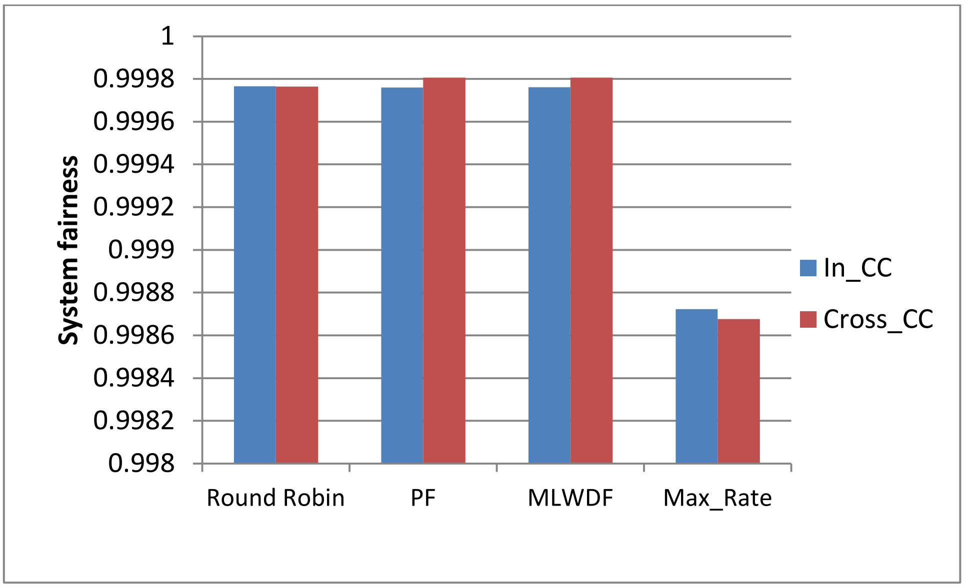

Figure 4-5: System fairness

For confirmation, the output result was checked by another fairness algorithm [68] which was presented in Section 3.2.3.iv. In this algorithm, the lower the fairness index, the better the PS algorithm. It shows the same result that PF and M-LWDF are the best PS algorithm.

Figure 4-6: System fairness, new algorithms of fairness

The simulation can show other system performance criteria like system delay and packet loss ratio, as illustrated in the figures below.

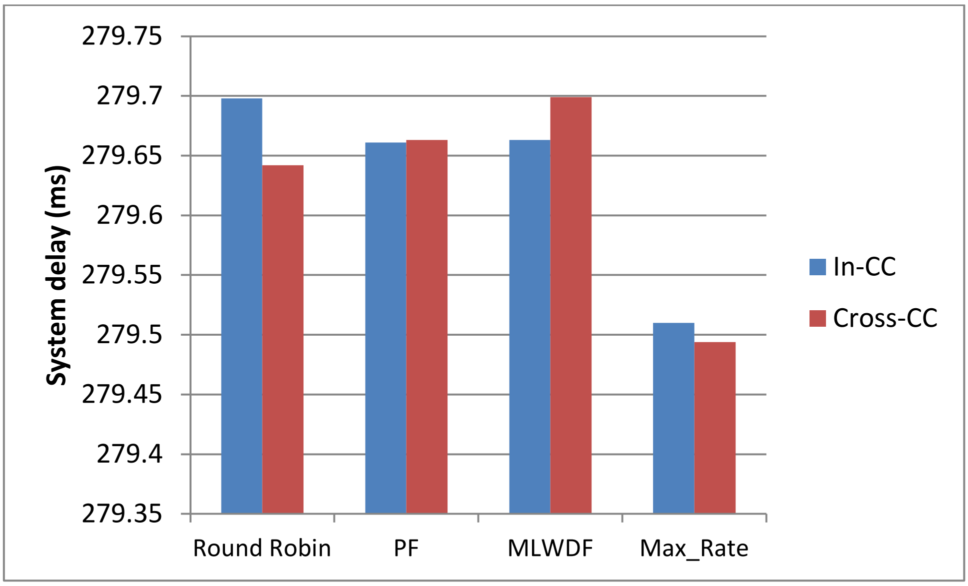

Figure 4-7: System delay

There is no major difference among these PS algorithms in terms of system delay, since the differences are so small, under 1 ms. In terms of packet loss ratio (PLR), the logic of the result is the higher throughput, the lower the packet loss.

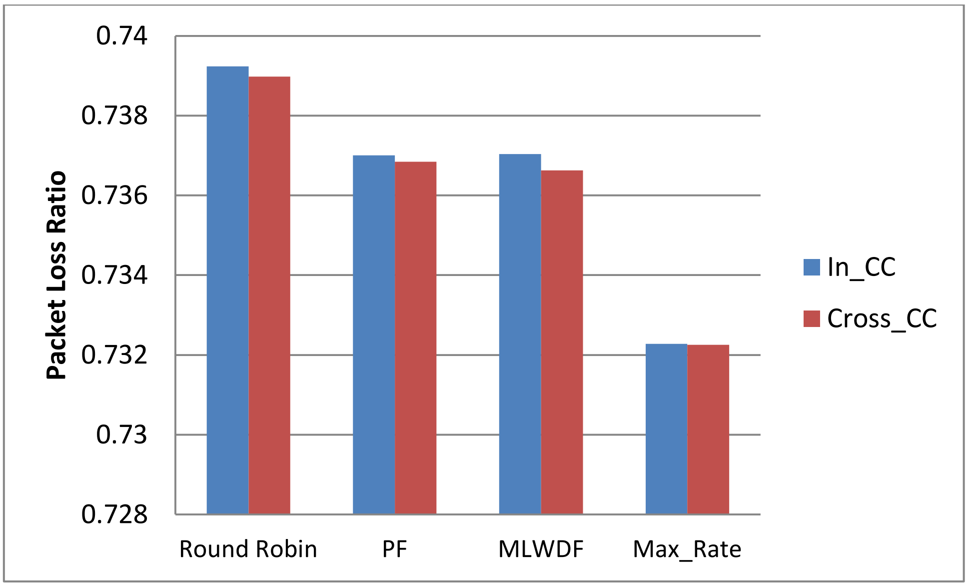

Figure 4-8: Packet Loss Ratio

With four algorithms carried out by two different types of schedulers tested so far, simulation results prove that cross-CC scheduler using Proportional Fair and its modified version, M-LWDF, are the best algorithm for LTE-Advanced. It can provide good system throughput and best fairness for all users including LTE, LTE-Advanced, and especially for cell-edge users.

In above graphs, there is no difference between PF and M-LWDF. It is because the incoming traffic pattern of eNodeB in this simulation scenario is full buffer. This is the unrealistic traffic for testing only. It cannot be used for real services with defined QoS requirements. The difference between PF and M-LWDF as well as full buffer traffic and finite traffic will be discussed later in section 4.3.2.B.

4.3. Proposed PS algorithm for LTE-Advanced

4.3.1. Theory discussion

A. Optimized Cross-CC PF algorithm

As discussed above, cross-CC PF algorithm is the best algorithm for LTE-Advanced. However, there is a major disadvantage of this algorithm that can make it become infeasible.

Consider a case that there are two users – one LTE and one LTE-A – with the same CQI for whole transmission (e.g. they are located at the same place), their instantaneous data rate in all RBs are correspondingly the same. If LTE-A user want to be allocated in any RB, its metric M must be higher than the LTE user's metric:

$$M_{LTE\text{-}A} \geq M_{LTE}$$

So based on Equation (4-1) or (4-3):

$$R_{LTE\text{-}A} \leq R_{LTE}$$

This means that total average data rate of LTE-A user must be less than or equal to LTE user's data rate, no matter how many CCs this LTE-A user operates on. To be clearer, if average data rate of LTE-A user is higher than average data rate of LTE user, LTE-A user will not be allocated any RB. Instead, LTE user is allocated for those RBs until LTE user's throughput is higher than LTE-A user's throughput. For the whole duration of a call, the average data rate of LTE-A user therefore cannot get higher than LTE user's.

This is unacceptable since the purpose of new feature "supporting wider bandwidth" of LTE-A is to increase the data rate of LTE-A users with multiple CCs multiple number of times. For example, LTE-A user who runs on five CCs may wish to get five times data rate than user on one CC with the similar radio condition, but this algorithm will constrain that LTE-A user so that its average data rate is as low as one CC user (in the context that a

LTE-A user have to compete with LTE users in every 5 CC, 1 LTE-A + 5 LTE users. If there are no other users in other bands, there's no competition, so it's not the case we need to discuss).

The following algorithm with a new metric calculation called Optimized Cross-CC PF (OCPF) can solve this problem while maintaining other advantages of cross-CC PF algorithm.

$$M_{k,i,j} = \frac{r_{k,i,j}(t)}{\frac{\sum_{k=1}^{N} R_{k,i}(t)}{N_i}} \tag{4-9}$$

N_i is the number of CCs that user i can transmit on.

The corresponding modification to Equation (4-4) is as follows

$$M_{k,i,j} = \frac{r_{k,i,j}(t)}{\frac{R_i(t)}{N_i}} \tag{4-10}$$

The denominator of cross-CC PF formula is changed from total average data rate to the average data rate per CC. N_i is not fixed but varied based on number of CCs that a user actually operates.

B. Optimized Cross-CC M-LWDF algorithm

This new concept can be applied to another well-known PS algorithm to support real-time services called the Modified-Largest Weighted Delay First (M-LWDF) [33]. This algorithm is an evolution of the PF algorithm to support different QoS requirements for the users as it accounts delay parameter into its metric formula. The scheduling metric of M-LWDF algorithm with cross-CC scheduler are given as follows:

$$M_{k,i,j} = a_i W_i \frac{r_{k,i,j}(t)}{R_i(t)} \tag{4-11}$$

and

$$a_i = -\frac{(\log \delta_i)}{\tau_i} \tag{4-12}$$

where W_i is the head-of-line (HOL) packet delay of user *i* at time *t*, τ_i is the delay threshold of user *i* and δ_i denotes the maximum probability for HOL packet delay of user *i* to exceed the delay threshold. Since M-LWDF jointly considers HOL delay along with PF properties, it can maximize the number of users that can be supported with the desired QoS, as well as obtain a good throughput and fairness performance along with a relatively low PLR.

The modified formula for M-LWDF (called Optimized Cross-CC M-LWDF algorithm, OCM) following proposed concept is:

$$M_{k,i,j} = a_i W_i \frac{r_{k,i,j}(t)}{\frac{R_i(t)}{N_i}} \tag{4-13}$$

The simulation results in the following sections will explain and prove the advantages of these new algorithms, namely Optimized Cross-CC PF (OCPF) for Equation (4-10) and Optimized Cross-CC M-LWDF (OCM) for Equation (4-13).

4.3.2. Simulation results

A. Optimized Cross-CC PF Algorithm

This section will discuss the simulation results of Optimized Cross-CC PF, which was explained in Section 4.3.1.A, in comparison with other PF algorithms.

The simulation scenario consists of two CCs on the 800 MHz band with 280 users using five algorithms:

- In-CC PF following Equation (4-1).
- Cross-CC PF from Equation (4-3), named cross-CC PF type A and from (4-4), named cross-CC PF type B.
- Optimized Cross-CC PF, the new proposed algorithm following Equation (4-9) named OCPF type A and (4-10), named OCPF type B.

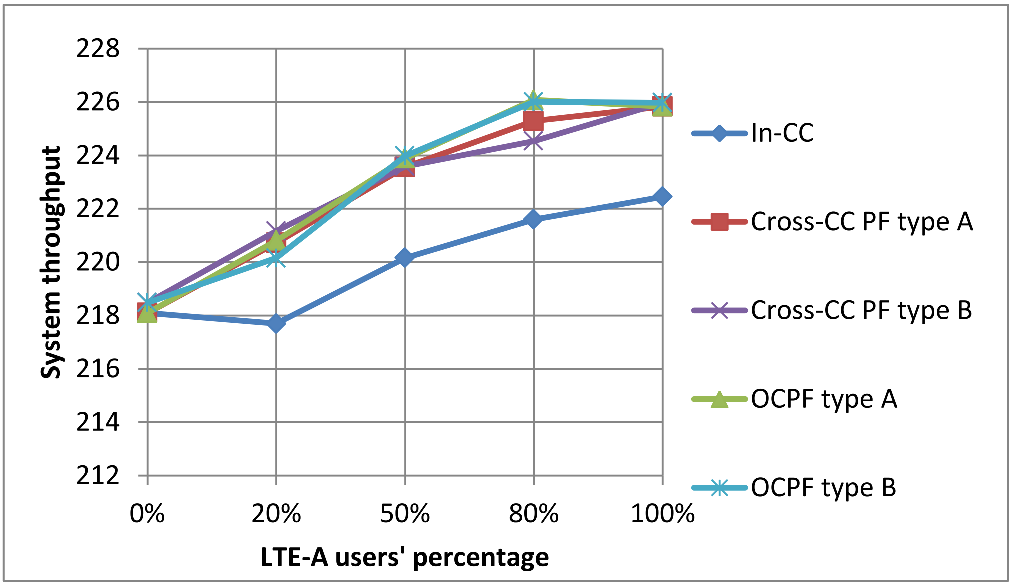

Figure 4-9: System throughput

Figure 4-9 shows the system throughputs in all seven cells for the five algorithms. New optimized algorithms have similar system throughputs with the cross-CC PF in most cases, and all four of them have higher throughput than the in-CC PF.

Meanwhile, LTE-A users' throughput in the new algorithm increase significantly comparing to the cross-CC PF. In Figure 4-10 at 20% LTE-A users' case, the improvement can reach as high as 96%. This is logical since the new algorithm liberates the transmission capacity of LTE-A users so that it could double its data rate since LTE-A users operate on two CCs. By the same logic, in case system has four or five CCs, this algorithm can increase LTE-A users' throughput four or five times that of the cross-CC PF algorithm.

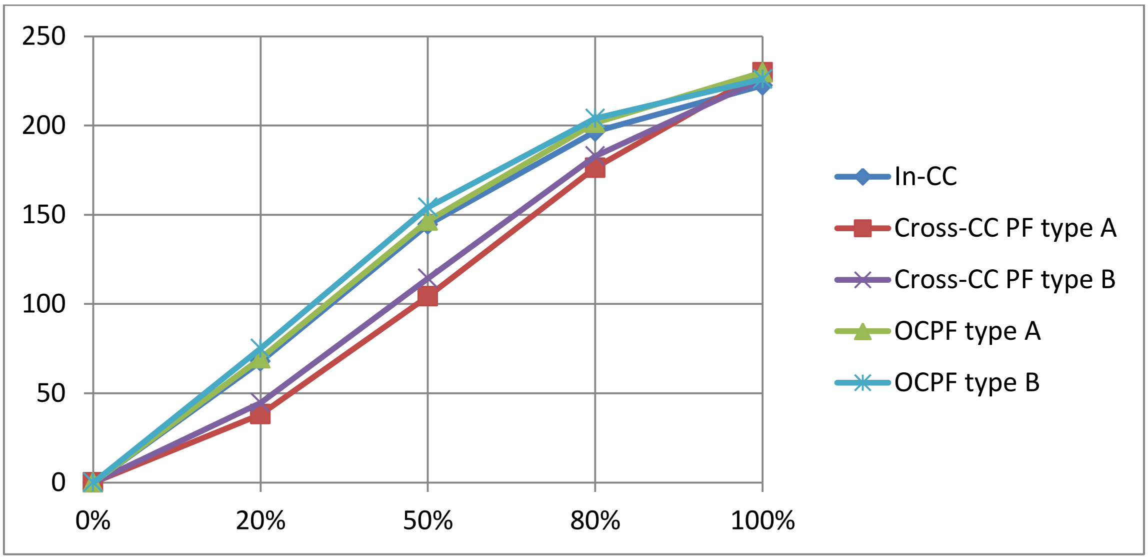

Figure 4-10: LTE-A users' throughput

Percentage of LTE-A users	0%	20%	50%	80%	100%
In-CC	0	67.79	144.49	196.6	222.45
Cross-CC PF type A	0	38.21	104.28	176.3	229.833
Cross-CC PF type B	0	44.72	114.33	182.84	225.978
OCPF type A	0	69.56	146.58	201.47	229.833
OCPF type B	0	75.12	154.17	203.99	225.978
Improvement of OCPF type B to Cross-CC PF type A		**96.6%**	47.8%	15.7%	

Table 4-2: LTE-A users' throughput

With the criteria of throughput shown in the graphs above and other performance criteria, there are minor differences between the results of Equation (4-3) and (4-4), also with (4-9) and (4-10), but for simple and clear presentation, the simulation results for other criteria just display the cross-CC PF algorithm from Equation (4-4) and Optimized Cross-CC PF from Equation (4-10).

For throughput of the cell-edge users or the worst 5% users, Figure 4-11 shows that the new algorithm is similar as the In-CC PF. While in another case, the throughput of best 5% users with new algorithm is the best among three algorithms, as presented in Figure 4-12. The highest improvement is 30% at 20% LTE-A user case.

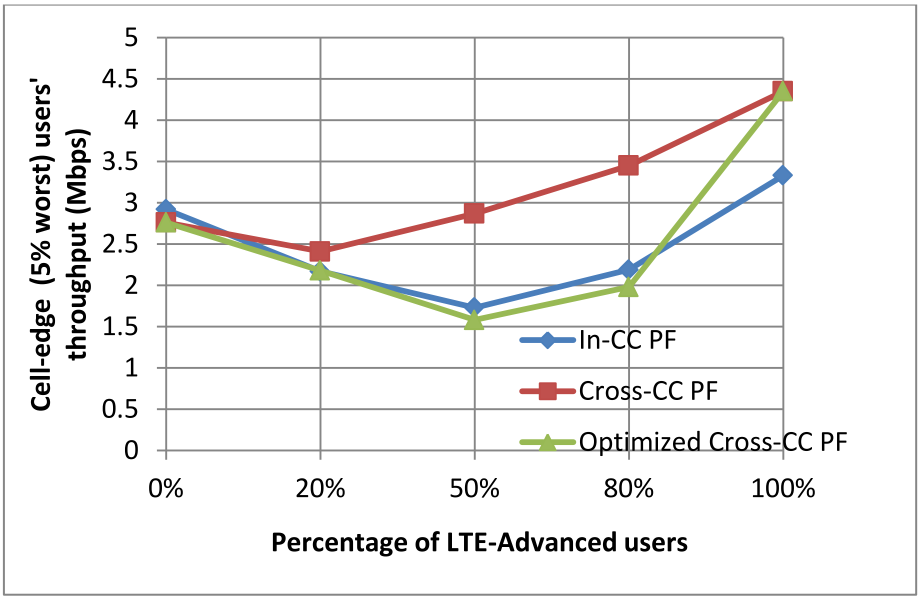

Figure 4-11: Cell-edge users' throughput

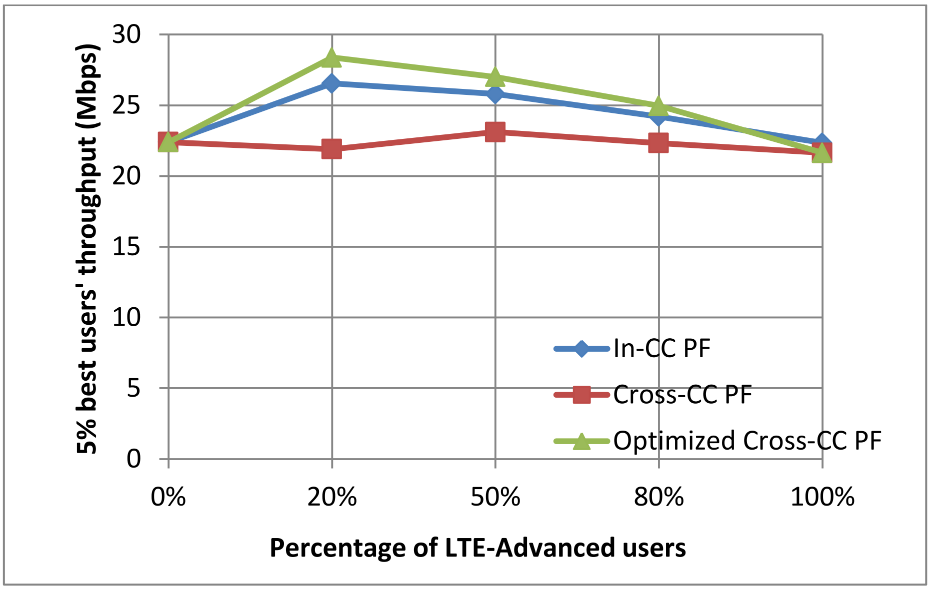

Figure 4-12: 5% best users' throughput

Percentage of LTE-A users	0%	20%	50%	80%	100%
In-CC PF	22.4	26.54	25.8	24.2	22.34
Cross-CC PF	22.4	21.9	23.11	22.33	21.64
Optimized Cross-CC PF	22.4	28.37	27.01	24.96	21.64
Improvement of OCPF to Cross-CC PF		30%	17%	12%	

Table 4-3: 5% best users' throughput

Furthermore, this optimized cross-CC PF algorithm is also being tested in other contexts and settings. The graph shown in the Figure 4-13 displays the differences of system throughputs in three algorithms as number of user increases with 50% LTE-A users. The simulation result shows that the effect of the new algorithm is more significant in this scenario, as the system throughput of the new algorithm is always higher than the cross-CC PF by around 6% in all cases.

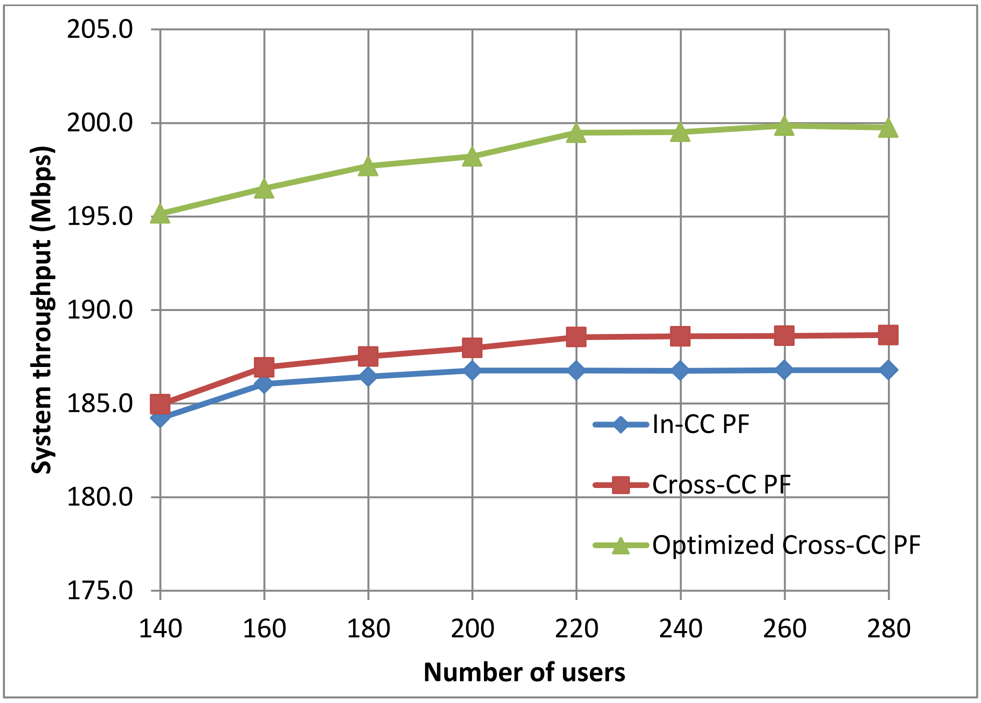

Figure 4-13: System throughput with 50% LTE-A users

Number of Users	140	160	180	200	220	240	260	280
In-CC PF	184.2	186.1	186.4	186.8	186.8	186.8	186.8	186.8
Cross-CC PF	185.0	186.9	187.5	188.0	188.6	188.6	188.6	188.7
Optimized Cross-CC PF	195.2	196.5	197.7	198.2	199.5	199.5	199.9	199.7
Improvement of OCPF to Cross-CC PF	6%	5%	5%	5%	6%	6%	6%	6%

Table 4-4: The system throughput of 3 algorithms

In the setting of two CCs in different bands, one in 800 MHz and one in 2 GHz, the simulation result shows similar improvement. In this scenario, LTE-A users who are located outside the coverage of 2 GHz CC can work on 800 MHz CC only, while LTE-A users in 2 GHz can communicate on 2 CCs simultaneously, as shown in Figure 2-23. So in case of 100% LTE-A users, it does not mean all users are served on 2 CCs. Therefore, the logic of new algorithm still impacts the metric calculation in this case. The improvements of OCPF algorithm comparing to In-CC PF and Cross-CC PF are around 12% and 6%, respectively (Figure 4-14).

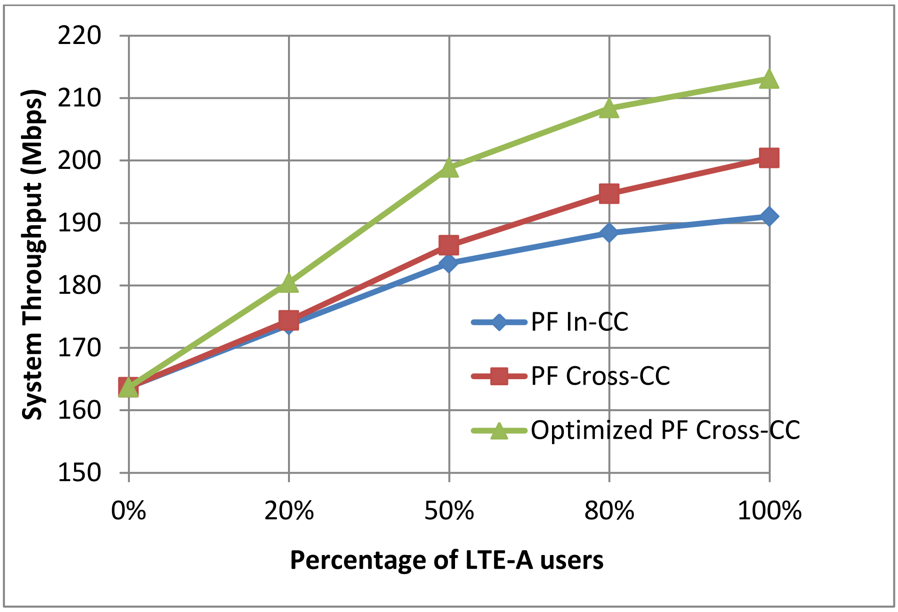

Figure 4-14: System throughput in scenario of different CC bands (800MHz + 2GHz)

	0%	20%	50%	80%	100%
In-CC PF	163.686	173.67	183.573	188.396	191.03
Cross-CC PF	163.697	174.37	186.416	194.665	200.408
Optimized Cross-CC PF	163.697	180.439	198.882	208.375	213.111
Improvement of OCPF to In-CC PF		4%	8%	11%	12%
Improvement of OCPF to Cross-CC PF		3%	7%	7%	6%

Table 4-5: System throughput in scenario of 2 different CC bands (800MHz & 2GHz)

In terms of fairness, the simulation results show that the new cross-CC PF decrease slightly compared to other algorithms but it is still much better than the Max Rate algorithm (0.6 of PCPF compare to 1.2 of Max Rate). In Figure 4-15, the smaller the fairness index, better the fairness is.

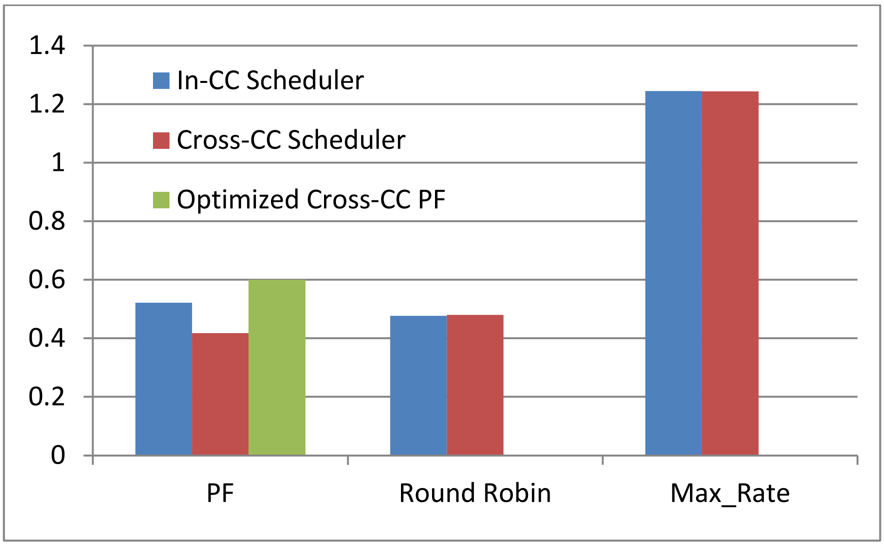

Figure 4-15: System fairness

B. Optimized Cross-CC M-LWDF algorithm

With M-LWDF, an upgraded version of PF to support different QoS requirements of users, the results of Optimized Cross-CC M-LWDF (OCM) algorithm is almost the same with OCF in all performance criteria with full buffer traffic, as described in section 4.3.1.B. But taking QoS requirements of users into consideration, the traffic pattern is changed to finite buffer traffic (1 Mbps per user, more realistic traffic than full buffer) so that the difference and advantage of M-LWDF can be recognized.

The QoS requirements are specified by 3GPP in [72] as presented by Table 4-6, e.g. for conversational voice service, the end-to-end delay threshold is 100 ms, the packet loss ratio (PLR) threshold is 10^{-2}.

QCI	Resource Type	Priority	Packet Delay Budget	Packet Error Loss Rate	Example Services
1	GBR (RT)	2	100 ms	10^{-2}	Conversational Voice
2		4	150 ms	10^{-3}	Conversational Video (Live Streaming)
3		3	50 ms	10^{-3}	Real Time Gaming
4		5	300 ms	10^{-6}	Non-Conversational Video (Buffered Streaming)
5	Non-GBR (NRT)	1	100 ms	10^{-6}	IMS Signalling
6		6	300 ms	10^{-6}	Video (Buffered Streaming) TCP-based (e.g., www, e-mail, chat, ftp, p2p file sharing, progressive video, etc.)
7		7	100 ms	10^{-3}	Voice, Video (Live Streaming) Interactive Gaming
8		8	300 ms	10^{-6}	Video (Buffered Streaming) TCP-based (e.g., www, e-mail, chat, ftp, p2p file sharing, progressive video, etc.)
9		9			

Table 4-6: Standardized QCI characteristics [72]

In the mentioned context, the OCM algorithm has the similar performance when compared with OCPF in most criteria: throughput, fairness. The throughput of OCM is slightly higher than others, as shown in Table 4-7 or Figure 4-16.

		20	40	60	80	100	120	140	160	180	200
Cross-CC	**PF**	20.5	41.0	61.4	81.7	101.7	121.2	139.8	159.2	173.1	188.5
	MLWDF	20.5	41.0	61.4	81.8	102.2	122.7	142.2	159.9	172.4	185.3
Optimized Cross-CC	**PF**	20.5	41.0	61.4	81.7	100.5	120.3	139.9	159.2	173.5	186.4
	MLWDF	20.5	41.0	61.4	81.8	102.2	122.7	142.6	159.9	173.0	186.6

Table 4-7: System throughput with M-LWDF

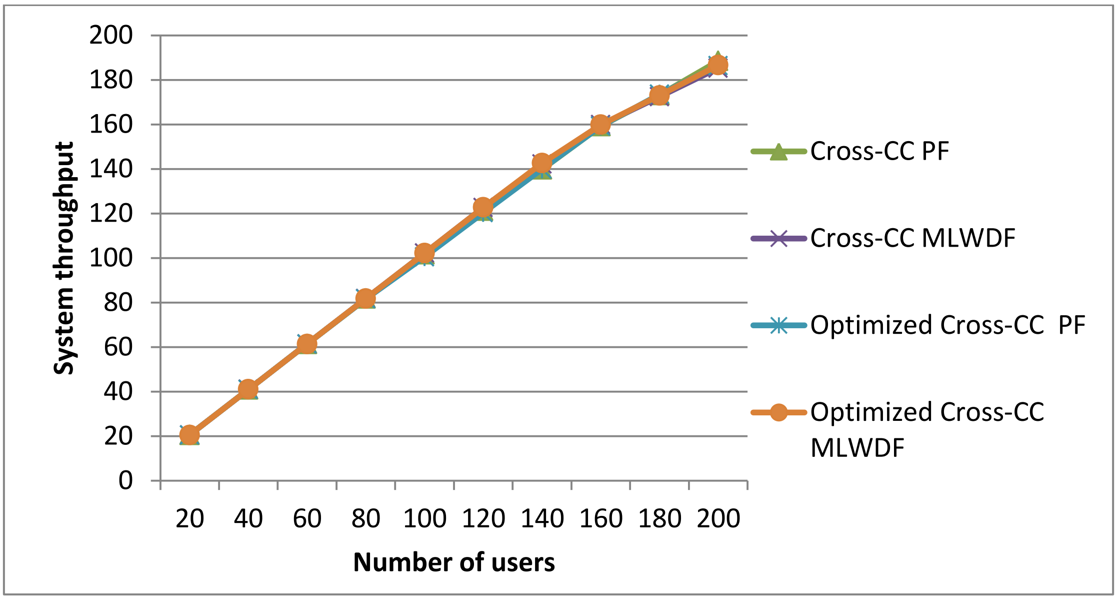

Figure 4-16: System throughput with M-LWDF

The most signification improvement is resided on PLR criterion. In the setting of packet delay budget of 150 ms for live streaming video service and the acceptable PLR is 10^{-3}, the simulation results are given in the table below:

		20	40	60	80	100	120	140	160	180	200
Cross-CC	PF	0	0	0	1.2E-05	0.002	0.008	0.017	0.018	0.043	0.057
	MLWDF	0	0	0	3.8E-05	0	0	2.35E-05	0.004	0.027	0.049
Optimized Cross-CC	PF	0	0	0	0	0.013	0.016	0.018	0.021	0.042	0.065
	MLWDF	0	0	0	0	0	0	0	0.005	0.02	0.044

Table 4-8: Packet loss ratio data

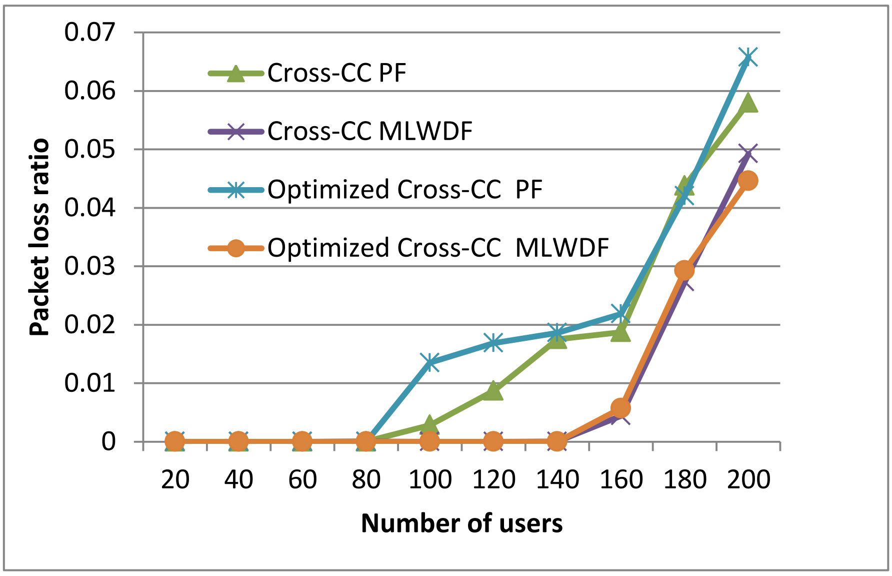

Figure 4-17: Packet loss ratio

According to Figure 4-17, M-LWDF algorithm can increase the number of user that can be supported with the PLR lower than 10^{-3} from 80 users to 140 users, comparing to PF algorithms. This graph also shows that the OCM algorithm has the same effect with original M-LWDF. Meanwhile, the OCPF has the same PLR with cross-CC PF in low system load, zero percentage up to 80 users. While above that load, it is worse than cross-CC PF insignificantly.

In summary, while maintaining all the advantages of OCPF, the OCM algorithm also has the ability to maintain low packet loss ratio in order to support more services with different QoS requirements. It can provide the best system throughput and LTE-A users' throughput as well as maintain QoS for data transmission from the eNodeB to all mobile devices in the LTE-Advanced network.

4.4. Summary

In this chapter, the comparison between cross-CC and in-CC scheduler is discussed. The simulation results confirm that cross-CC scheduler is far better than in-CC. Several well-known algorithms such as Round Robin, Max Rate, Proportional Fair and M-LWDF are evaluated by the LTE-Advanced simulator. Finally, two algorithms have been proposed for packet scheduling in LTE-A. The simulation results show that these two algorithms are optimized solutions that should be applied when the LTE-A system is deployed in reality.

CHAPTER 5: CONCLUSION

The thesis has presented research works that had been conducted for developing a new packet scheduling algorithm for LTE-Advanced. A comprehensive literature review of the topics covering LTE, LTE-A, PS mechanisms, PS algorithms was presented. This thesis also briefly explains how a new simulation tool is developed to model LTE-A technology as well as to adopt several well-know algorithms for LTE-A. The results of the tool prove that this simulation tool is working as anticipated. Based on this work, new algorithms for LTE-Advanced can be modeled and simulated by this tool. Its performance can be evaluated and compared with other algorithms.

The thesis also reviews proposed algorithms for LTE-A. It shows that the cross-CC PF is the most recommended for LTE-A with the good performance on fairness, as well as system and cell-edge users' throughput. However, cross-CC PF has a big drawback as it limits the data rate of LTE-A users running on multiple carriers so that the LTE-A users cannot get higher data rate than a single carrier user.

The simple solution modified from traditional PF algorithm can solve that problem completely. This proposed algorithm is named Optimized Cross-CC PF (or OCPF). Furthermore, the simulation results show that this new algorithm can improve performance criteria like system throughput and LTE-A users' throughput in most scenarios, while other criteria like fairness, packet loss ratio and system delay remain the same or mitigate slightly. Furthermore, as taking the QoS requirements of user into account, the modified cross-CC M-LWDF algorithm based on proposed concept, named Optimized Cross-CC M-LWDF (or OCM), can provide more realistic and effective solution for PS mechanism with the best PLR and system delay. The simulation results have proved that these algorithms are more optimized algorithm for LTE-A with multiple component carriers.

In terms of the future research works, this project can be expanded to analyze carefully on other new features of LTE-A such as CoMP, Relaying and MIMO. Although some of these features such as CoMP were already built into this simulation tool, the effects of these functions were not studied in detail due to time limitations. Relaying and MIMO functions were not fully developed in the simulation tool. These new features need considerable effort to precisely model in this computer simulation tool. The mathematical throughput analysis of the new PS algorithms should be discussed in the future works.

To conclude, the packet scheduling algorithms proposed in this project are suitable not only for LTE-A technology but also for any technology using multiple component carriers such as WirelessMAN-Advanced, the new 4G technology from WiMAX family [73], or CDMA EVDO [74]. It is strongly believed that these algorithms are highly practical and it will be applied in the real network once this LTE-A technology is launched in the near future.

APPENDIX

The actual images of the simulation tool

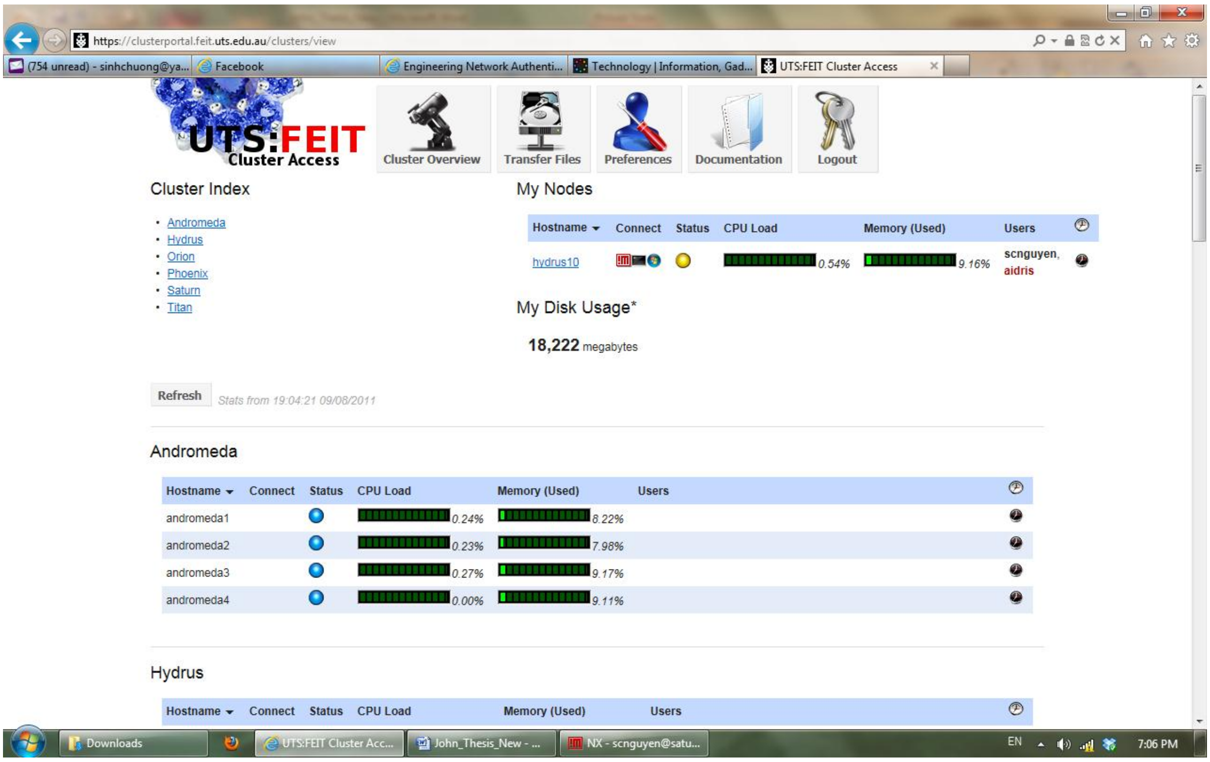

UTS cluster interface

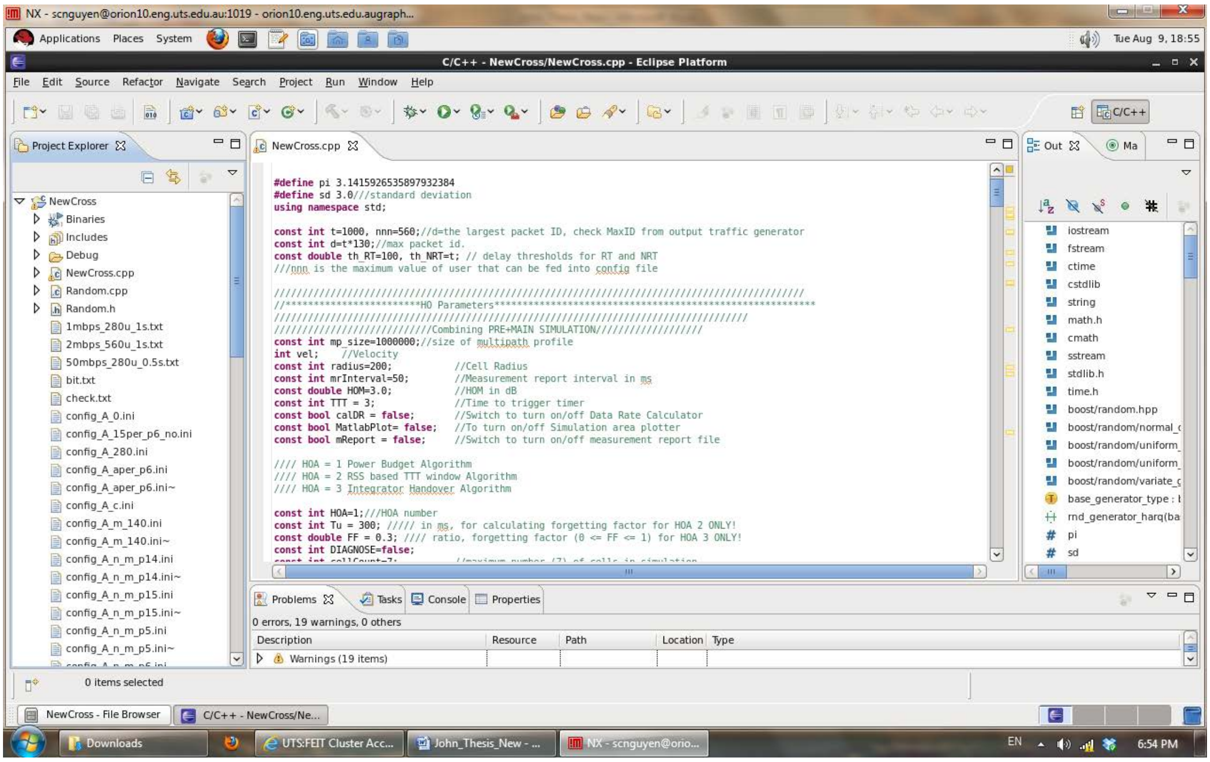

C++ Eclipse Platform

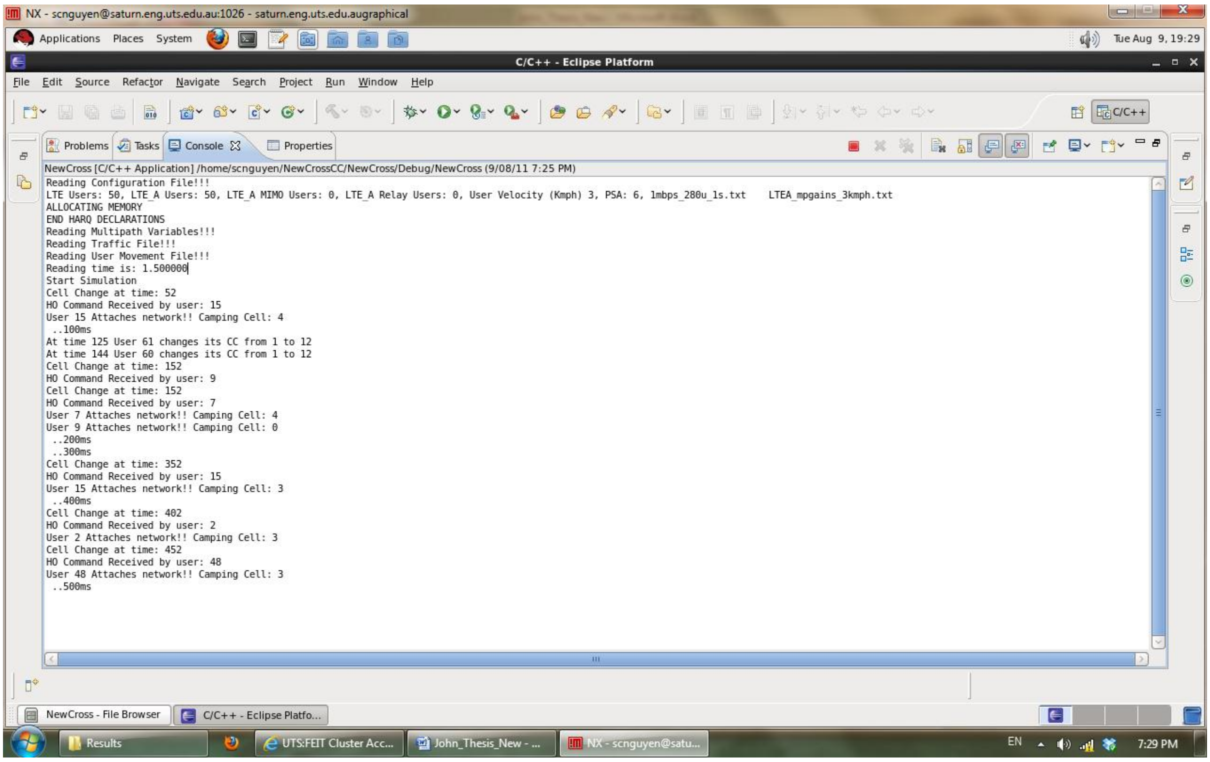

The image of the simulation when it starts running

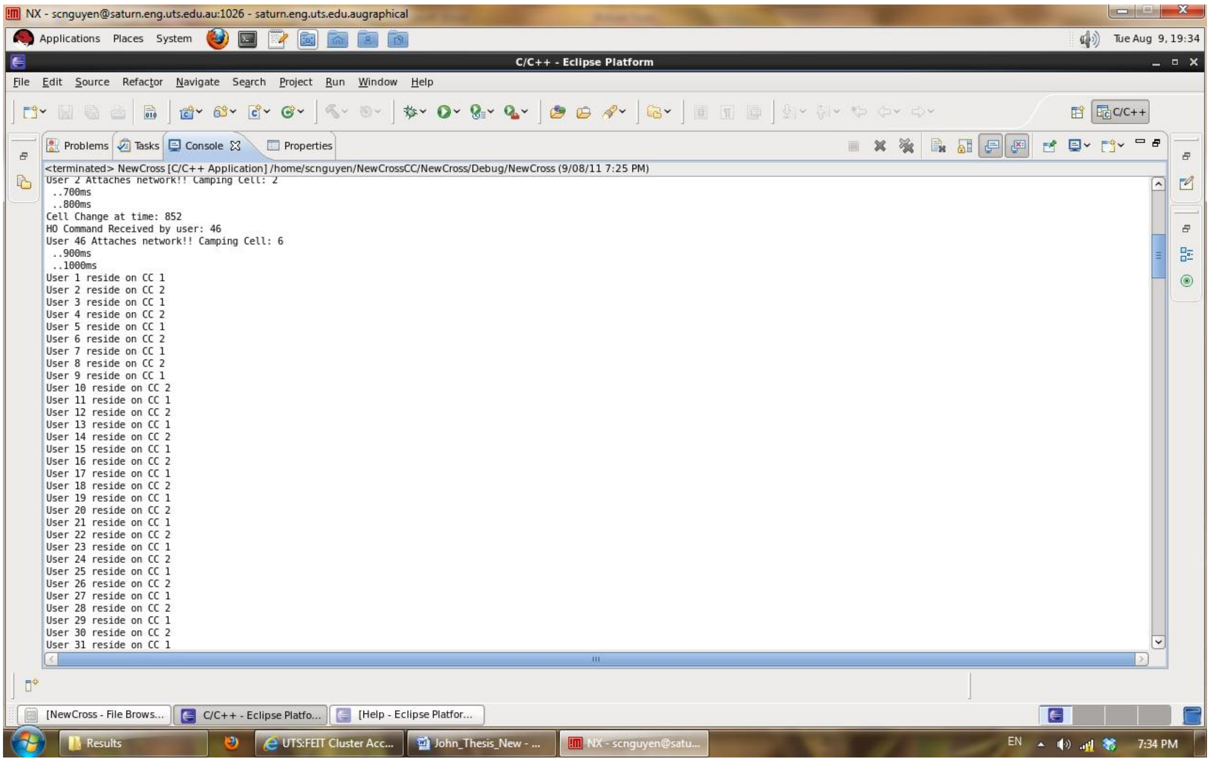

The simulation displays users with their located CC.

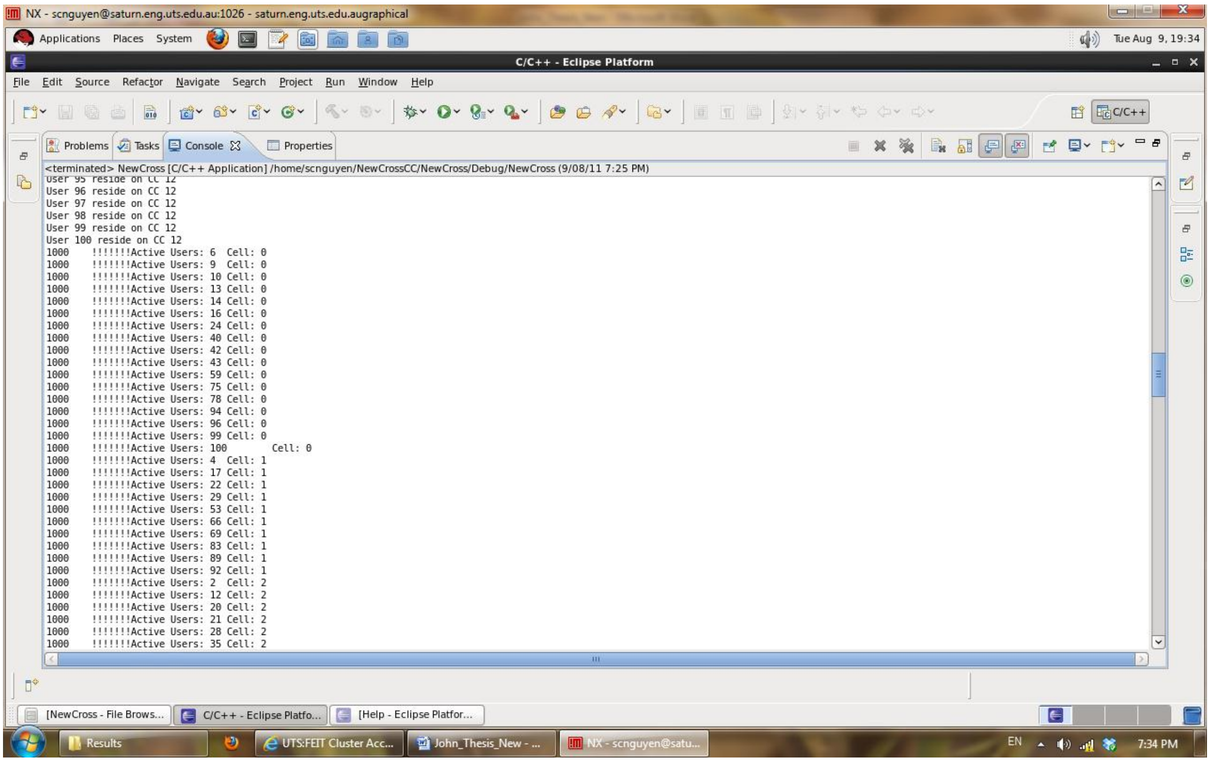

The simulation displays users with their serving cell.

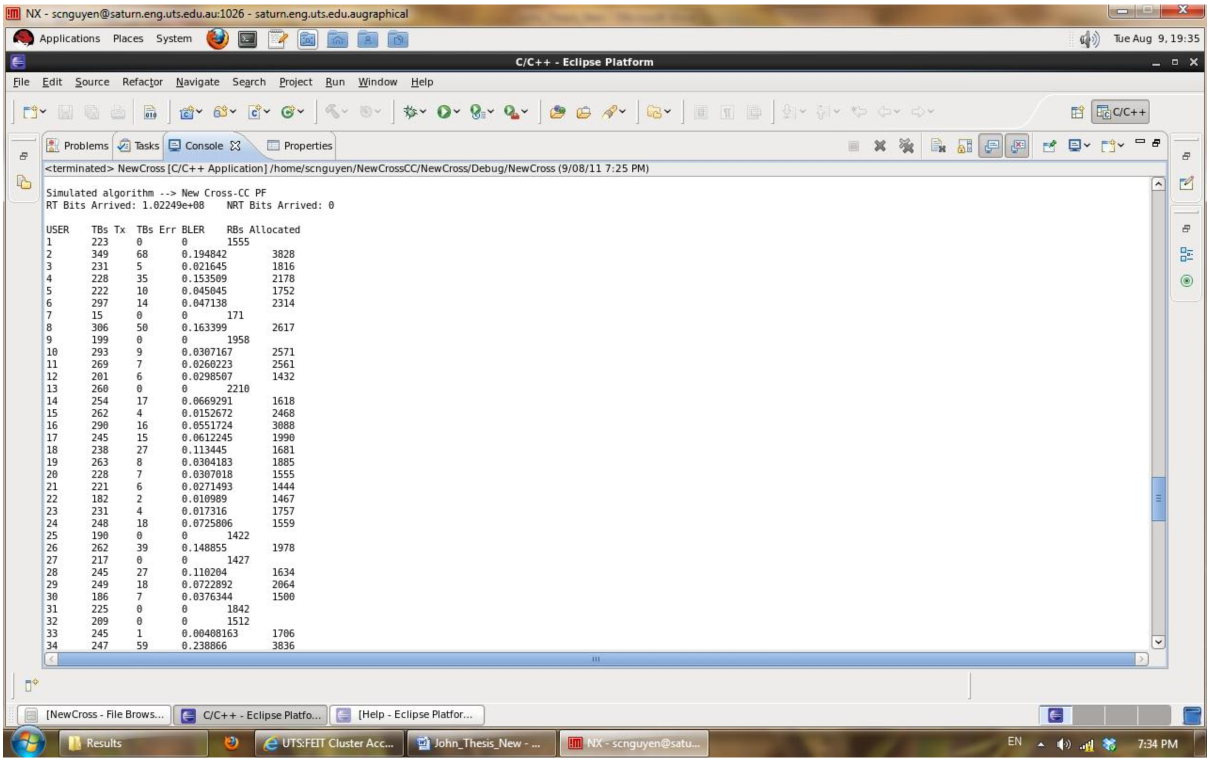

As the simulation finish, it displays users with their number of TB (Transport Block), number of allocated RBs, etc.

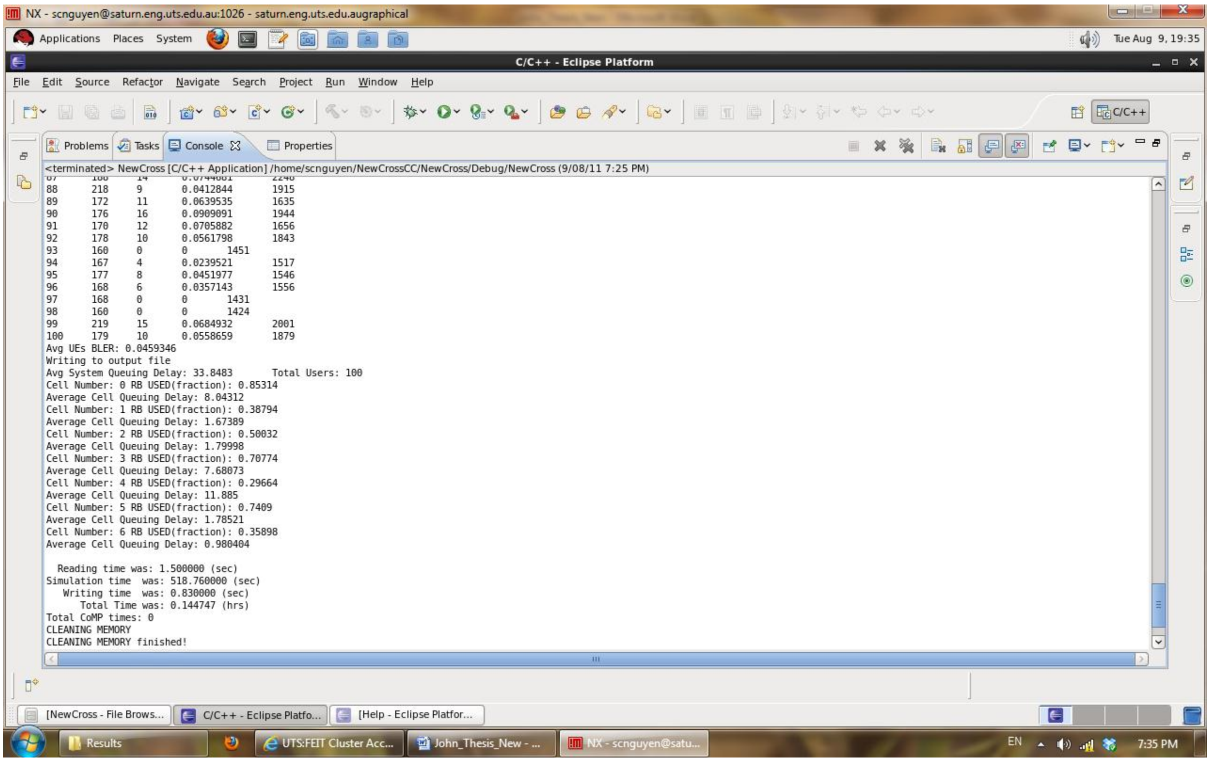

The image when the simulation finished, with information about total simulation time and so on.

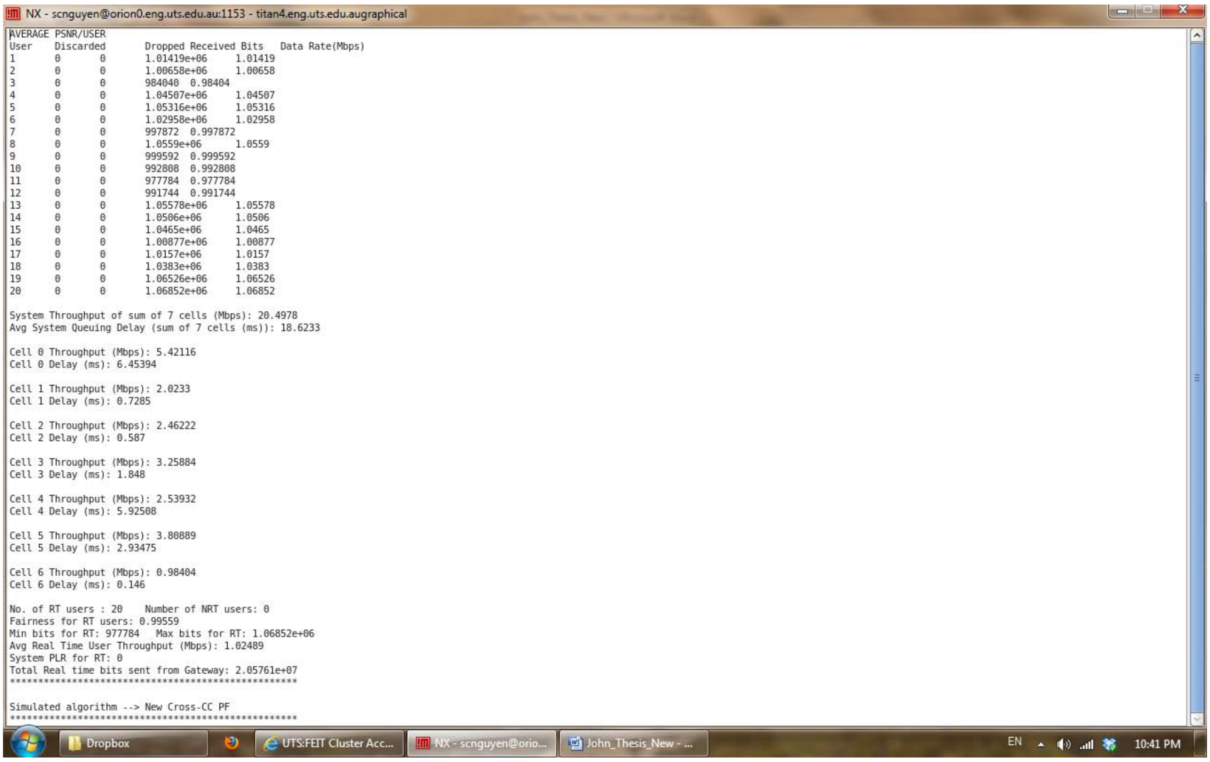

The simulator's final outputs (after the post-processing block) showing the data rate of all users and all cells; fairness index; delay; and packet loss ratio.

LIST OF SYMBOLS

ε	:	A constant
λ	:	Average talk spurt arrival rate
δ_i	:	The maximum probability for HOL packet delay of user i to exceed the delay threshold of user i
τ	:	Alignment delay for the first packet in the talk spurt
τ_i	:	The delay threshold of user i
τ_{max}	:	The maximum delay constraint out of RT service users
$\theta_{i,n}$	:	Discrete Doppler phase
$\xi\ (t)$	:	Rayleigh process
$\xi_i(t)$	:	The shadow fading of user i at time t
$\eta(t)$	:	Suzuki process
$\zeta(t)$	:	Log-normal process
$\delta(t)$	:	Continuous Dirac delta function
$\gamma_{i,j}(t)$	:	The SNR level of user i on sub-carrier j at time t
$\mu\ (t)$	:	Complex Gaussian random process
$\mu_i(t)$	:	Priority metric of user i at time t
		White Gaussian noise process
μ_1	:	Average service rate of the signalling channel
μ_2	:	Average service rate of the traffic channel
$\tilde{\mu}_i(t)$	:	Approximated Gaussian process
ρ	:	Normalized threshold level
$\rho_i(t)$	:	The shadow fading autocorrelation function of user i at time t
$\gamma_i(t)$	:	The number of urgent packets for user i at time t

a	:	A slope of a NRT service
$Bcurr_i(t)$	:	The buffer size of user i at time slot t
$Bcurr\_avg_i$	:	The average value of $Bcurr_i(t)$
c	:	The speed of light
$c_{i,n}$	:	Doppler coefficient
$C(t)$	:	The number of HARQ cycles between the i-1th packet's arrival with the start of ith packet's transmission
$C_{avg}(t)$	:	The average value of $C_{ij}(t)$
$C_{max}(t)$	:	The maximum value of $C_{ij}(t)$
$C_{ij}(t)$	:	The MCS level of user i for sub-band j at time slot t
$\tilde{d}$	:	Total packet delay
$data\_rate(t)$	:	The achievable data rate of a user time t
f_c	:	The carrier frequency
$f_{i,n}$	:	Discrete Doppler frequency
f_{max}	:	The maximum Doppler frequency
$f_{w\|r}(t)$	:	The conditional probability density function of HOL packet delay of user i, given the instantaneous achievable rate of RB j at time $n+1$
$Gain_{i,,j}(t)$	:	The channel gain of user i on RB j at time t
$H(t)$	:	Channel matrix
h_n	:	HARQ early termination probability
H_r	:	Height of mobile or receiver in meters
h_b	:	Height of base station or transmitter in meters
h_m	:	Height of mobile station.
I	:	Inter-cell Interference
$I_i(t)$	:	Indicator function of the event that user i is scheduled to transmit at time t
$I(t)$	:	Index matrix

j	:	Radio Block position.
k	:	Number of component carrier
$k(t)$	:	The index number of the user who is selected for transmission at time t
K	:	The total number of users
$mpath_{i,j}(t)$	:	The multi-path gain of user i on sub-carrier j at time t
m_1	:	Number of available tile-interlace resources for signalling transmission within one interlace period
m_2	:	Number of available tile-interlace resources for traffic transmission within one interlace period
M	:	Metric of packet scheduling algorithm
N	:	Total number of Component Carrier
N_i	:	The number of component carrier of user i
N_s	:	The period of HARQ retransmission in slots
N_0	:	The noise power spectral density
$nbits_{i,j}(t)/symbol$	:	The number of bits per symbol of user i at time t on a sub-carrier within RB j
$nsymbols/slot$	:	The number of symbols per slot
$nslot/TTI$	:	The number of slots per TTI
nsc/RB	:	The number of sub-carriers per RB
$p_j(n)$	:	The probability that n talk spurt are present in the jth queue
$PLR_i(t)$	:	Packet loss ratio of user i at time t
$PLR_{req,i}$	:	PLR threshold of user i
P_{total}	:	Total eNodeB downlink transit power
$pdiscard_i(t)$	:	The size of discarded packets of user i at time t
$pdrop_i(t)$	:	The size of dropped packets of user i at time t
$pl_i(t)$	:	The path loss of user i at time t
$psize_i(t)$	:	The size of all packets that have arrived into eNodeB buffer of

		user i at time t
$ptotaltransmit_{max}$	:	The total size of the transmitted packets of the most served user
$ptotaltransmit_{min}$	:	The total size of the transmitted packets of the least served user
$ptransmit_i(t)$	:	The size of transmitted packets of user i at time t
r	:	Instantaneous achievable data rate
$r_i(t)$	:	The achievable data rate of user i at time t
$R_i(t)$	:	The average data rate of user i at time t
R_{thr}	:	The threshold level
$SDF_i(t)$	:	SDF of user i at time t
$shd_i(t)$	:	The shadow fading gain of user i at time t
s_j	:	The multi-server service time seen by a talk spurt waiting for resource assignment
$\tilde{s}_j$	:	The service time experienced by a talk spurt with assigned resources
T	:	The total simulation time
T_s	:	Time slot duration
T_0	:	Regular Interval of the vocoder
t_c	:	The size of an update window
$total_{RB\_used}(t)$	:	Total number of RBs that have been used for transmission at time t
$UDF_j(t)$	:	UDF of sub-band j at time t
UT_i	:	Throughput of user i
UT_{aver}	:	Average throughput of all user
v	:	The user's velocity
$\tilde{v}$	:	Transmission time experienced by the transmitted packet itself
v_i	:	Transmission time of ith packet in the talk spurt seen by other packets waiting in the queue

w	:	Overall packet waiting time
w_i	:	Waiting time of *i*th packet in the talk spurt
w_b	:	Total queue delay experienced by a new talk spurt
w_{b1}	:	Waiting time in the signalling server
w_{b2}	:	Waiting time in the traffic server
W_{max}	:	The maximum HOL packet delay of all RT service users
$W_{max,i}$	:	Maximum allowable delay of user i
$W_i(t)$	:	The HOL packet delay for user i at time t

GLOSSARY

1G	The first generation of analogue mobile phone technologies including AMPS, TACS and NMT
1xEVDO	1xEvolution-Data Optimized, a short name for CDMA 1xEV-DO
2.5G	The enhancement of GSM which includes technologies such as GPRS
2G	The second generation of digital mobile phone technologies including GSM, CDMA IS-95 and D-AMPS IS-136
3G	The third generation of mobile phone technologies covered by the ITU IMT-2000 family
3GPP	The 3rd Generation Partnership Project, a grouping of international standards bodies, operators and vendors with the responsibility of standardising the WCDMA based members of the IMT-2000 family, an upgrade version of GSM technology.
3GPP2	The counterpart of 3GPP with responsibility for standardising the CDMA2000-based members of the IMT-2000 family.
Bandwidth	A term meaning both the width of a transmission channel in terms of Hertz and the maximum transmission speed in bits per second that it will support
BER	Bit Error Rate; the percentage of received bits in error compared to the total number of bits received
BLER	Block Error Rate
Bit	A bit is the smallest unit of information technology. As bits are made up using the binary number system, all multiples of bits must be powers of two i.e. a kilobit is actually 1024 bits and a megabit 1048576 bits. Transmission speeds are given in bits per second (bit/s)
BSC	Base Station Controller; the network entity controlling a number of Base Transceiver Stations
BTS	Base Transceiver Station; the network entity which communicates with the mobile station
CC	Component Carrier, a range in frequency with the limited bandwidth, usually from 1.25MHz to 20MHz in LTE-Advanced.
CDMA	Code Division Multiple Access; also known as spread spectrum, CDMA cellular systems utilise a single frequency band for all

traffic, differentiating the individual transmissions by assigning them unique codes before transmission. There are a number of variants of CDMA (see W-CDMA, B-CDMA, TD-SCDMA et al)

CDMA 1x	The first generation of cdma2000; the standardisation process indicated that there would be CDMA 2X and CDMA 3X but this no longer appears likely
CDMA 1xEV-DO	A variant of CDMA 1X which delivers data only
CDMA2000	A member of the IMT-2000 3G family; backwardly compatible with cdmaOne
cdmaOne	The first commercial CDMA cellular system; deployed in North America and Korea; also known as IS-95
Cell	The area covered by a cellular base station. A cell site may sectorise its antennas to service several cells from one locationCell site
	The facility housing the transmitters/receivers, the antennas and associated equipment
CoMP	Coordinated MultiPoint transmission and reception, new technique of LTE-Advanced to receive and transmit from and to many base stations.
Cross-CC	Cross-Component Carriers, refer to the mechanism that can control multiple component carriers concurrently.
DCS1800	Digital Cellular System at 1800MHz, now known as GSM1800
DECT	Digitally Enhanced Cordless Telecommunications system, a second generation digital cordless technology standardised by ETSI
DFTS-OFDM	DFT-spread OFDM, or Direct Fourier Transform spread – Orthogonal Frequency Division Multiplexing
DPSK	Digital Phase Shift Keying
DQPSK	Digital Quadrature Phase Shift Keying
EDGE	Enhanced Data rates for GSM Evolution; effectively the final stage in the evolution of the GSM standard, EDGE uses a new modulation schema to enable theoretical data speeds of up to 384kbit/s within the existing GSM spectrum. An alternative upgrade path towards 3G services for operators, such as those in the USA, without access to new spectrum. Also known as Enhanced GPRS (E-GPRS)
eNodeB	evolved-Node B, new name of Base Station in LTE system.
EPC	Evolved Packet Core, main component of the SAE architecture,

	also known as SAE Core
ETSI	European Telecommunications Standards Institute: The European group responsible for defining telecommunications standards
FDD	Frequency-division duplex, the method of transmitter and receiver operate at different carrier frequencies
FDMA	Frequency Division Multiple Access-a transmission technique where the assigned frequency band for a network is divided into sub-bands which are allocated to a subscriber for the duration of their calls
FSK	Frequency Shift Keying; a method of using frequency modulation to send digital information
GBR	Guarantee Bit Rate, same meaning with Real Time, to distinguish 2 kind of services: Real Time and Non Real Time.
GGSN	Gateway GPRS Support Node, main component of the GPRS network, responsible for the interworking between the GPRS network and external packet switched networks
GMSC	Gateway Mobile Services Switching Centre; the gateway between two networks
GPRS	General Packet Radio Service; standardised as part of GSM Phase 2+, GPRS represents the first implementation of packet switching within GSM, which is a circuit switched technology. GPRS offers theoretical data speeds of up to 115kbit/s using multislot techniques. GPRS is an essential precursor for 3G as it introduces the packet switched core required for UMTS
GPS	Global Positioning System; a location system based on a constellation of US Department of Defence satellites. Depending on the number of satellites visible to the user can provide accuracies down to tens of meters. Now being incorporated as a key feature in an increasing number of handsets
GSM	Global System for Mobile communications, the second generation digital technology originally developed for Europe but which now has spread all over the world. Initially developed for operation in the 900MHz band and subsequently modified for the 850, 1800 and 1900MHz bands. GSM originally stood for Groupe Speciale Mobile, the CEPT committee which began the GSM standardization process
Handoff	The transfer of control of a cellular phone call in progress from one cell to another, without any discontinuity

HARQ	Hybrid Automatic Retransmission Request
HLR	Home Location Register; the database within a GSM network which stores all the subscriber data. An important element in the roaming process
HOL	Head of Line, the time difference between the current time and the arrival time of a packet
HOM	Higher Order Modulations
HSCSD	High Speed Circuit Switched Data; a special mode in GSM networks which provides higher data throughput by concatenating a number of timeslots, each delivering 14.4kbit/s, much higher data speeds can be achieved
HSDPA	High Speed Downlink Packet Access, 3.5G technology of 3GPP family.
HSUPA	High Speed Uplink Packet Access, upgrade version of HSDPA.
HSPA+	Evolved HSPA technology, upgrade version of HSUPA.
IMEI	International Mobile Equipment Identity
IMSI	International Mobile Subscriber Identity; an internal subscriber identity used only by the network
IMT-2000	The family of third generation technologies approved by the ITU, also named 3G. There are five members of the family: IMT-DS, a direct sequence WCDMA FDD solution IMT-TC, a WCDMA TDD solution IMT-MC, a multicarrier solution developed from cdma2000 IMT-SC, a single carrier solution developed from IS-136/UWC-136 IMT-FT, a TDMA/TDD solution derived from DECT
IMT-Advanced	International Mobile Telecommunications-Advanced, or 4G, next generation of IMT-2000.
In-CC	Independent-Component Carriers, refer to the mechanism that works separately on each component carrier.
IS-95	Cellular standard know also as cdmaOne
ITU	International Telecommunications Union
LTE	Long Term Evolution, 3.9G technology of 3GPP family
LTE-Advanced (or **LTE-A**)	Long Term Evolution- Advanced, 4G technology of 3GPP.
MBMS	Multimedia Broadcast/Multicast Services

MCS	Modulation and Channel coding Schemes
MIMO	Multi-Input Multi-Output
M-LWDF	Modified-Largest Weighted Delay First, a well-known packet scheduling algorithm.
MMS	Multimedia Messaging Service; an evolution of SMS, MMS goes beyond text messaging offering various kinds of multimedia content including images, audio and video clips
Modulation	The process of imposing an information signal on a carrier. This can be done by changing the amplitude (AM), the frequency (FM) or the phase, or any combination of these
MS	Mobile Station
MSC	Mobile Switching Centre; the switching centre of a mobile phone network, the MSC has interfaces to the BSCs, HLR, VLR and other MSCs
Node B	The element in a UMTS network which interfaces with the mobile station, analogous to a BTS in a GSM network
Non GBR	Non Guarantee Bit Rate, same meaning with Non Real-Time
NRT	Non Real-Time
O&M	Operations and Maintenance
OCM	Optimized Cross-CC M-LWDF, new proposed packet scheduling algorithm for LTE-Advanced technology with multiple component carriers
OCPF	Optimized Cross-CC Proportional Fair, new proposed packet scheduling algorithm for LTE-Advanced technology with multiple component carriers
OFDMA	Orthogonal Frequency Division Multiple Access
PCMCIA	Personal Computer Memory Card Interface Association the body responsible for defining the standards and formats for memory expansion cards for laptop computers and PDAs. Now extended to cover cards for mobile phones
PCS 1900	Personal Communications Systems 1900MHz; the terminology used in the US to describe the new digital networks being deployed in the 1900MHz band; rarely used today
PCU	Packet Control Unit, part of the Base Station Subsystem in a GSM network

PF	Proportional Fair, a well-known packet scheduling algorithm
PLMN	Public Land Mobile Network; any cellular operator's network
PLR	Packet Loss Ratio
PS	Packet Scheduling, RRM mechanism to allocate the radio resources for all users
PSDN	Public Switched Data Network
PSK	Phase Shift Keying
PSTN	Public Switched Telephone Network
QAM	Quadrature Amplitude Modulation
QoS	Quality of Service; a broad term to describe the performance attributes of an end-to-end connection
QPSK	Quadrature Phase Shift Keying (4QAM)
RAN	Radio Access Network, includes some network elements like base station (BTS, NodeB), base station controller (BSC, RNC).
RB	Radio Resource Block, 180KHz x 0.5ms, the basic unit for all LTE radio resource activities.
RF	Radio Frequency
RN	Relay Node, new network element in LTE-Advanced that extends the coverage of base station.
RNC	Radio Network Controller, the element controls the NodeBs within a UMTS network. It is roughly analogous to a BSC in a GSM network
RNP	Radio Network Planning
Roaming	A service unique to GSM which enables a subscriber to make and receive calls when outside the service area of his home network e.g. when travelling abroad
RRM	Radio Resource Management, refer to some mechanisms like handover, radio admission, power control, packet scheduling.
RT	Real-Time
SAE	System Architecture Evolution, core network architecture of 3GPP's LTE system.
SC-FDMA	Single Carrier Frequency Division Multiple Access
SCP	Switching/Service Control Point

SDMA	Spatial Division Multiple Access
SGSN	Serving GPRS Support Node; the gateway between the RNC and the core network in a GPRS/UMTS network
SIM	Subscriber Identity Module; A smart card containing the telephone number of the subscriber, encoded network identification details, the PIN and other user data such as the phone book. A user's SIM card can be moved from phone to phone as it contains all the key information required to activate the phone
SINR	Signal to Interference plus Noise ratio, same as signal to noise ratio (SNR) when there is no interference.
SMS	Short Message Service; a text message service which enables users to send short messages (160 characters) to other users.
SMSC	SMS Centre-the network entity which switches SMS traffic
TB	Transport Block
TDD	Time-Division Duplex, the application of time-division multiplexing to separate outward and return signals.
TDMA	Time Division Multiple Access; a technique for multiplexing multiple users onto a single channel on a single carrier by splitting the carrier into time slots and allocating these on a as-needed basis
TTI	Transmit Time Interval, 1ms interval in LTE technology.
UE	User Equipment, new name for Mobile Station.
UMB	Ultra Mobile Broadband, 3.9G technology of 3GPP2
UMTS	Universal Mobile Telecommunications System; the European entrant for 3G; now subsumed into the IMT-2000 family as the WCDMA technology.
UPE	User Plane Entity
USIM	Universal Subscriber Identity Module; the 3G equivalent of the GSM SIM
UTRAN	Universal Terrestrial Radio Access Network; the UMTS radio access network comprising the RNC, Node B and the air interface
VLR	Visitor Location Register
VoIP	Voice over Internet Protocol
WAP	Wireless Application Protocol; a de facto standard for enabling mobile phones to access the Internet and advanced services. Users can access websites and pages which have been converted by the

use of WML into stripped-down versions of the original more suitable for the limited display capabilities of mobile phones

WCDMA Wideband CDMA; the technology created from a fusion of proposals to act as the European entrant for the ITU IMT-2000 family

WiBro Wireless Broadband, a version of mobile WiMAX developed by South Korean telecoms industry.

WiMAX Worldwide Interoperability for Microwave Access

REFERENCES

[1] ITU. (2011, 2 July). *2 billion people now surfing the net: UN*. Available: http://www.abc.net.au/news/stories/2011/01/27/3122545.htm

[2] Internet World Stats. (2011, 11 July). *World Internet Users and Population Stats*. Available: http://www.internetworldstats.com/stats.htm

[3] 3GPP. *3rd Generation Partnership Project*. Available: http://www.3gpp.org

[4] 3GPP2. *3rd Generation Partnership Project 2*. Available: http://www.3gpp2.org

[5] IEEE. *IEEE 802 LAN/MAN Standards*. Available: http://www.ieee802.org

[6] ITU. (21/10/2010). *ITU-R IMT-Advanced 4G standards to usher new era of mobile broadband communications*. Available: http://www.itu.int/net/pressoffice/press_releases/2010/40.aspx

[7] 3GPP TSG-RAN1, "3GPP Self-evaluation Methodology and Results," 17-18/12/2009.

[8] ITU-R, "Requirements related to technical performance for IMT-Advanced radio interface(s)," M.2134, 2008.

[9] Nokia. *World's first GSM call*. Available: http://www.nokia.com/about-nokia/company/story-of-nokia/the-move-to-mobile/first-gsm-call

[10] J. Bensimon, "From 2G to 4G and beyond," Logtel 2007.

[11] T. Nakamura, "Proposal for Candidate Radio Interface Technologies for IMT-Advanced Based on LTE Release 10 and Beyond (LTE-Advanced)," 3GPP TSG-RAN 15/10/2009.

[12] Cisco, "Evolving to LTE – Cisco's Seamless Migration for UMTS Operators."

[13] 3G Americas, "3GPP Mobile Broadband Innovation Path to 4G: Release 9, Release 10 and Beyond: HSPA+, SAE/LTE and LTE-Advanced," Febuary, 2010.

[14] K. Sandrasegaran, "Title," unpublished|.

[15] NBN. (2011). *What is the NBN?* Available: http://www.nbn.gov.au/about-the-nbn/what-is-the-nbn/

[16] NBN Co Limited. (1 June, 2011). *NBN Co selects fixed wireless network partner for mid-2012 service start*. Available: http://www.nbnco.com.au/news-and-events/news/nbnco-selects-fixed-wireless-network-partner-for-mid-2012-service-start.html

[17] E. Dahlman, *3G evolution : HSPA and LTE for mobile broadband*, 2nd ed. Amsterdam ; Boston ; London: Academic, 2008.

[18] Agilent, "3GPP Long Term Evolution: System Overview, Product Development, and Test Challenges," 2008.

[19] Ericsson, "Long Term Evolution (LTE): an introduction," White Paper 284 23-3124 Uen, October 2007 2007.

[20] F. Rayal. (2010, June 20) An overview of the LTE physical layer. *EE Times* [Design > RF and Microwave].

[21] Z. Ghadialy. (2009, 6 February). *MIMO schemes in LTE* Available: http://3g4g.blogspot.com/2009/02/mimo-schemes-in-lte.html

[22] H. G. Myung and D. J. Goodman, *Single carrier FDMA : a new air interface for long term evolution*. Chichester, U.K. ; New York: J. Wiley & Sons, 2008.

[23] 3GPP, "Overview of 3GPP Release 10," 2011-06.
[24] C. Li, *et al.*, "Analysis and Simulation for Spectrum Aggregation in LTE-Advanced System," in *Vehicular Technology Conference Fall (VTC 2009-Fall), 2009 IEEE 70th*, 2009, pp. 1-6.
[25] Tata Consultancy Services, "LTE-Advanced: Future of Mobile Broadband," White Paper,2009.
[26] P. E. Mogensen, *et al.*, "LTE-Advanced: The path towards gigabit/s in wireless mobile communications," in *Wireless Communication, Vehicular Technology, Information Theory and Aerospace & Electronic Systems Technology, 2009. Wireless VITAE 2009. 1st International Conference on*, 2009, pp. 147-151.
[27] 3GPP TR 36.814, "Further Advancements for E-UTRA Physical Layer Aspects (Release 9)," January 2009.
[28] H. Holma and A. Toskala, *LTE for UMTS : OFDMA and SC-FDMA based radio access*. Chichester, U.K.: Wiley, 2009.
[29] H. A. M. Ramli, *et al.*, "Performance of Well Known Packet Scheduling Algorithms in the Downlink 3GPP LTE System," presented at the IEEE 9th Malaysia International Conference on Communications (MICC), 2009.
[30] E. Dahlman, *et al.*, *3G Evolution: HSPA and LTE for Mobile Broadband*, First ed.: Elsevier Ltd., 2007.
[31] Tsung-Yu Tsai; Yao-Liang Chung and Zsehong Tsai, "Introduction to Packet Scheduling Algorithms for Communication Networks," in *Communications and Networking*, ed, 2010.
[32] A. Jalali, *et al.*, "Data Throughput of CDMA-HDR a High Efficiency-High Data Rate Personal Communication Wireless System," presented at the IEEE 51st Vehicular Technology Conference Proceedings, 2000.
[33] M. Andrews, *et al.*, "Providing Quality of Service over a Shared Wireless Link," *IEEE Communications Magazine,* vol. 39, no. 2, pp. 150-154, Feb. 2001.
[34] J.-H. Rhee, *et al.*, "Scheduling of Real/Non-Real Time Services: Adaptive EXP/PF Algorithm," presented at the The 57th IEEE Semiannual Vehicular Technology Conference, 2003.
[35] J.-H. Rhee, *et al.*, "Performance Analysis of the Adaptive EXP/PF Channel Scheduler in an AMC/TDM System," *IEEE Communications Letters,* vol. 8, no. 8, pp. 4978-4980, Aug. 2004.
[36] M. Xue, "Performance Analysis of Packet Scheduling Algorithms for Long Term Evolution " Master of Engineering (Research), Faculty of Engineering and Information Technology, University of Technology, Sydney, 2010.
[37] K. K. L. Erwu Liu, "Throughput Analysis of Opportunistic Scheduling under Rayleigh Fading Environment," presented at the Vehicular Technology Conference, 2008.
[38] L. Erwu and K. K. Leung, "On theThroughput Characteristics of Utility-based Fair Scheduling," in *Personal, Indoor and Mobile Radio Communications, 2008. PIMRC 2008. IEEE 19th International Symposium on*, 2008, pp. 1-5.
[39] L. Erwu and K. K. Leung, "Proportional Fair Scheduling: Analytical Insight under Rayleigh Fading Environment," in *Wireless Communications and Networking Conference, 2008. WCNC 2008. IEEE*, 2008, pp. 1883-1888.
[40] E. Liu and K. K. Leung, "Fair Resource Allocation under Rayleigh and/or Rician Fading Environments," in *Personal, Indoor and Mobile Radio*

Communications, 2008. PIMRC 2008. IEEE 19th International Symposium on, 2008, pp. 1-5.
[41] M. S. P. J. Smith, "On a Gaussian Approximation to the Capacity of Wireless MIMO Systems," in *Proc. IEEE ICC*, New York, 2002, pp. 460-410.
[42] H. P. Hsu, *Schaum's Outline of Theory and Problems of Probability, Random Variables, and Random Processes*: The McGraw-Hill Companies, Inc., 1997.
[43] S. V. Qi Bi, Yifei Yuan, Qinqing Zhang, "Performance and Capacity of Cellular OFDMA Systems With Voice-Over-IP Traffic," *IEEE TRANSACTIONS ON VEHICULAR TECHNOLOGY,* vol. 57, pp. 3641-3652, Nov. 2008.
[44] W. Yuanye*, et al.*, "Carrier load balancing and packet scheduling for multi-carrier systems," *Wireless Communications, IEEE Transactions on,* vol. 9, pp. 1780-1789.
[45] K. Takeda*, et al.*, "Effects of Wideband Scheduling and Radio Resource Assignment in OFDMA Radio Access for LTE-Advanced Downlink," in *Vehicular Technology Conference Fall (VTC 2009-Fall), 2009 IEEE 70th*, 2009, pp. 1-5.
[46] Y.-L. Chung*, et al.*, "An efficient downlink packet scheduling algorithm in LTE-Advanced systems with Carrier Aggregation," in *Consumer Communications and Networking Conference (CCNC), 2011 IEEE*, 2011, pp. 632-636.
[47] S. Shi*, et al.*, "A Resource Scheduling Algorithm Based on User Grouping for LTE-Advanced System with Carrier Aggregation," in *Computer Network and Multimedia Technology, 2009. CNMT 2009. International Symposium on*, 2009, pp. 1-4.
[48] W. Yuanye*, et al.*, "Resource allocation considerations for multi-carrier LTE-Advanced systems operating in backward compatible mode," in *Personal, Indoor and Mobile Radio Communications, 2009 IEEE 20th International Symposium on*, 2009, pp. 370-374.
[49] L. Lingjia*, et al.*, "Proportional fair scheduling for multi-cell multi-user MIMO systems," in *Information Sciences and Systems (CISS), 2010 44th Annual Conference on*, pp. 1-6.
[50] Balamurali, "A low complexity resource scheduler for cooperative cellular networks," in *Internet Multimedia Services Architecture and Applications (IMSAA), 2009 IEEE International Conference on*, 2009, pp. 1-6.
[51] L. Jianhua*, et al.*, "Semi-persistent scheduling for VoIP service in the LTE-Advanced relaying networks," in *Communications, Circuits and Systems (ICCCAS), 2010 International Conference on*, pp. 54-58.
[52] H. A. M. Ramli*, et al.*, "Modeling and simulation of packet scheduling in the downlink long term evolution system," in *Communications, 2009. APCC 2009. 15th Asia-Pacific Conference on*, 2009, pp. 68-71.
[53] C. Komninakis, "A fast and accurate Rayleigh fading simulator," in *Global Telecommunications Conference, 2003. GLOBECOM '03. IEEE*, 2003, pp. 3306-3310 vol.6.
[54] O. S. Rice, "Mathematical Analysis of Random Noise," in *Bell Syst. Tech. J.* vol. 23, ed, 1944, pp. 282-332.
[55] M. Patzold*, et al.*, "A deterministic digital simulation model for Suzuki processes with application to a shadowed Rayleigh land mobile radio channel," *Vehicular Technology, IEEE Transactions on,* vol. 45, pp. 318-331, 1996.
[56] A. Papoulis, *Probability, Random Variables, and Stochastic Processes*. New York: McGraw-Hill, 1991.

[57] K. Sandrasegaran, *et al.*, "Delay-Prioritized Scheduling (DPS) for Real Time Traffic in 3GPP LTE System," in *Wireless Communications and Networking Conference (WCNC), 2010 IEEE*, 2010, pp. 1-6.
[58] 3GPP, "Feasibility Study for Orthogonal Frequency Division Multiplexing (OFDM) for UTRAN Enhancement (Release 6)," TR25.892, version 6.0.0, June 2004.
[59] 3GPP2, "cdma2000 Evaluation Methodology," December 10 2004.
[60] R. Basukala, *et al.*, "Performance analysis of EXP/PF and M-LWDF in downlink 3GPP LTE system," in *Internet, 2009. AH-ICI 2009. First Asian Himalayas International Conference on*, 2009, pp. 1-5.
[61] H. Holma and A. Toskala, *WCDMA for UMTS : HSPA evolution and LTE*, 4th ed. Chichester, England ; Hoboken, NJ: Wiley, 2007.
[62] J. Zhang, *et al.*, "An Adaptive Resource Reservation Strategy for Handoff in Wireless CDMA Cellular Networks," *Canadian Journal of Electrical and Computer Engineering,* vol. 29, no. 1/2, pp. 77-84, 2004.
[63] M. Gudmundson, "Correlation model for shadow fading in mobile radio systems," *Electronics Letters,* vol. 27, pp. 2145-2146, 1991.
[64] K. Kim, *et al.*, "Interference Analysis and Subchannel Allocation Schemes in Tri-Sectored OFDMA Systems," presented at the IEEE 66th Vehicular Technology Conference, 2007.
[65] L. Cheng-Chung, *et al.*, "Optimization of handover algorithms in 3GPP long term evolution system," in *Modeling, Simulation and Applied Optimization (ICMSAO), 2011 4th International Conference on*, 2011, pp. 1-5.
[66] X. Qiu and K. Chawla, "On the Performance of Adaptive Modulation in Cellular Systems," presented at the IEEE Transactions on Communications, 1999.
[67] K. Sandrasegaran, *et al.*, "Delay-Prioritized Scheduling (DPS) for Real Time Traffic in 3GPP LTE System," in *Wireless Communications and Networking Conference (WCNC), 2010 IEEE*, pp. 1-6.
[68] H. Ayoub and M. Assaad, "Scheduling in OFDMA Systems with Outdated Channel Knowledge," in *Communications (ICC), 2010 IEEE International Conference on*, 2010, pp. 1-5.
[69] A. Jalali, *et al.*, "Data throughput of CDMA-HDR a high efficiency-high data rate personal communication wireless system," in *Vehicular Technology Conference Proceedings, 2000. VTC 2000-Spring Tokyo. 2000 IEEE 51st*, 2000, pp. 1854-1858 vol.3.
[70] S. C. Nguyen and K. Sandrasegaran, "Adaptations of Proportional Fair Algorithm for Packet Scheduling in LTE-Advanced," in *The 2010 International Conference on Communication and Vehicular Technology (ICCVT 2010)*, Hanoi, Vietnam, 2010, pp. 1-4.
[71] S. C. Nguyen and K. Sandrasegaran, "Modeling and Simulation of Packet Scheduling in the Downlink LTE-Advanced," in *The 17th Asia-Pacific Conference on Communication (APCC 2011)*, Sabah, Malaysia, 2011, pp. 1-4.
[72] 3GPP, "Policy and Charging Control Architecture (Release 10)," TS 23.203, version 10.0.0, June 2010.
[73] I. K. Fu, *et al.*, "Multicarrier technology for 4G WiMax system [WiMAX/LTE Update]," *Communications Magazine, IEEE,* vol. 48, pp. 50-58, 2010.
[74] R. Attar, *et al.*, "Evolution of cdma2000 cellular networks: multicarrier EV-DO," *Communications Magazine, IEEE,* vol. 44, pp. 46-53, 2006.